FROM FATS TO FLUORESCENT FISH: LIPID MODIFICATIONS OF SONIC HEDGEHOG LIGAND DICTATE CELLULAR RECEPTION AND SIGNAL RESPONSE

By

VANDANA KAMINIE GROVER

Dissertation

Submitted to the Faculty of the

Graduate School at Vanderbilt University

in partial fulfillment of the requirements

for the degree of

DOCTOR OF PHILOSOPHY

in

Neuroscience

December, 2011

Nashville, Tennessee

Approved:

Lilianna Solnica-Krezel, Ph.D.

Chin Chiang, Ph.D.

Michael K. Cooper, M.D.

Louis J. De Felice, Ph.D.

Ethan Lee, M.D., Ph.D.

For my parents, Rani and Viren Grover, who instilled their love of science in me,
and to my loving and supportive husband, Joshua Decker.

ACKNOWLEDGMENTS

“There's an old saying that victory has a hundred fathers and defeat is an orphan.”
President John F. Kennedy, April 21, 1961

President John F. Kennedy made that statement when he took responsibility for the Bay of Pigs fiasco. Though my graduate career is as far removed from a Cuban invasion as anything could be, his logic holds. My doctorate and this thesis would not have happened but for the warm, constant contributions of friends, family, mentors, and colleagues. I am privileged to thank them.

I first must thank my advisor, Michael Cooper, for his tireless advice and mentorship. He combined a passion for science and good arguments with ceaseless support, patience, warmth, and good humor. Our discussions made me into a stronger, critically thinking scientist.

Michael gave me an academic home, but Elaine Sanders-Bush and the Neuroscience Graduate Program made that home possible. Thank you for admitting me into this program and for providing a learning environment full of interesting classes, stimulating talks, and enjoyable extracurricular activities, all of which enabled me to grow and mature as a scholar. I also thank the entire Vanderbilt Brain Institute staff for their administrative assistance throughout the years.

Thank you to my thesis committee, Lilianna Solnica-Krezel, Chin Chiang, Michael Cooper, Louis De Felice, and Ethan Lee, for their fruitful discussions and

useful ideas. I appreciate that they each freely gave their time, thoughts, and wisdom. They were instrumental in suggesting areas of investigation and honing my experimental course. Thank you specifically to Ethan for suggesting the HPLC experiments, to Chin for our detailed conversations about sonic hedgehog and for the joint Chiang-Cooper lab meetings, and to Lila for her expertise and assistance with zebrafish development. Lila was also a terrific committee chair: after every committee meeting, she provided me with wonderfully specific notes about each member's suggestions: these were fundamental to my success. Finally, but certainly not least, thank you to Lou, who was not only a committee member, but also a kind mentor and a generous friend. As Neuroscience's former Director of Graduate Studies, he immensely helped me during the beginning of my career. Lou is a fabulous teacher and provided me with a sense of confidence when I really needed it; without him, I would not be here today.

For me, Juan Gerardo Valadez-Sánchez is heart of the Cooper Lab. Gerardo is a true friend. Gerardo helped me with experiments (I especially owe him for countless Maxi Preps), kept me well fed with his homemade Mexican specialties, and was always there with open ears and wise counsel. I am eternally grateful and cannot imagine my graduate career without his support. I also thank Tina Ho for introducing me to the world of molecular cloning and Nishka Narula for helping with ELISAs for a few weeks during the summer of 2009.

I thank Aaron Bowman for allowing us to use his HPLC. I could not have performed these experiments without Aaron's troubleshooting skills and advice.

In the summer of 2006, I was fortunate to be awarded a space at the Marine Biological Laboratory in Woods Hole, Massachusetts. This was an amazing experience: I learned new techniques, I met scientists who were passionate about their research, and I ate as much Cape Cod seafood as I could stomach. I am grateful to MBL for fostering a stimulating, inquisitive environment and for giving me a set of skills that I continue to use.

I spent much of my graduate studies in the fish room with zebrafish. Adi Inbal is the one who taught me how to work with them and make transgenic lines. I owe my zebrafish skill to Adi. I also thank Alex Flynt and Chunyue Yin for imparting their expertise on zebrafish antibody staining and live imaging.

Though Athena is the goddess of wisdom and skill, scientific knowledge does not spring full-born from anyone's head: it is the product of intelligent dialogue and enlightened discussion. Thank you to Sunday Abiria, Catherine Au, Alexandre Benedetto, Iris Castro, Xi Huang, Wasif Khan, Wenyi Lo, Leta Moser, Sarah Rush, Anuraag Sarangi, Emily Schwartz Todd, and Niranjana Vijayakrishnan, for coffee, companionship, lunch breaks, and friendship through the years. All of them are wonderful people and gifted scientists; for their advice and thoughtful conversations, I am in their debt.

I thank the Department of Neurology administrative staff, especially Rosemary Madill, Sandra Camp, and Brenda Farley for taking care of all the little things throughout the years and making my graduate career a more pleasant one.

Robert Frost wrote, “Good fences make good neighbors.” Apparently, he never visited Vanderbilt’s Medical Research Building III. I thank the members of the Appel, Barnes, Bowman, Chiang, Ess, Gallagher, Hedera, and MacDonald labs for sharing reagents, for their collaborative working atmosphere, and for being great neighbors.

Thank you to Gina Oka, Vijay Menon, Rita Dubey, Kruti Patel, and Ketevan Kulidzhanova for their years of friendship and support; I am honored to have these amazing people as some of my closest friends.

Last, but certainly not least, thank you to my two wonderful and supportive parents, Rani and Viren Grover, who have provided me with all the opportunities in the world. Thank you finally to my husband, Joshua Decker, for his boundless love, unending kindness, and ceaseless assistance.

PREFACE

There once was a video game character,
That created much joy and laughter.
His inspiration was ironic,
For he was a break from work, a tonic.
And so a Hedgehog protein was named Sonic.

Eponymous,
With a name as funny as a hippopotamus,
Sonic hedgehog has its character's traits:
Twisted, powerful, and small,
Adducts of palmitoyl,
And a carboxy terminus of cholesterol,
It affects zebrafish, mice, and humans all.

Itself, inspiring Ancient Greeks to tell tales of cyclopia,
Damning modern men with glioma and basal cell carcinoma.
From genesis to death,
Our two nostrils, with every breath.

Neural tubes and Limbs,
Regulated by Patched and Smoothened.
Bilateral split, digits, not thumbs
Governed by a morphogen.
Its importance, mega.
Not bad, for a protein named after Sega.

Vandana K. Grover
One sleepless night.
circa ~ 2010

TABLE OF CONTENTS

LIST OF TABLES

LIST OF FIGURES

Figure Page

LIST OF APPENDIX FIGURES

LIST OF ABBREVIATIONS

ADAM	a disintegrin and metalloprotease
AGNSC	adherent glioma neural stem cell medium
Ala/A	alanine
AP	alkaline phosphatase
Arg/R	arginine
Asp/D	aspartate
BOC	Brother of CDO
CDO	cell-adhesion molecule-related, down-regulated by oncogenes
CSF	cerebrospinal fluid
C-W	Cardin-Weintraub
Cys/C	Cysteine
Dhh	Desert hedgehog
Dlp	Dally like protein
E/CFP	enhanced/cyan fluorescent protein
E/GFP	enhanced/green fluorescent protein
E/YFP	enhanced/yellow fluorescent protein
Ech	Echidna hedgehog
ER	endoplasmic reticulum
FGF	fibroblast growth factor
FL	fluorescently labeled
FRAP	fluorescence recovery after photobleaching

FRET	fluorescence resonance energy transfer
Gas1	Growth Arrest Specific 1
GCP	glypican
Gly/G	glycine
GPCR	G-protein coupled receptor
Hh	Hedgehog
HH	Hamburger-Hamilton
Hhat	Hedgehog acyltransferase
Hhip	Hedgehog interacting protein
Hint	Hedgehog intein
HSPG	heparin sulfate proteoglycan
Ihh	Indian hedgehog
Ihog	interference hedgehog
IR/DR	inverted repeat/direct repeat
Lrp	lipoprotein receptor-related protein
MEF	mouse embryonic fibroblast
MFCS	mammals-fish conserved sequence
mRFP	monomeric red fluorescent protein
NT	neural tube
Phe/F	phenylalanine
Ptc	Patched
RNAi	RNA-interference
RND	resistance-nodulation division

SB	Sleeping Beauty
SBE	Shh brain enhancer
SBE2	Shh brain enhancer-2
SFPE	Shh floor plate enhancer
Shh	Sonic hedgehog
Shha	Sonic hedgehog a
Shhb	Sonic hedgehog b
Ski	Skinny Hedgehog (*Drosophila*)
Skn	Skinny Hedgehog (vertebrate)
Smo	Smoothened
SRR	sterol recognition region
SSD	sterol sensing domain
Tg	transgenic
Twhh	Tiggywinkle hedgehog
VNT	ventral neural tube
ZPA	zone of polarizing activity
zShh	zebrafish Shh (Shha)

CHAPTER I

INSIGHTS INTO HEDGEHOG PROCESSING, SIGNAL TRANSDUCTION, AND TISSUE PATTERNING

1.1 Background

Development of a multicellular organism from a single cell into discrete and organized structures requires the coordinated action of multiple factors. Cell specification is one of development's quintessential questions. How a cell acquires its fate and what mechanisms underlie and facilitate the interactions and communications between cells is fundamental to our understanding of developmental biology. During gastrulation three germ layers, the endoderm, mesoderm, and ectoderm, originate from somatic cells. It is at this junction that pluripotent embryonic stem cells begin to undergo differentiation (Sasai and De Robertis 1997). Among the foremost players in this field is Hedgehog (Hh). Hh is a morphogen, a secreted signaling protein released from a localized source, and acts in a concentration dependent manner to pattern a field of tissue (Roelink et al. 1995; Teleman et al. 2001). Hh signals are varied and profound; in addition to its role as a morphogen, Hh controls a plethora of processes, including proliferation, cell survival, and axon guidance, in a multitude of systems from brain and spinal cord to limb and pancreatic development (Jessell 2000; Charron et al. 2003). Not only is Hh paramount during embryogenesis, but it plays a significant lifelong role in homeostasis and regeneration (Jiang and Hui 2008; Varjosalo and Taipale 2008). These processes are tightly regulated;

misregulation of the Hh signal transduction pathway results in numerous pathologies and malformations, including cancers such as meduloblastoma and basal cell carcinoma (Hahn et al. 1996; Johnson et al. 1996; Goodrich et al. 1997; Oro et al. 1997; Taipale and Beachy 2001; Berman et al. 2003), and holoprosencephaly, a condition characterized by a spectrum of defects in midline facial and forebrain structures (Belloni et al. 1996; Chiang et al. 1996; Roessler et al. 1996; Cohen 2002). Gaining mechanistic insight into the role of Hh cellular secretion, reception and signaling is fundamental to our understanding of tissue patterning as it pertains to birth defects, tissue repair, and malignancies.

1.2 Introducing Sonic hedgehog

Historical background and expression profile

Since Nüsslein-Volhard and Wieschaus discovered the *Hedgehog* gene in the fruit fly, *Drosophila melanogaster*, its study has helped illuminate the mystery of cell-cell interactions. The *Hh* gene belongs to the class of segment polarity genes and was identified in a large-scale screen that examined impairments in the *Drosophila melanogaster* body plan. The normal *Drosophila melanogaster* larvae contains approximately eight abdominal segments. Anterior to the segments is a band of bristles, while the posterior side is smooth. The Hh mutation effects segment patterning, resulting in partial or complete segment deletion within the larvae and is named for its appearance, which includes an abnormal bristle pattern (Nusslein-Volhard and Wieschaus 1980). In the most

severe *Hh*$^{-/-}$ phenotype, the head segment fails to involute and all smooth cuticles from the posterior surface of each segment are lost, resulting in a lawn of bristles and an embryo that is approximately halved in size (Lee et al. 1992; Tabata et al. 1992). *Hh* homologs have been discovered in several organisms, both vertebrates and invertebrates, including *Diadema antillarum* or sea urchins (Walton et al. 2009) and *Petromyzon marinus* or lampreys (Sugahara et al. 2011). This thesis, though, will focus on Hh studies in *Mus musculus* (mouse), *Danio rerio* (zebrafish), and *Drosophila melanogaster* (fruit fly). For simplicity, I will abbreviate *Drosophila melanogaster* as *Drosophila.*

Drosophila Hh was cloned in the early 1990s (Lee et al. 1992; Mohler and Vani 1992; Tabata et al. 1992; Tashiro et al. 1993) followed by the cloning of vertebrate *Hh* (Echelard et al. 1993; Krauss et al. 1993; Riddle et al. 1993). During vertebrate evolution, genome duplication and divergence of the *Hh* gene, resulted in three types of *Hh* subgroups in mammals and avian, *Sonic hedgehog* (*Shh*), *Indian hedgehog* (*Ihh*) and *Desert hedgehog* (*Dhh*). Shh expression is conserved across species in the notochord and floor plate, while Dhh and Ihh have varied expression patterns and can be found in the gonads and in bone growth plates respectively (Bitgood et al. 1996; Vortkamp et al. 1996; Shimeld 1999). In the embryonic mouse, the absence of *Shh* leads to several defects including but not limited to, mispatterning of the midline structures resulting in cyclopia and a proboscis (remnants of the nose and forebrain structures), shortening of the long bones, neural tube mispatterning, and loss of digits two through five (Chiang et al. 1996). Zebrafish, as a result of additional whole-

genome duplication and other rearrangements (Jaillon et al. 2004), has two *Shh* homologs, *tiggywinkle hedgehog* (*Twhh* or *Shhb*) and *Sonic hedgehog* (*Shh or Shha*) (Ekker et al. 1995). *Echidna hedgehog* (*Ehh*), a homolog of *Ihh* is expressed also in the notochord (Currie and Ingham 1996; Varjosalo and Taipale 2008).

Little is known about the initiation of *Hh* transcription. Some possible candidates that may be involved in regulating *Shh* expression include FoxA2, HNF3β, and Six3. FoxA2, a transcription factor, is an upstream positive and negative regulator of Shh expression. Chromatin immunoprecipitation studies in dopaminergic progenitors revealed that FoxA2 may act by binding directly to genomic regions of Gli2, a transducer of the Hh signal (Mavromatakis et al. 2010). In zebrafish, *Shh* is co-expressed with *axial* (*HNF3β*), a transcription factor in the winged helix family, and improper regulation of axial leads to ectopic *Shh* expression. Additionally, in cell culture studies, *HNF3β* expression leads to activation of *Shh* gene promoter (Chang et al. 1997). Six3, a homeobox protein, binds Shh brain enhancer-2 (SBE2), an enhancer known to drive *Shh* expression in the forebrain. Furthermore, in the mouse diencephalon, Shh was determined to be a direct target of Six3 as reduced Six3 protein fails to induce Shh expression (Geng et al. 2008; Jeong et al. 2008).

Multiple enhancer elements, unique to specific tissue types, also influence Shh transcription. Shh floor plate enhancer 1 (SFPE1) and SFPE2, direct Shh expression in the floor plate of the hindbrain and spinal cord, while SBE1, facilitates Shh expression in the ventral midbrain and parts of the diencephalon.

SBE2, SBE3, and SBE4, located farther upstream of the Shh transcription start site, lead to Shh expression in the ventral forebrain (Epstein et al. 1999; Jeong et al. 2006; Varjosalo and Taipale 2008). Loss-of-function studies demonstrate that another enhancer, mammals-fish conserved sequence 1 (MFCS1), is required for Shh expression in the limb bud zone of polarizing activity (ZPA) and mutations in MFCS1 in humans results in limb malformations (Sharpe et al. 1999; Lettice et al. 2003; Sagai et al. 2004; Varjosalo and Taipale 2008).

1.3 Hedgehog Structure, Processing and Lipidation

Hedgehog structure

Full length Hh includes an amino terminal (N-terminal) signaling and a carboxy terminal (C-terminal) autoprocessing domain. A signal sequence peptide precedes the Hh amino terminal. The carboxy end consists of a Hint module that is commonly found in the intein region within self-splicing proteins. The Hh C-terminus also contains a sterol-recognition region (SRR) that may be involved in the addition of the cholesterol moiety (see Hedgehog Biogenesis section for details) (Hall et al. 1997; Mann and Beachy 2004; Ingham et al. 2011).

Shh has homology with zinc hydrolases. The zinc ion associated with the Shh signaling domain is tetrahedrally coordinated with two histidines, an aspartate (D148) and usually a water molecule within a large cleft. The water molecule may form a hydrogen bond with glutamate acting as a base deprotonating water and making it available for nucleophilic attack of substrates.

In addition, mutational analysis of the Shh zinc coordinating residues highlighted their importance in Shh signaling and stability. These point mutations not only resulted in diminished Shh activity, but these mutants were also more susceptible to proteolysis. These zinc associated residues are conserved in vertebrates, but not *Drosophila*. (Hall et al. 1995; Hall et al. 1997; Day et al. 1999; Fuse et al. 1999) (Reviewed in (Beachy et al. 2010)).

Several other studies have also looked at the structure of Shh and its interaction with additional proteins (McLellan et al. 2006; McLellan et al. 2008; Bosanac et al. 2009; Kavran et al. 2010), but one study in particular examines the interactions between Shh and the monoclonal mouse Shh 5E1 antibody. This antibody has been used several times and in different contexts throughout our studies, so it deserves a bit of attention. 5E1 is an anti-Shh monoclonal antibody and Hh pathway antagonist with neutralizing properties that has been extensively utilized in the study of Shh signaling in development and cancer. Mutation of specific surface residues disrupts binding to 5E1 and these same mutations also disrupt Shh and Patched (Ptc, a Shh pathway regulator that binds Hh) binding. Therefore, 5E1 most probably inhibits Hh signaling by competing with Ptc for the Shh zinc cleft binding site, thus acting as a negative pathway regulator (Fuse et al. 1999; Maun et al. 2010). Additional cell culture based studies also illustrate that pre-incubation of 5E1 with Shh inhibits binding to Ptc-expressing cells (Bosanac et al. 2009; Beachy et al. 2010).

Hedgehog biogenesis and lipid modifications

Sonic hedgehog (Shh) undergoes substantial processing and post translational modifications prior to cellular release. There are putative Shh glycosylation sites in mice and four have been found in human Shh. Shh glycosylation is possible and has been shown *in vitro* studies that subject Shh proteins to pancreatic microsomal membranes, an artificial environment that promotes glycosylation (Bumcrot et al. 1995; Dorus et al. 2006). Unlike other similar proteins, glycosylation has not been conclusively demonstrated in the secreted signaling form of Shh protein (Nusse 2003).

Furthermore, upon entry into the secretory pathway, Shh precursor peptides undergo two nucleophilic displacement reactions in the endoplasmic reticulum (ER), resulting in a signaling domain and an autoprocessing domain. Following signal sequence elimination, cholesterol serves as a cofactor in an autocatalytic intramolecular cleavage reaction mediated by amino acid residues in the autoprocessing domain. Hedgehog cleavage occurs at an absolutely conserved Gly-Cys-Phe tripeptide site (Lee et al. 1994; Porter et al. 1995; Porter et al. 1996a; Hall et al. 1997; Chen et al. 2011). The first step of the internal cleavage reaction occurs between the Gly (G197 or G198 depending on the vertebrate species) and neighboring Cys that form the conserved tripeptide and involves rearrangement to replace the main chain peptide with a thioester from the Cys side chain. In the following step, the same carbonyl is attacked by a hydroxyl oxygen, this second nucleophilic attack displaces the sulfur atom and severs the link between the amino terminal (signaling domain) and carboxy end

of the full length Hh protein. Cholesterol remains covalently bound via an ester linkage to the newly formed carboxy terminus of the signaling domain at the Gly 198 residue (Figure 1) (Lee et al. 1994; Porter et al. 1995; Porter et al. 1996a; Porter et al. 1996b). *In vitro* experiments demonstrate that other steroidal compounds such as desmosterol, 7-dehydrocholesterol, and lathosterol can be substituted for cholesterol and thus may be potential adducts in the autocatalytic cleavage reaction (Cooper et al. 1998).

A second lipophilic modification, catalyzed by the acyl transferase endoplasmic reticulum transmembrane protein Skinny hedgehog (Ski in *Drosophila* and Skn or Hhat (Hedgehog acyltransferase) in vertebrates), results in an amide linkage, via a thioester intermediate, of a fatty acid, typically palmitate, with the amino-terminal Cys (C24 or C25 depending on the vertebrate species) of the signaling domain. The modified Cys25 residue is part of pentapeptide, CGPGR that is conserved among species (Figure 1). Hhat, a member of the family of multi-pass transmembrane proteins MBOAT (membrane-bound O-acyl-transferase), is specific to Shh palmitoylation and is, for example, unable to modify other proteins such as Wnt or PSD95. Palmitoylation most likely occurs in the lumen of the ER or Golgi (Pepinsky et al. 1998; Chamoun et al. 2001; Lee and Treisman 2001; Buglino and Resh 2008). Furthermore, the efficiency of Shh palmitoylation is diminished in the absence of the cholesterol modification and may be due to reduced acylation or the lack of some processing sequences that are not available in the truncated or mutated Shh protein (Pepinsky et al. 1998; Mann and Beachy 2004). Shh palmitoylation, however, still

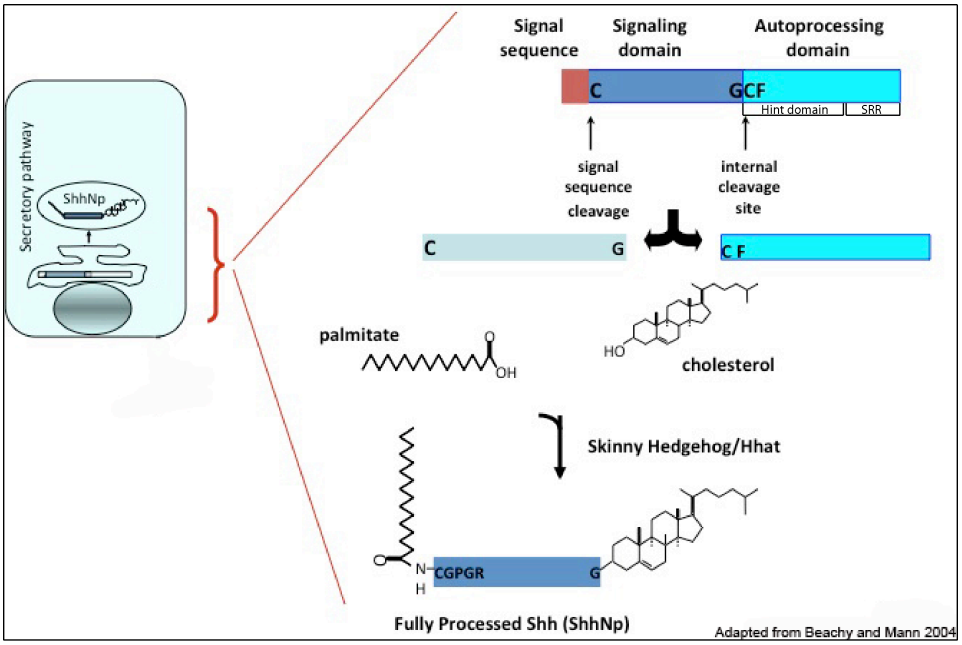

Figure 1. Shh biogenesis and lipid modifications. Upon entry into the secretory pathway, Shh undergoes an autocatalytic cleavage reaction resulting in a signaling domain modified by palmitate on the amino terminus and cholesterol on the newly formed carboxy terminus. This fully processed dual lipid modified form of Shh is the predominant signaling molecule in vivo.

occurs in the absence of Shh cholesterol modification. Radiolabeling experiments demonstrate that cholesterol modification of Shh is not required for palmitoylation and that in cell culture Shh lacking cholesterol (ShhN) still incorporates considerable amounts of radiolabeled palmitate (Chen et al. 2004; Buglino and Resh 2008). Additionally, *in vitro*, an artificially constructed N-myristoylated form of Shh also maintains signaling capability and cellular association (Taylor et al. 2001). Dual lipid modified or fully processed Shh is the predominant form of the signaling molecule *in vivo*. Lack of one or both lipids influences Shh signaling, trafficking, and potency (Pepinsky et al. 1998; Chamoun et al. 2001; Taylor et al. 2001; Gallet et al. 2003; Chen et al. 2004; Mann and Beachy 2004; Li et al. 2006).

Until recently all known signaling functions of Hh were mediated by the Shh amino terminus or signaling domain. New studies, however, demonstrate a potential role for the full length unprocessed form of Shh protein as well. Hh responsive cells transfected with full length Shh, containing a point mutation (Shh-U) prohibiting the autocatalytic cleavage reaction, retain the ability to signal. Furthermore, Shh-U colocalizes with the Hh receptor Ptc and has the ability to induce cellular differentiation in chick embryos, albeit significantly diminished compared to the fully processed lipid modified Shh. A larger percentage of Hh-U was found in *Drosophila* embryos, suggesting that there may be a role for Hh-U in short range signaling or autocrine signaling (Hh is thought to act over short distances in the *Drosophila* eye) and not in tissues that require long range Shh

signaling for patterning (Tokhunts et al. 2010). The relevance of Shh-U *in vivo* has yet to be determined.

1.4 Hedgehog Signal Transduction

Hedgehog receptors and its signaling cascade

Several proteins coordinate Hh signal reception. Hh signaling occurs by direct binding of Hh ligand to Ptc (Marigo et al. 1996; Stone et al. 1996; Fuse et al. 1999). Ptc is a twelve transmembrane protein with sequence and structural similarity to related resistance-nodulation division (RND) family of bacterial proton driven pumps. These proton pumps employ a proton gradient to transport lipophilic molecules across the membrane (Paulsen et al. 1996; Ma et al. 2002; Piddock 2006). It is speculated that Ptc may be involved in translocating a small molecule that modulates Smoothened (Smo) activity (Taipale et al. 2002). Ptc also contains a sterol sensing domain (SSD), however, the Shh cholesterol adduct is not needed for Ptc binding, in fact, neither lipid moiety is required for Shh to bind Ptc (Williams et al. 1999). There are two *Ptc* genes, *Ptc1* and *Ptc2* (Motoyama et al. 1998). For the purpose of this thesis, Ptc refers to Ptc1 and is mentioned as either Ptc or Ptc1.

In the absence of Shh ligand, Ptc is concentrated in primary cilia (Huangfu and Anderson 2005; Rohatgi et al. 2007) and acts catalytically to suppress the activity of Smo, a seven pass transmembrane domain (van den Heuvel and Ingham 1996; Taipale et al. 2002). Inactivation of Ptc by Shh binding inhibits its

catalytic activity (Stone et al. 1996; Taipale et al. 2002) and removes Ptc from the primary cilium, which thereby enables Smo to accumulate in ciliary membranes (Rohatgi et al. 2007; Milenkovic et al. 2009). This accumulation is followed by a secondary process converting Smo to an active state (Rohatgi and Scott 2008; Rohatgi et al. 2009) resulting in a transcriptional response through Gli proteins in vertebrates (Reviewed in (Jacob and Briscoe 2003)) (Figure 2).

Due to its structure, Smo has long been thought to be a G-protein coupled receptor (GPCR). Recent studies from *Drosophila* and vertebrate cell culture suggest that Hh signaling may be occurring via the alpha subunit of the G_i family of G-proteins, however Smo can still signal independent of G-proteins (DeCamp et al. 2000; Riobo et al. 2006; Ogden et al. 2008). Thus, the requirement for G-proteins may be context dependent. Furthermore, whether vertebrate Smo signaling requires G-proteins *in vivo* remains to be determined.

Ptc, and additionally Hedgehog interacting protein (Hhip) in vertebrates, negatively regulate Hh signaling and availability by restricting its range of movement through tissue via a negative feed back loop that regulates Smo in the absence of Hh; both are also Shh transcriptional targets (Chen and Struhl 1996; Chuang and McMahon 1999; Goodrich et al. 1999; Jeong and McMahon 2005). In contrast, cell surface proteins cell-adhesion molecule-related down-regulated by oncogenes (CDO), Brother of CDO (BOC), and Growth Arrest Specific 1 (Gas1) are positive regulators of the Hh pathway and directly bind Shh. Either CDO/BOC or Gas1, in addition to Ptc, are required for Shh mediated differentiation and proliferation. These accessory proteins may also form a

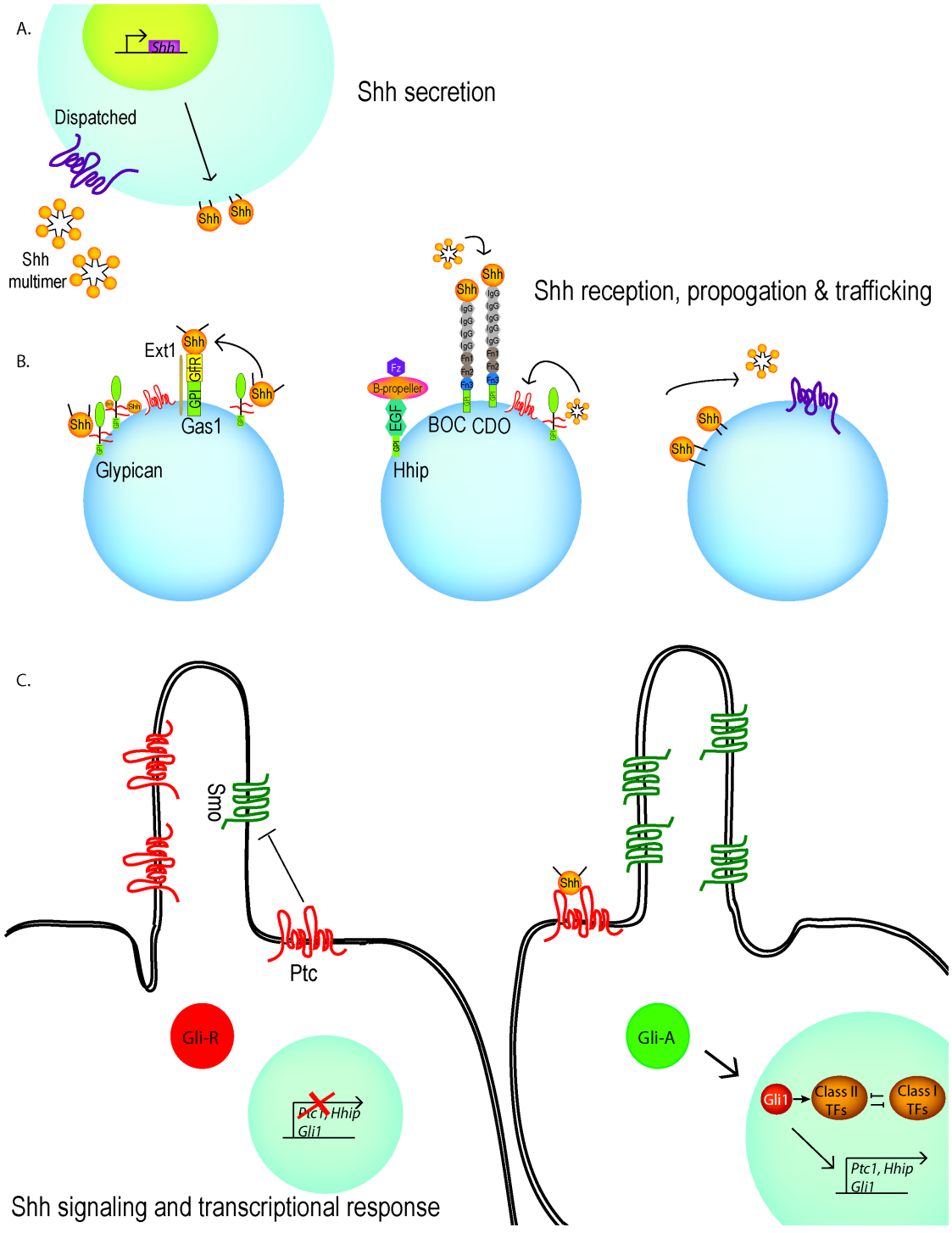

Figure 2. Figure legend on following page.

Figure 2. Vertebrate Sonic hedgehog signaling pathway. Shown is the vertebrate Shh pathway from post translational modification and protein release, to cellular reception and generation of a transcriptional response modulated by a family of Gli transcriptional activators (Gli-A) and repressors (Gli-R). **(A)** Shh is secretion is mediated by Dispatched and is presumed to be secreted as a multimeric complex. **(B)** Shown are receiving cells and the various proteins that are involved in Shh trafficking. **(C)** Shown is the Shh signal transduction pathway, which can be mediated via the primary cilium. In the absence of Shh, Ptc is concentrated in the primary cilium and acts catalytically to suppress Smo. Upon Shh binding to Ptc, Ptc is inactivated and Smo accumulates in the cilium and is activated resulting in a transcriptional response mediated through Gli proteins. See text for details.

complex with Shh and Ptc to initiate signaling, but are not required for Shh to bind Ptc (Tenzen et al. 2006; Yao et al. 2006; Allen et al. 2007; Kavran et al. 2010; Allen et al. 2011; Izzi et al. 2011). Shh binding to Cdo occurs independently of the Shh cholesterol adduct (McLellan et al. 2006; McLellan et al. 2008).

Hedgehog accessory proteins and reception

Additionally, several accessory proteins are implicated in Shh signal regulation. Heparin sulfate proteoglycans (HSPG) are cell surface extracellular matrix molecules containing a core protein with covalently linked glycosaminoglycan chains (Perrimon and Bernfield 2000). Glypicans (GPC), a member of the HSPG protein family, have glycosylphosphatidyl inositol (GPI) anchors tethering them to the cell membrane, and are required for Hh reception and signaling (Lum et al. 2003; Yan and Lin 2009). *Dally like protein* (*Dlp* – *Drosophila* homolog of vertebrate HSPG) is essential for Hh movement and distribution (Han et al. 2004) and genetic evidence indicates that *Dlp* is required at or upstream of *Ptc* for Hh signal response in *Drosophila* embryos (Desbordes and Sanson 2003; Lum et al. 2003; Han et al. 2004). Specific regions on the surface of the Dlp core protein are required for normal responsiveness to Hh signaling, however the Dlp protein core does not directly interact with Hh (Kim et al. 2011).

In vertebrates, there are six GPC encoding genes that act as both positive and negative regulators of the Shh pathway. GPC4 shares the greatest

homology with *Dlp* (Bernfield et al. 1999). GPC4 and GPC6 are positive Hh pathway modulators and rescue Dlp function and Hh response in *Drosophila* cultured cells, whereas GPC 1, 2, 3, and 5 show no effect (Williams et al. 2010). In contrast, GPC3 inhibits Shh signaling by competing with Ptc for Shh and promotes endocytosis and degradation (Capurro et al. 2008; Jiang and Hui 2008). To initiate proliferation, however, Shh interacts with HSPGs via the Cardin-Weintraub motif, which binds heparin. This region though, is not required for Shh to bind Ptc (Rubin et al. 2002; Chan et al. 2009). In addition to signaling, HSPGs also modulate Hh distribution. Shh can be found concentrated in clusters around HSPGs. In a mutated form of HhN that negatively affects clustering, Hh was unable to interact with HSPGs and failed to signal over a long distance, but retained autocrine signaling activity (Vyas et al. 2008). HSPGs may also be involved in Hh transport to target cells (The et al. 1999) or multimerization (Ohlig et al. 2011). Thus, glypicans are involved in trafficking Shh while also positively and negatively modulating signaling.

Sonic hedgehog as a morphogen in graded signaling

Cellular exposure to developmental factors are a heterogeneous function of signal type, signal duration, and cellular location. The Hedgehog family of signaling proteins are morphogens secreted from localized sources such as the zone of polarizing activity (ZPA) in the limb bud, and the notochord and floor plate in the developing spinal cord. Morphogens directly elicit concentration-dependent responses in neighboring cells to influence the patterning of embryonic structures, such as the ventral neural tube (VNT) and limb bud

thereby impacting cellular specialization (Teleman et al. 2001; Harfe 2011). Changing as a function of concentration, Hh signaling influences cells in close proximity to the signal source (short range signaling) as well as those a greater distance away (long range signaling) (Jessell 2000; Teleman et al. 2001).

The concept of a morphogen gradient is best characterized in the VNT and was brought on by studies in the developing spinal cord of chick embryos. Neural plate explants were subjected to varying concentrations of Shh protein. Unique cell fates were induced depending on the concentration of Hh. The dose requirement needed correlates well with the position that domain would occupy in the dorsal to ventral position in the VNT. The threshold concentration of Shh required to induce motor neurons, for example, is higher than that required to define more dorsally located interneurons (Roelink et al. 1994; Roelink et al. 1995; Chiang et al. 1996; Ericson et al. 1996; Ericson et al. 1997; Briscoe et al. 2001) (Figure 3). The activity of Shh ligand is not only based on concentration, but also on duration of signal (Harfe et al. 2004; Dessaud et al. 2007). In chick neural cell experiments, signal duration is proportional to Shh concentration. Over time cells become desensitized to Shh resulting in up-regulation of Ptc; Gli expression decreases as Ptc is upregulated. This leads to a conversion of Shh concentration to a specific period of Gli activity and more ventral target genes are expressed. Neural cells convert different concentrations of Shh into specific periods of signaling (Jeong and McMahon 2005; Stamataki et al. 2005; Dessaud et al. 2007).

Varying combinations of homeodomain transcription factors are induced in

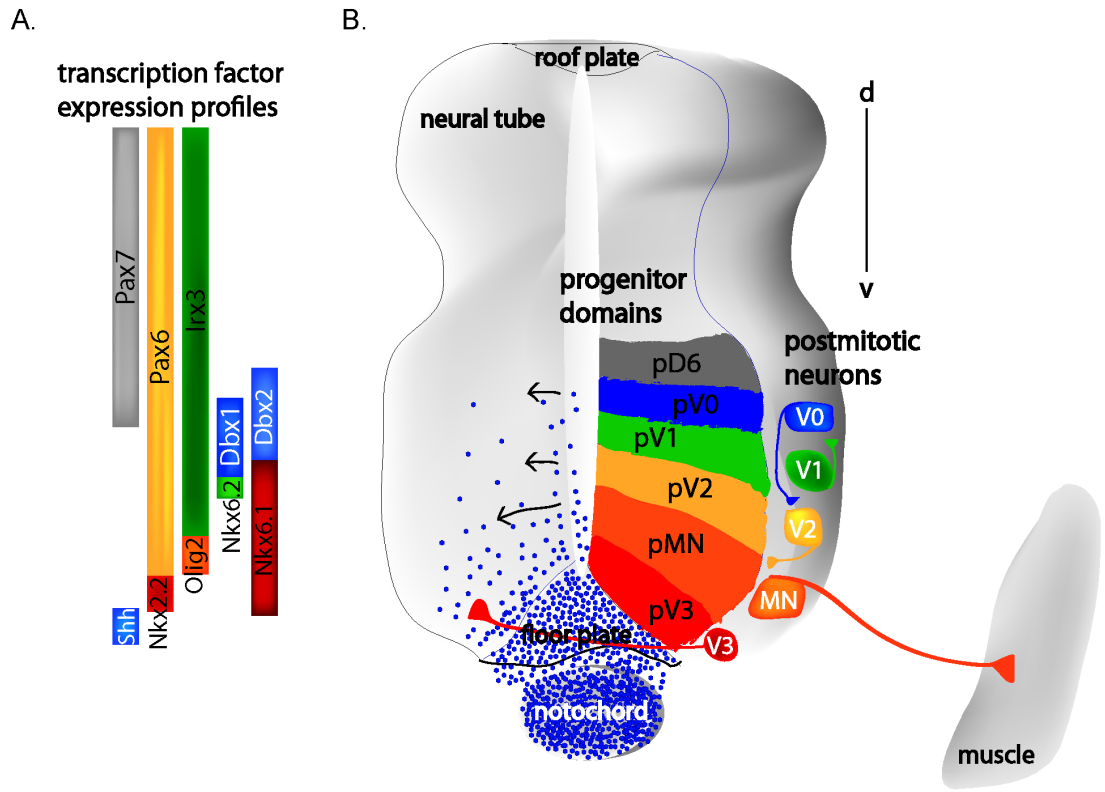

Figure 3. Shh regulated gene expression profiles within progenitor cell domains in the ventral spinal cord. (A) Shown are the expression profiles of transcription factors regulated by graded Shh signaling. **(B)** Along the dorsal-ventral axis of the developing neural tube are six domains of progenitor cells (floor plate, p3, pMN, p2, p1, and p0) which generate different ventral motor and interneurons. This spatial organization is formed by a gradient of Shh protein (blue dots) secreted from the notochord and floor plate. Not shown is the effect of time and duration of Shh protein signal in shaping the morphogen gradient. After neural tube closure, postmitotic cells migrate to various positions within the spinal cord.

response to graded signaling within progenitor cells to yield at least five distinct neuronal subtypes. Homeodomain proteins are divided into two classes on the basis of their patterns of expression and regulation by Shh. Shh represses class I proteins (e.g. PAX6 and PAX7), thus they are expressed in the dorsal half of the neural tube. Conversely, Shh signaling is required for class II protein expression (e.g. Nkx2.2) which is focused in the ventral half of the neural tube (Figure 3). The interaction between these two classes of proteins, regulated by Shh among other signaling molecules, maintains and defines the boundaries of progenitor domains in the neural tube (Briscoe et al. 2000; Ribes and Briscoe 2009).

The distribution and spread of Shh ligand in target tissue is also regulated by extracellular transmembrane proteins such as CDO, BOC, and Gas1 that were described previously as positive regulators of the Shh pathway. The floor plate is reduced in *Cdo-/-* mice and in Gas1-/-; CDO-/- mouse embryos, the floor plate in addition to ventral interneuron 3 and motor neurons are absent. Thus these factors may be involved in enhancing Shh signaling in the VNT (Tenzen et al. 2006; Allen et al. 2007). Furthermore, Ptc negatively regulates Shh signaling and is also transcriptionally upregulated by Shh (Chen and Struhl 1996; Chuang and McMahon 1999; Goodrich et al. 1999). When chick embryos were electroporated with a mutant form of Ptc no longer able to bind Shh, there was a reduction in Shh signaling in the electroporated area and a ventral to dorsal shift in neuronal fate (Briscoe et al. 2001). Additionally, the family of Gli activator and repressor proteins form their own gradients within the neural tube that also

control cellular differentiation (Reviewed in (Ribes and Briscoe 2009)). Thus, there are many regulatory factors that influence differentiation in the VNT.

1.5 Hedgehog Trafficking, Secretion, and Reception

Secretion and release of Hedgehog protein

Shh lipid adducts modulate cellular secretion and reception. Lipid modified Hh is targeted to lipid raft microdomains within the cell, associating the ligand with cell membranes (Rietveld et al. 1999), such that the secreted signaling domain is tightly associated with Hh generating cells. Specialized machinery, namely Dispatched1 (Disp1), has evolved to secrete and release Shh for distribution. Disp1 is structurally similar to Ptc, has a SSD, and is also a member of the RND family of transport proteins. Disp1 mediates secretion of cholesterol modified Shh and also plays a role in long range signaling. In addition, loss of Disp1 leads to Hh accumulation in producing cells; HhN on the other hand does not require Disp1 for cellular release (Burke et al. 1999; Caspary et al. 2002; Kawakami et al. 2002; Ma et al. 2002). Though, Disp1 is not required to generate a Shh response, it thought to be involved in Shh spread and distribution as well as long range signaling (Burke et al. 1999; Ma et al. 2002; Saha and Schaffer 2006; Etheridge et al. 2010). Additionally, in other proteins with SSDs, this sterol sensing domain regulates the stability of these proteins response to cholesterol. It is still unclear whether Disp responds to sterol levels or what the specific roles of the Shh lipid adducts are in cellular release (Chang et al. 2006; Eaton 2008).

Shh multimeric complexes

Hh signal is released as a multivalent particle or multimer (Zeng et al. 2001), and in *Drosophila* these multimers are associated with lipoproteins (Panakova et al. 2005). The role or existence of lipoprotein in vertebrate Shh is, however, unknown (Eaton 2008). Multimerization requires both the palmitoyl and cholesterol lipid adducts and is thought to be the biologically active form of Shh (Zeng et al. 2001; Chen et al. 2004; Goetz et al. 2006). Smaller sized multimers, however, have also been described and need only one lipid adduct to form (Feng et al. 2004). Shh multimers are also thought to be more potent than Shh monomers and may be involved in long range signaling (Zeng et al. 2001; Chen et al. 2004). The multimeric form of Shh, however, has not been observed via rigorous structural analysis (Kavran et al. 2010).

Hedgehog cholesteryl and palmitoyl modifications

Lipid modifications influence the localized release, propagation, and reception of Hh signal over several cell diameters. The mechanisms by which these lipid modifications influence trafficking have been the subject of many, often conflicting, studies. Neither cholesterol nor palmitate is required for Hh binding to Ptc (Williams et al. 1999) or to initiate signaling, but both are needed for proper secretion and spatial distribution of Shh (Chamoun et al. 2001; Lewis et al. 2001; Chen et al. 2004; Li et al. 2006).

The cholesterol adduct appears to function as a lipid anchor. In cultured cells, cholesterol modified Shh is membrane associated, while those lacking the cholesteryl moiety (ShhN) are more freely secreted into the culture medium (Porter et al. 1995). Both *Drosophila* and murine Hh partition into detergent insoluble glycolipid complexes (called DIGs, lipid microdomains, or lipid rafts) (Simons and Vaz 2004), so the cholesterol adduct appears to influence the subcellular localization of Hh proteins and may tether Hh to the site of production while restricting its spread across the field of neighboring cells. Similarly, localized expression of Hh lacking only cholesterol broadens tissue distribution and range of signaling (Porter et al. 1996a; Burke et al. 1999; Li et al. 2006; Huang et al. 2007) as Shh is secreted farther and results in ectopic pathway activation (Li et al. 2006; Guerrero and Chiang 2007). In fact the cholesterol moiety enhances local concentration while anchoring Hh to the cell membrane (Saha and Schaffer 2006). Interpretation of these data have been complicated by conflicting results stating that cholesterol is required for long range signaling (Lewis et al. 2001). This disparity may be due to the different Hh expression levels of the mutant forms of ShhN used in the studies (Varjosalo and Taipale 2008).

The palmitoyl adduct also imparts an additive membrane anchoring effect (Feng et al. 2004) and the hydrophobic nature of the amino-terminal lipid enhances Shh potency (Taylor et al. 2001). Palmitoylation also influences proteolytic removal of Shh amino terminal residues allowing multimeric Shh to bind Ptc (Ohlig et al. 2011). In cell-based assays removal of either of the lipid

adducts abolishes (Chen et al. 2004) or greatly reduces signaling (Williams et al. 1999; Taylor et al. 2001). In *Drosophila*, Hh protein that lacks a palmitoyl adduct (ShhC25S) fails to signal (Chamoun et al. 2001) and ventral neural tube patterning is disrupted in ShhC25S and Skinny Hedgehog $(Skn)^{-/-}$ mice (Chen et al. 2004). Localized expression of Hh lacking only the palmitoyl moiety decreases long range signaling (Chamoun et al. 2001; Chen et al. 2004) while the opposite is true in the absence of the cholesterol adduct (Porter et al. 1996a; Burke et al. 1999; Li et al. 2006; Huang et al. 2007).

As discussed, Hh protein is post-translationally modified by two lipids, cholesterol and palmitate. In fact, it is the only known protein to be covalently modified by cholesterol (Mann and Beachy 2004). Curiously, Hh is involved in long range signaling, and it is not spatially restricted by anchoring cell membranes (Porter et al. 1996a; Porter et al. 1996b; Chamoun et al. 2001). A better understanding of this dichotomy between Hh biochemistry and morphogen activity requires an in depth look at the roles of both lipid adducts, their biological relevance, and their influences on Hh trafficking and signaling.

CHAPTER II

LIPID MODIFICATIONS OF SONIC HEDGEHOG LIGAND DICTATE CELLULAR RECEPTION AND SIGNAL RESPONSE

2.1 Introduction

The Hedgehog (Hh) family of signaling proteins are secreted from localized sources and elicit concentration-dependent cellular responses to specify tissue pattern during development and homeostasis (Jessell 2000; Jiang and Hui 2008). Proper Hh ligand distribution and reception are essential for the full repertoire of graded cellular responses; human birth defects and malignancies are attributed to the misregulation of Hh signaling (Hahn et al. 1996; Johnson et al. 1996; Muenke and Beachy 2000; Cohen 2002). A unique biochemical property of the secreted Hh signaling domain is covalent modification by cholesterol and palmitate. Following signal sequence cleavage, cholesterol serves as a cofactor in an autocatalytic intramolecular cleavage reaction and remains covalently bound to the carboxy-terminal Gly residue of the newly formed signaling domain (Lee et al. 1994; Porter et al. 1995; Porter et al. 1996a; Porter et al. 1996b; Hall et al. 1997). The second hydrophobic modification is catalyzed by the acyl-transferase Skinny hedgehog, which results in the amide linkage of palmitate to the amino-terminal Cys residue of the signaling domain (Pepinsky et al. 1998; Chamoun et al. 2001; Lee et al. 2001).

Hydrophobic modification confers membrane affinity such that the secreted signaling domain is tightly associated with Hh-generating cells (Lee et

al. 1994; Porter et al. 1996a; Feng et al. 2004). The cellular release of cholesterol modified Hh ligand is regulated by the transmembrane protein Dispatched (Burke et al. 1999; Ma et al. 2002; Saha and Schaffer 2006). Thus, one biological function of the lipid moieties is to restrict the spatial deployment of Hh morphogens. Hh is secreted as multivalent particles (Zeng et al. 2001; Panakova et al. 2005) whose formation requires the presence of both lipid additions to the signaling domain (Zeng et al. 2001; Chen et al. 2004; Goetz et al. 2006). Thus, it has been proposed that both lipid moieties are required for long range signaling (Lewis et al. 2001; Zeng et al. 2001; Chen et al. 2004; Goetz et al. 2006). Conspicuously, however, lipid modification is not a requisite for high-affinity binding of Hh ligand to Patched1 (Ptc1) and other receptor complex proteins (Fuse et al. 1999; Williams et al. 1999; Taylor et al. 2001; McLellan et al. 2008; Zheng et al. 2010).

A clear understanding of how lipid modification influences signal reception has been hampered by conflicting results. Notably, the earliest *in vitro* signaling assays utilized purified Sonic hedgehog (Shh) lacking both cholesterol and palmitate adducts (Hall et al. 1995) to elicit the full repertoire of graded signaling responses in explanted chick neural plate ectoderm (Roelink et al. 1995; Ericson et al. 1997). Conversely, in cell-based assays, removal of either of the lipid adducts abolished (Chen et al. 2004) or greatly diminished signaling (Williams et al. 1999; Taylor et al. 2001). In *Drosophila* and mouse embryos, localized expression of Hh lacking only the palmitoyl moiety decreased long range signaling (Chamoun et al. 2001; Chen et al. 2004) whereas the localized

expression of Hh lacking only cholesterol broadened tissue distribution and range of signaling (Porter et al. 1996a; Burke et al. 1999; Li et al. 2006; Huang et al. 2007).

A major constraint of *in vivo* model systems to elucidate the influences of the lipid adducts on Hh signaling is the inability to distinguish an effect on tissue distribution, and thus local concentration, from an effect on signal potency. Another limitation centers on tissue-specific differences in sensitivity to Hh signaling (Huang et al. 2007). With regard to cell-based assays, we report a profound loss of signal reception sensitivity in cloned and high-passage cell lines used in prior studies (Cooper et al. 2003; Chen et al. 2004; Goetz et al. 2006). To circumvent some of these limitations, we used early-passage NIH3T3 fibroblasts and assays with enhanced sensitivity to integrate quantitative measurements of Shh concentration, cellular localization, and potency to evaluate the influences of lipid modification on Shh signaling. We demonstrate that the lipid adducts serve critical functions in cellular reception, governance of cell concentration, and signal potency of Shh ligand.

2.2 Materials and Methods

Preparation of complementary DNA (cDNA) constructs

The pRK5-Shh construct was used to express full length mouse Shh. The pRK5-ShhN construct carries an open reading frame truncated after Gly-198 and was used to express Shh lacking cholesterol (Roelink et al. 1995). To eliminate palmitoylation, PCR site-specific mutagenesis by overlap extension (Sambrook and Russell 2001) was performed with pRK5-Shh as cDNA template (Platinum® Blue PCR SuperMix, Invitrogen) with the following primers: 1) 5' -CCC GGG CTG GCC GCT GGG CCC GGC AG- 3' (mutates Cys-25 to Ala-25; ShhC25A), 2) 5'-CCC GGG CTG GCC AGT GGG CCC GGC AG- 3' (mutates Cys-25 to Ser-25; ShhC25S) and 3) 5' -TGT GCC CCG GGC TGG CCG GGT TTG GAA AGA GGC GGC ACC C- 3' (deletes Cys-25 through Arg-29; Shh(n-5)). To eliminate both cholesterol and palmitate modification, the primers listed above were used in conjunction with 5'-GCG GCC AAA TCC GGC GGC TAG GTC GAC TGC-3' to create a stop codon after Gly-198. All constructs were sequenced for verification (Genepass Inc.).

Cell culture and transfection

NIH3T3 mouse embryonic fibroblasts cultured in 6-well plates were co-transfected (FuGene® 6, Roche) with Shh constructs (Shh, ShhC25A, ShhC25S, ShhN, or ShhNC25A) over a range of 0.06 ng to 1000 ng in two fold increments, pEGFP-C1, a Gli-reporter (pGL3-8xGli-luciferase) (Sasaki et al. 1997; Cooper et

al. 2003), pCMV-LacZ, (a transfection control with a 9:1 ratio of Gli-reporter:LacZ), and variable amounts of empty vector (pcDNA) to normalize the total DNA quantity in each well. Shh constructs were eliminated from the co-transfection mix for controls. Twelve hours later, cells were changed to low-serum medium (0.5% calf serum) and cultured for an additional forty hours (Taipale et al. 2000; Taipale et al. 2002). Time course of reporter activity in signaling assays is shown (Figure 4). Cells were then processed by flow cytometry, ELISA, or used chemiluminescent signaling assays. Cells from each well (9.6 cm^2) were harvested and allocated for flow cytometry, Guava EasyCyte and ELISA. All experiments were conducted in parallel with identical culture conditions. The conditioned medium from each well was also collected for ELISA.

In other studies, NIH3T3 cells were transfected with Gli-reporter (pGL3-8xGli-luciferase) and pCMV-LacZ (in a 9:1 ratio) changed to low-serum medium with exogenous recombinant Shh protein, incubated at 37˚C for 42 hours, and then analyzed by ELISA or chemiluminescent signaling assays. For recombinant Shh protein, HEK293T cells were transfected with a Shh expression construct (Shh, ShhC25A, ShhC25S, ShhN, ShhNC25A, or ShhNC25S), and changed to low serum medium. Thirty-six hours later, conditioned medium was filtered and concentrated (Amicon® Ultra-15 centrifugation filter units; Millipore). For control assays, NIH3T3 cells were transfected as above and exposed to conditioned medium from untransfected HEK293T cells.

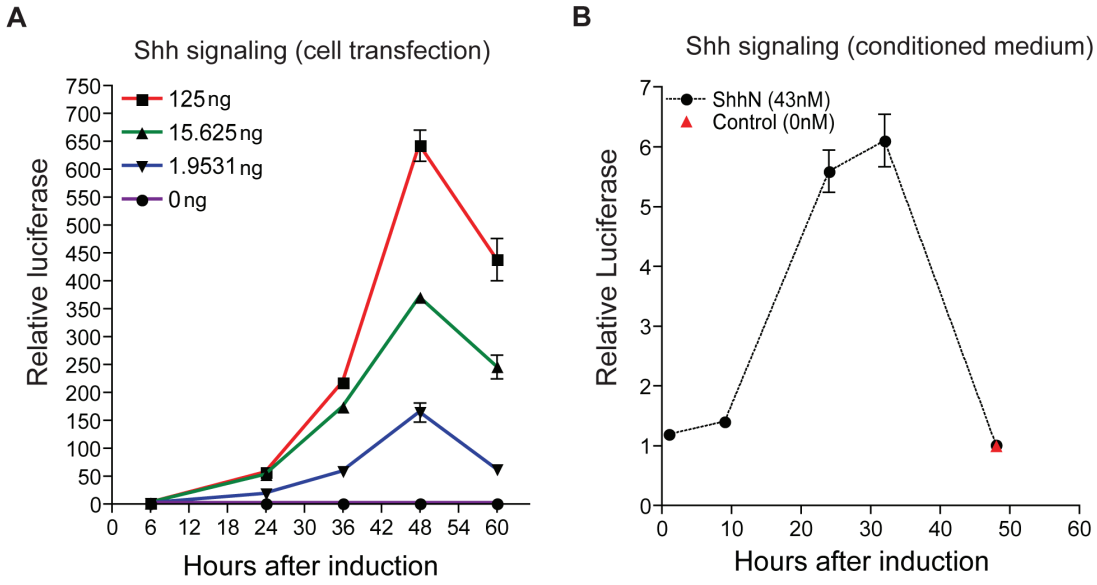

Figure 4. Time course of reporter activity in Shh signaling assays. (A) To determine the linear phase of reporter activity (shown to be between 24 and 48 hours), NIH3T3 fibroblasts were co-transfected with expression plasmids for recombinant Shh (125 ng, 15.63 ng, 1.95 ng, and 0 ng), EGFP, Gli-reporter and LacZ, changed to low serum medium and assayed at varying time points. **(B)** For signaling assays with conditioned medium, NIH3T3 cells were co-transfected with Gli-reporter and LacZ, changed to low serum medium containing ShhN protein, and then assayed at the indicated time points. Experiments were performed in replicates of three (± s.e.m.).

Flow cytometry

NIH3T3 cells were dissociated with trypsin (Invitrogen) and then washed at 4 °C with FACS buffer (phosphate-buffered saline, 2% fetal bovine serum, and 0.05% sodium azide). Anti-Shh antibody (5E1, Developmental Studies Hybridoma Bank) was fluorescently conjugated as directed by the manufacturer (Zenon® Alexa Fluor-647; Invitrogen) and cells were then stained with 5E1-Alexa Fluor-647 anti-Shh antibody (8 mg/mL diluted at 1:10,000), washed with FACS buffer and fixed in 2% paraformaldehyde. To measure total cellular expression levels, cells were permeabilized and fixed (BD Cytofix/Cytoperm) prior to staining. To measure internal expression, cells were first incubated with a saturating level of unlabeled 5E1 antibody (1:50; Figure 5) for 1 hour, washed with FACS buffer, and then fixed, permeabilized and stained with fluorescent conjugated 5E1 antibody. Samples were run on a 5-laser BD LSRII system (BD Biosciences) and at least 50,000 viable cells were analyzed per sample. Non-viable cells were excluded from analysis based on forward and side scatter profiles as well as 7-aminoactinomycin D (Invitrogen) staining. Data were acquired using FACSDiva (BD Biosciences) and analyzed using FloJo (Treestar, Inc). Both EGFP (excited at 488 nm Argon Laser, and detected with a 505LP mirror and a 530/30 bandpass filter) and Alexa 647 (excited at 633 nm He-Ne Laser, detected with no LP mirror and a 670/14 bandpass filter) signals were analyzed simultaneously in all cells. Mean fluorescence index (MFI) was calculated by multiplying the percentage of positively stained cells by the mean fluorescence intensity (cells with fluorescence intensity greater than 99% of

A.

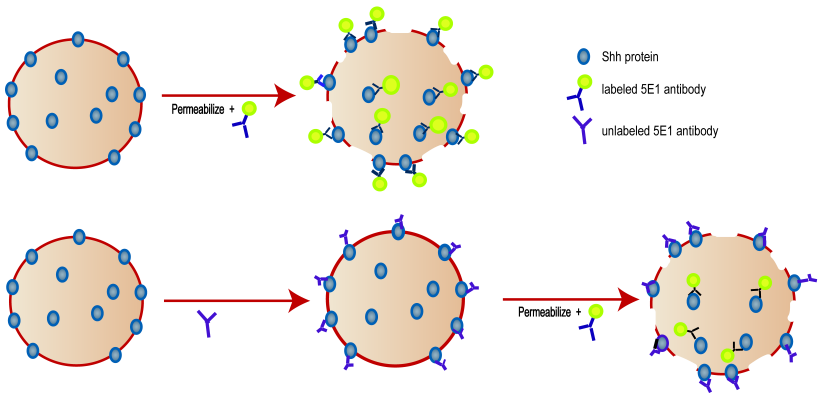

B.

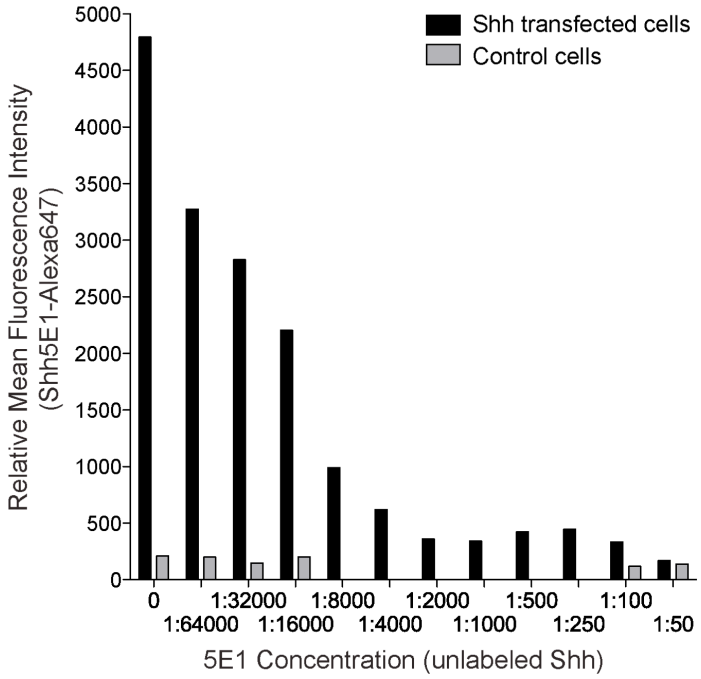

Figure 5. Determination of concentration of unlabeled 5E1 antibody required to saturate the cell surface prior to staining with labeled 5E1 antibody. (A) Total Shh cellular expression: Schematic showing Shh transfected cells permeabilized and then stained with labeled 5E1 antibody. Internal Shh expression: Schematic illustrating Shh transfected cells first incubated with unlabeled 5E1 for cell surface saturation and then permeabilized with labeled 5E1. **(B)** NIH3T3 cells were transfected with Shh cDNA (500 ng) and EGFP (1100 ng), while control cells were transfected with EGFP (1100 ng) alone. The cells were then incubated with varying concentrations of unlabeled 5E1 antibody, fixed, permeabilized, and stained with 5E1 antibody conjugated to Alexa 647 (1:10000). Saturation, or capping, of surface staining was observed with unlabeled 5E1 antibody over a range of dilutions from 1:50 to 1:2000.

control transfected cells (Figure 6 and 7)). For cell counts, NIH3T3 cells were suspended in phosphate-buffered saline (PBS) and analyzed with the Guava EasyCyte as directed by the manufacturer (Guava® ViaCount® Reagent; Guava Technologies).

Enzyme-linked immunosorbent assay (ELISA)

Culture medium was collected and then NIH3T3 cells were washed three times with PBS and lysed in RIPA Buffer (50 mM Tris-HCl at pH 7.4, 150 mM NaCl, 2 mM EDTA, 0.1% SDS, 1% NP-40) with protease inhibitors (Complete Mini, Roche Applied Science) on a rotator for 4 hours at 4 °C. Recombinant Shh protein concentration was measured in the cell lysate and culture medium as instructed by the manufacturer (DuoSet® ELISA Development System, R&D Systems). ELISA was performed on a series of eight, two-fold dilutions with a starting concentration of 1:1 (reagent diluent:sample). The colorimetric optical density was measured at 450 nm (FLUOstar Omega, BMG Labtech). An internal positive control (purified Shh protein, 0.063 nM) was included in each assay for normalization. Culture medium and cell lysate from untransfected NIH3T3 cells were used as negative controls.

Shh signaling assays

Chemiluminescence (Dual-Light® Luciferase and ß-Galactosidase Reporter Gene Assay System) was measured in lysed (Passive Lysis Buffer; Promega) NIH3T3 cells as directed by the manufacturer (FLUOstar Omega, BMG Labtech).

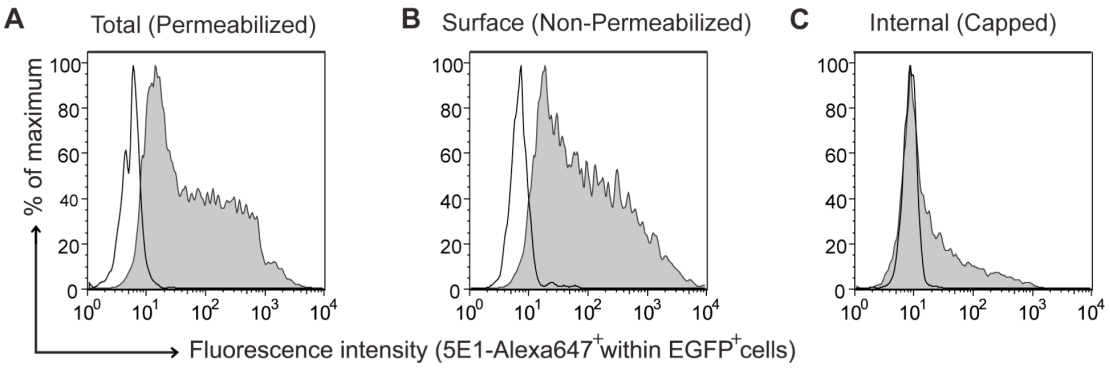

Figure 6. Representative histograms of total, surface, and internal cell staining for Shh. Shown are histograms for the fluorescent intensity of total **(A)**, surface **(B)**, and internal **(C)** cell staining for Shh within viable EGFP-positive cells (filled histogram) relative to control cells (unfilled histogram).

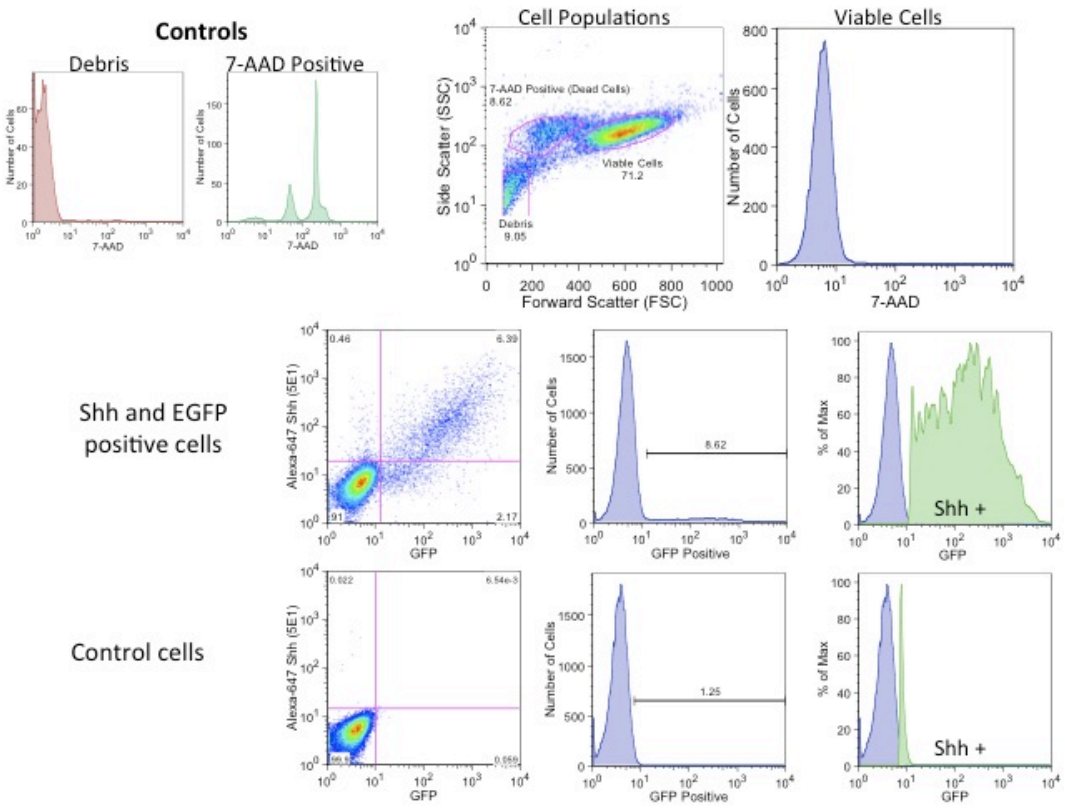

Figure 7. Flow cytometry gating schematic. NIH3T3 cells were co-transfected with recombinant Shh and EGFP. Non-viable cells and debris were excluded from analysis based on forward (FSC) and side scatter (SSC) properties and by positive staining for 7-AAD (7-aminoactinomycin D), a DNA intercalating agent that permeabilizes dead cells. Shown is an example of how Shh expression was determined within EGFP positive cells. Mock transfected cells were used as controls.

Statistical analysis and data manipulation

The half-maximal excitatory concentrations (EC_{50}) were determined by obtaining the non-linear regression (plotted with a 95% confidence interval) of transformed (X=Log(X)) and normalized (highest value set at 100) data. Significance was determined using one-way analysis of variance and a Bonferroni post-test with 99% confidence intervals. All statistical analyses were performed using GraphPad Prism. To determine the cell-associated concentrations of recombinant Shh protein in transfected cells, the total amount of protein measured in the lysate by ELISA was divided by the number of transfected cells ($EGFP^+$) for that well.

Column fractionation, analysis, and sample preparation

Conditioned media (DMEM with N2 supplement; Invitrogen) from recombinant ShhN and ShhNC25S transfected and control (untransfected) HEK293T cells were collected, filtered, and then loaded (1 mL loop) on a 15PHE Tricorn 5/100 column (GE Healthcare Life Sciences) equilibrated in buffer (3.9 M ammonium sulfate, 50 mM Tris pH 8). Prior to loading, samples were brought up to a final concentration of 1.5 M ammonium sulfate using a 3.9 M saturated ammonium sulfate in ddH_2O stock. Bound proteins were eluted after 12 mL wash in equilibration buffer by a 70 mL linear salt gradient beginning with 100% equilibration buffer at fraction 7 to 100% elution buffer (50 mM Tris pH 8) ending at fraction 42. HPLC was performed at 4 °C using the Amersham Biosciences ÄKTA Purifier P-900 (GE Healthcare Life Sciences). Fractions were collected in 2

mL increments and analyzed by ELISA or by chemiluminescence signaling assays.

Conditioned medium (DMEM with N2 supplementation; Invitrogen) from recombinant Shh (Shh, ShhC25A, ShhC25S, ShhN, ShhNC25A, or ShhNC25S) transfected and untransfected control HEK293T cells were collected, filtered, and analyzed by HPLC (High Pressure Performance Liquid Chromatography) using the Amersham Biosciences ÄKTA Purifier P-900 (GE Healthcare Life Sciences). Conditioned medium (400 µL) was fractionated using a Superose 6 10/300 GL column (GE Healthcare Life Sciences) equilibrated and ran using PBS with 0.0001% NP-40. Some experiments described were performed using Superose 12 10/300 GL and varying amounts of PBS with NP-40 (0.1% NP-40 – 0.0001% NP-40). These details are specified in the figure legends. Gel filtration HPLC was performed at 4 °C and 0.5 mL fractions were collected. The column void volume is 7.5 mL (fraction 8), and elution volumes of gel filtration standards are 12.7 mL (fraction 13) for thyroglobulin (669 kDa), 14.5 mL (fraction 14.5) for apoferritin (443 kDa), 16.2 mL (fraction 16.5) for alcohol dehydrogenase (150 kDa), and 18.4 mL (fraction 18.5) for carbonic anhydrase (29 kDa). Elution fractions were analyzed by ELISA as described above and confirmed by western blot analysis (data not shown). Conditioned medium from HEK293T cells was concentrated (Amicon® Ultra-15 centrifugation filter; Millipore) and fractionated using a Superose 12 10/300 GL column (GE Healthcare Life Sciences) equilibrated PBS with 0.01% NP-40. The 0.5 mL elution fractions containing Shh multimer (> 29 kDa) and Shh monomer (< 29 kDa) were pooled, dialyzed (3,500 MW, Slide-A-

Lyzer Dialysis Cassette; Thermo Scientific) in DMEM and then used in chemiluminescence based Shh signaling assays.

2.3 Results

Either lipid adduct is sufficient for cellular association of Shh ligand.

The lipid adducts, cholesterol and palmitate, tightly associate Shh ligand with Hh-generating cells (Lee et al. 1994; Porter et al. 1995; Pepinsky et al. 1998; Feng et al. 2004). To quantify the contribution of each lipid modification to cellular association, NIH3T3 fibroblasts were co-transfected with expression vectors for recombinant Shh (ranging from 0.06 ng to 1000 ng in two-fold increments) and EGFP, and the concentrations of recombinant Shh protein in culture media and cell lysates were measured by ELISA (Figure 8). All the constructs conferred similar dose-dependent total expression levels of recombinant forms of Shh protein (Figure 9A). The proportions of cell-associated and secreted Shh, however, were significantly altered by lipid modification. Whereas only 89.7% of lipid-modified Shh was cell associated, virtually all (≥ 99.5%) was released into the culture medium when both lipid modifications were removed (ShhNC25A and ShhNC25S), indicating a strict requirement of lipid modification for cellular association (Figure 9B). Removal of the palmitoyl adduct alone decreased the cellular association of recombinant Shh (76.7% of ShhC25A and 56.3% of ShhC25S; Figure 9B), and the enhanced association of ShhC25A compared to ShhC25S is consistent with the greater hydrophobicity of alanine compared to serine (Taylor et al. 2001). Removal of the cholesteryl adduct resulted in the retention of 36.5% ShhN (Figure 9B), suggesting a greater contribution of cholesterol to cellular association. The efficiency of ShhN palmitoylation,

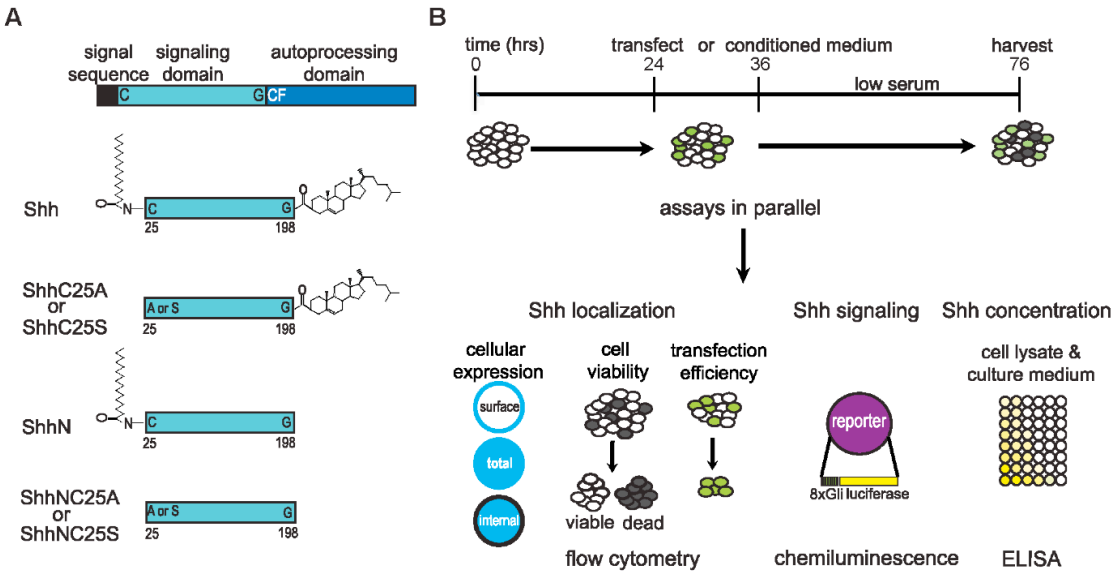

Figure 8. Schematics of experimentation. **(A)** Shh ligand lipidated with palmitate and cholesterol was generated from a full-length Shh open reading frame. Point mutation of the amino-terminal C25 to either an A or S was introduced to eliminate palmitoylation (ShhC25A, ShhC25S, ShhNC25A and ShhNC25S). Introduction of a stop codon after G198 eliminates cholesterol modification (ShhN, ShhNC25A, and ShhNC25S). **(B)** Assays of recombinant Shh protein concentration, cellular localization, and signaling were performed on transfected NIH3T3 fibroblasts harvested from the same or parallel wells. ELISA measurements of Shh protein concentration, flow cytometric analysis of cell expression, and chemiluminescence signaling assays in NIH3T3 fibroblasts co-transfected with recombinant Shh, EGFP, Gli-reporter, and LacZ were integrated to determine the contributions of each lipid adduct on Shh secretion, cellular localization, and signaling potency

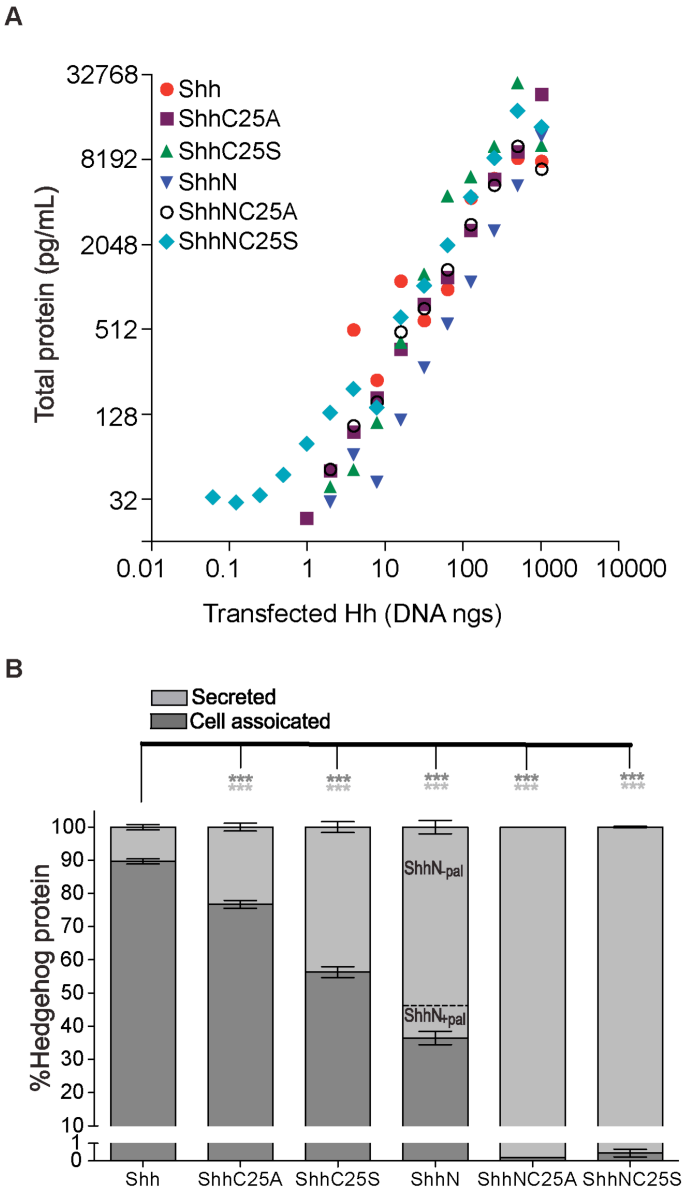

Figure 9. Figure legend on following page.

Figure 9. Shh lipid modifications enhance cellular association. **(A)** Each of the constructs conferred dose dependent and similar expression levels of recombinant Shh protein. Shown are the sums of protein measurements in cell lysate and culture medium from NIH3T3 cells transfected with a range of cDNA for Shh, ShhC25S, ShhN, and ShhNC25S. **(B)** Precise quantification of recombinant Shh protein concentrations in either the cell lysate or culture medium revealed both cholesterol and palmitate modifications confer cellular association. Shown are the averages of Shh protein measurements from cells transfected with cDNA (62.5 ng to 500 ng in two fold increments). With both lipid adducts, 89.7% of Shh was recovered in the lysate and 10.3% was secreted in the culture medium. Less protein was measured in lysates from cells expressing Shh without a palmitate adduct, (76% for ShhC25A and 56.3% for ShhC25S). Examination of the culture medium from cells transfected with ShhN by HPLC (Figure S1) revealed the presence of two species of protein, one that was palmitoylated ($ShhN_{+pal}$) and one that was not ($ShhN_{-pal}$). Approximately 13% of secreted ShhN was palmitoylated ($ShhN_{+pal}$). The portion of cell-associated ShhN (36.5%) represents the $ShhN_{+pal}$ species because in the absence of either lipid moiety, less than 0.5% of ShhNC25A and ShhNC25S protein was recovered from cell lysate. Protein measurements were performed in replicates of four (± s.e.m.) *** $p<0.001$ compared to Shh-transfected cells.

however, can be reduced *in vitro* expression systems (Pepinsky et al. 1998). Consistent with this observation, we determined that in our transfection system approximately 13% of secreted recombinant ShhN was palmitoylated ($ShhN_{+pal}$), while the remaining secreted protein lacked both cholesteryl and palmitoyl adducts ($ShhN_{-pal}$; Figure 10). Thirty-six percent of recombinant ShhN protein was measured in cell lysates, and appears to represent palmitoylated protein ($ShhN_{+pal}$) as less than 0.5% of recombinant Shh protein lacking both lipid modifications (ShhNC25A and ShhNC25S) was cell associated (Figure 9B). Therefore, in transfected NIH3T3 fibroblasts, approximately 81% of $ShhN_{+pal}$, was cell associated and 19% was secreted. These data demonstrate that either lipid modification is sufficient to confer cell association, however, ligand quantification by ELISA demonstrates that the palmitoyl adduct provides a greater contribution than previously recognized by Western blotting (Feng et al. 2004).

Cholesterol modification is required for cell surface retention and palmitate augments ligand internalization.

The contribution of each lipid adduct to cellular association was corroborated by flow cytometric analyses with the anti-ShhN monoclonal antibody 5E1 (Ericson et al. 1996). The 5E1 antibody blocks Hh signaling, and although 5E1 does not recognize Shh well by Western blotting (Fuse et al. 1999; Abe et al. 2008), excellent reactivity (low nanomolar) to the native conformation of Shh has been measured by FACS, ELISA, and signaling competition assays (Ericson et al. 1996; Pepinsky et al. 2000; Taylor et al. 2001; Bosanac et al.

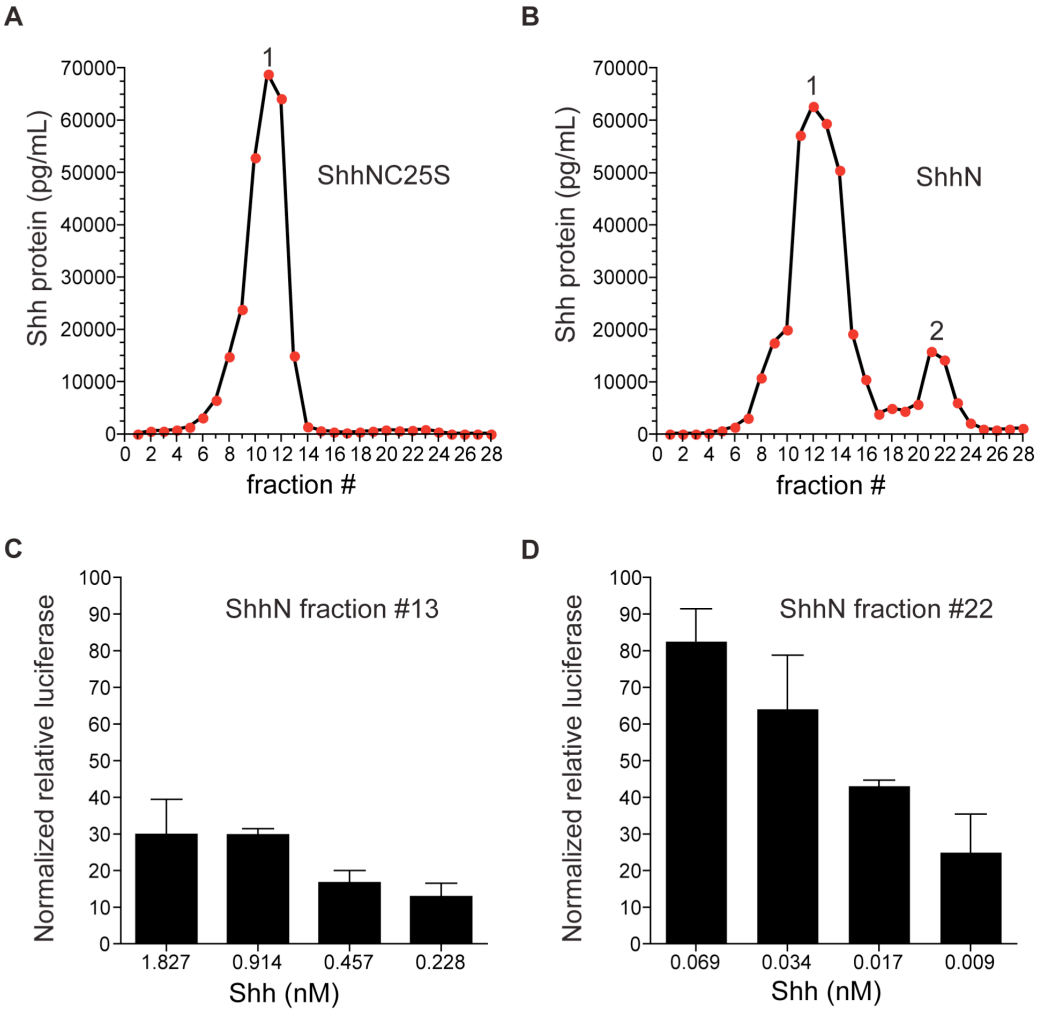

Figure 10. Two distinct species of recombinant protein in ShhN conditioned medium. (A–B) ShhNC25S and ShhN conditioned media were subjected to hydrophobic interaction chromatography and collected fractions were examined by ELISA. A single peak of ShhNC25S protein was measured in early elution fractions **(A)**. Two peaks of protein were measured for ShhN conditioned medium, one that corresponded to Shh protein devoid of lipid modifications (ShhNC25S), and a second in later elution fractions indicative of greater hydrophobicity. **(C–D)** ShhN protein in fractions 13 and 22 was quantified by ELISA and assayed for signaling in NIH3T3 fibroblasts transfected with Gli-reporter and LacZ (± s.e.m.).

2009; Maun et al. 2010). Notably, 5E1 binds a surface domain of Shh formed by non-continuous residues in the Shh linear sequence that is maintained in the absence of either cholesterol or palmitate modification (Pepinsky et al. 2000; Bosanac et al. 2009; Maun et al. 2010). Staining with Alexa 647-labeled 5E1 antibody was performed to detect recombinant Shh protein expression in transfected cells (GFP-positive) and neighboring cells (GFP-negative) (Figure 7). Total cellular expression was measured in permeabilized cells and surface expression was measured in non-permeabilized cells. To detect internal expression levels of recombinant Shh protein, non-permeabilized cells were first incubated with saturating levels of unlabelled 5E1 antibody, permeabilized, and stained with Alexa 647-labeled 5E1 antibody (Figure 5).

Quantitative flow cytometric analysis of Shh staining within permeabilized GFP-positive cells revealed that both lipid adducts are required to confer the highest degree of cell association (compare Figure 11D to 11P). Correspondingly, we observed a decrement in the percentage of GFP-positive cells that expressed ShhC25A (Figure 11G), ShhC25S (Figure 11J), and ShhN (Figure 11M). These findings were reiterated by examining total cell expression levels over a range of recombinant Shh expression in GFP-positive cells (Figure 12A), and are consistent with an interpretation of the ELISA studies that either lipid moiety can confer cell association. Yet, distinct contributions of the palmitoyl and cholesteryl adducts to steady state cell distribution were revealed. Surface expression was retained in the absence of the palmitoyl adduct (ShhC25A and ShhC25S; Figures 11H, 11K, 11T and 11B). Without the cholesteryl adduct, only

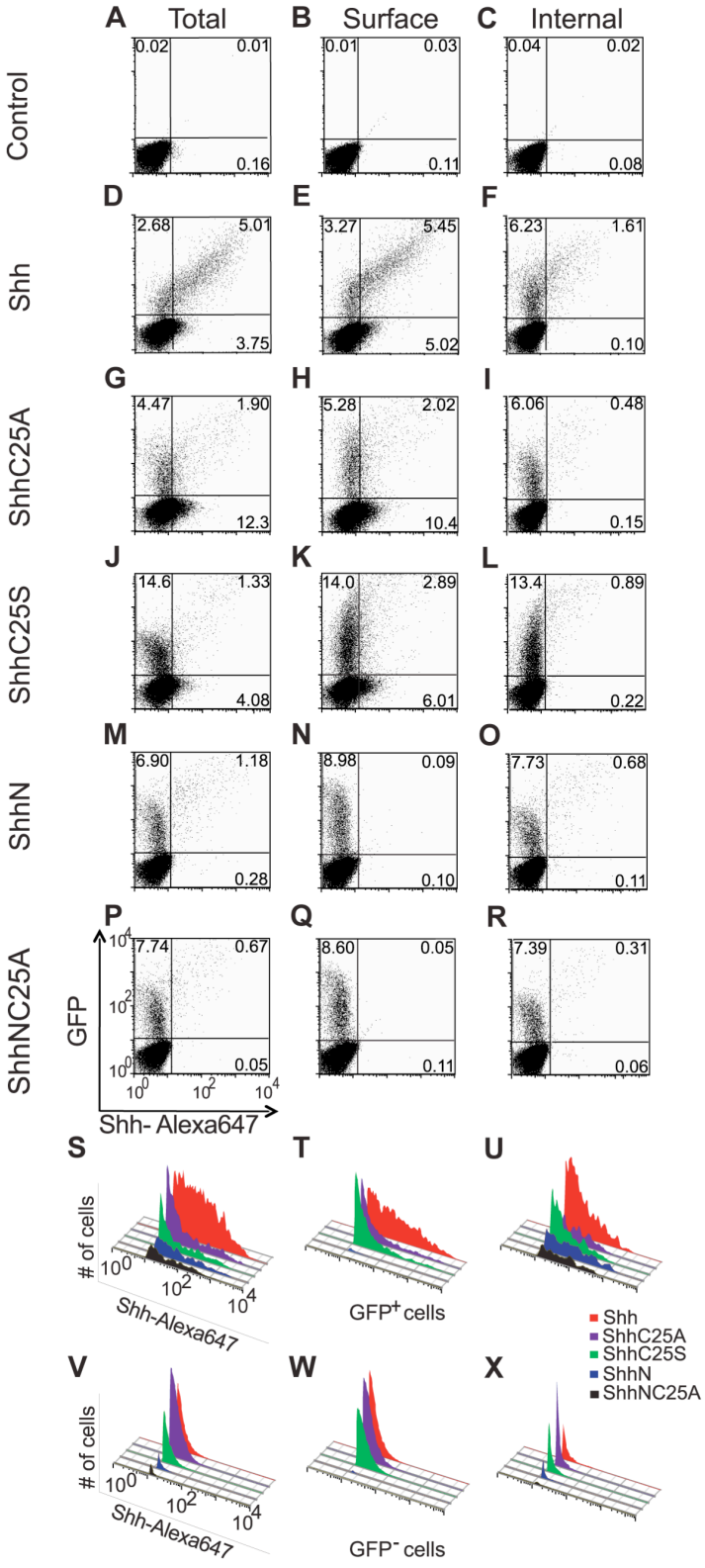

Figure 11. Figure legend on following page.

Figure 11. Cholesterol is required for expression of Shh on the cell surface. Shown are flow cytometric data from NIH3T3 fibroblasts co-transfected with recombinant Shh variants (0.125 ng) and EGFP (1000 ng), and stained with 5E1-Alexa 647 conjugated antibody. Total cell staining was measured in permeabilized cells and surface staining was measured in non-permeabilized cells. Internal staining was measured in cells that were pretreated with a saturating level of unlabeled 5E1 antibody prior to permeabilization and staining with 5E1-Alexa 647. Scatter plots **(A–R)** and histograms **(S–X)** of 5E1-Alexa 647 staining in transfected (GFP-positive) and untransfected (GFP-negative) cells revealed that cholesteryl modification is required for surface expression **(compare E, H & K to N & Q and T to W)**. In Shh transfected cells (GFP^+/5E1-Alexa 647^+) and untransfected cells (GFP^-/5E1-Alexa 647^+), the highest ligand staining levels are measured with fully lipidated Shh **(D*)***. Removal of either lipid moiety results in decreased cellular retention **(G, J, M, P)**. Shh surface expression **(E)** is reduced in the absence of palmitate **(H, K)** and eradicated by the removal of cholesterol **(N, Q)**. Internal expression is also diminished in the absence of either lipid moiety **(F, I, L, O, R)**. Histograms of the number of 5E1-Alexa 647-positive cells within GFP-positive or GFP-negative cells reiterate the above findings **(S-X)**. Experiments were done in replicates of two or more and representative images are shown.

2.9% of total Shh was available on the cell surface while the removal of both lipid adducts entirely eliminated surface expression (Figure 12D). Further, the percentage of cell-associated ligand localized to the surface was not significantly altered by removal of the palmitate (Figure 12D), indicating that the cholesteryl adduct alone is sufficient for cell surface expression and the palmitoyl adduct alone strongly enhances internal cellular localization (Figure 13). Supporting a requirement of cholesterol for localization to the plasma membrane, its removal (ShhN and ShhNC25A) virtually abolished surface staining (Figures 11N, 11Q, 11T, 12B and 12D). Additionally, the highest internal levels of recombinant Shh were measured within ShhN-transfected cells (Figure 12C). In conjunction with the ELISA data revealing that the $ShhN_{+pal}$ species is cell associated, these data indicate that in the absence of a cholesterol tether to the cell surface the palmitoyl adduct strongly enhances ligand internalization (Figure 13, note that 78.6% of $ShhN_{+pal}$ is expressed inside cells).

Analysis of 5E1 staining in GFP-negative fibroblasts suggests that lipid modification serves analogous functions in receiving cells. In Shh-transfected fibroblasts, 5E1 staining was measured in a significant population of GFP-negative cells (Figure 11D and 11V-11X) and was largely confined to the cell surface (compare 11E to 11F). Conversely, staining in GFP-negative cells was markedly reduced in the absence of both lipid adducts (ShhNC25A; Figure 11P-11R and 11V-11X). Thus, lipid modification strongly enhances ligand association with receiving cells. When solely modified by cholesterol (ShhC25A and ShhC25S), a similar population of GFP-negative cells stained with 5E1 antibody

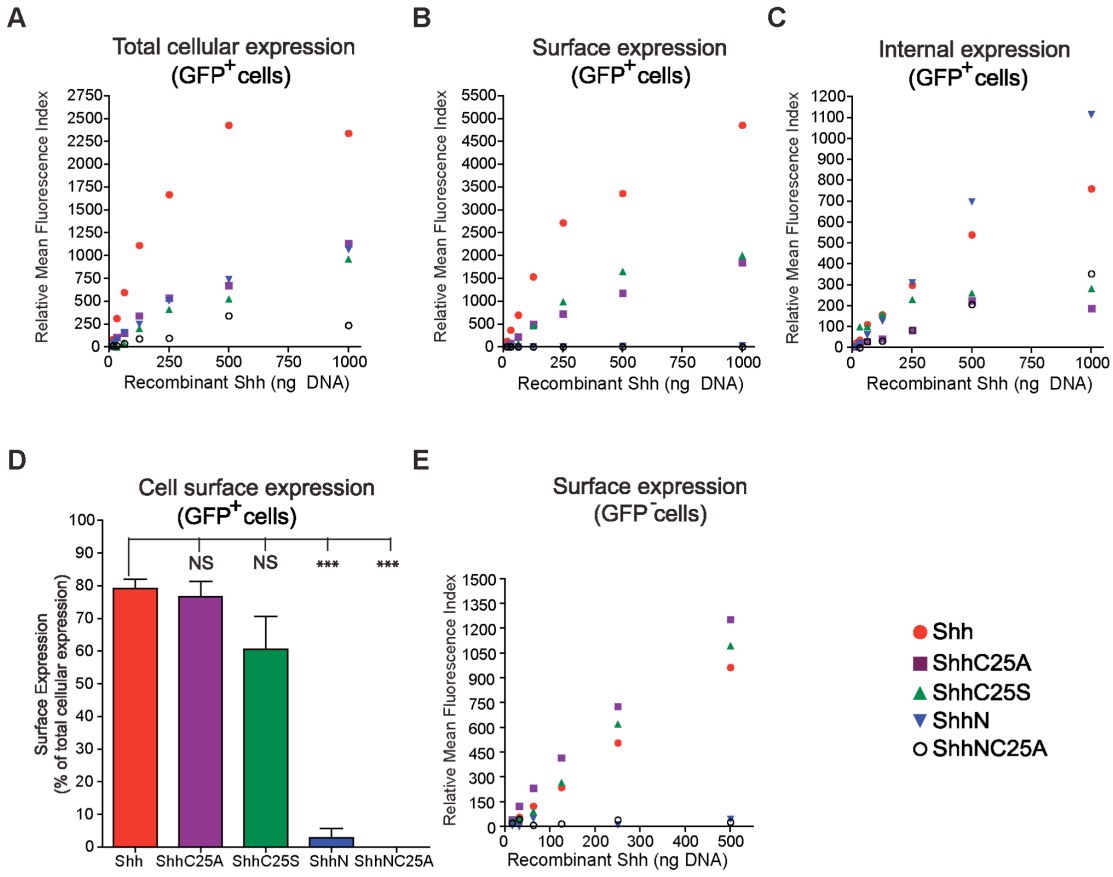

Figure 12. Figure legend on following page.

Figure 12. Distinct properties of cholesterol and palmitate modification on cellular localization of Shh ligand. (A–E) Distinct influences of the cholesterol and palmitate modifications on Shh cellular localization were revealed by quantification of mean fluorescence indices (MFI) for 5E1-Alexa 647 staining of NIH3T3 fibroblasts co-transfected with recombinant Shh (0.06 ng to 1000 ng) and EGFP (1050 ng). **(A–C)** In transfected cells (GFP^+), removal of both lipid adducts greatly diminished total cell MFI (compare ShhNC25A to Shh in **A**), and abolished surface expression (compare ShhNC25A in **B** and **C**). In ShhN transfected cells, where the vast majority of cell associated recombinant ligand appears to represent a palmitoylated species ($ShhN_{+pal}$), surface expression was greatly diminished and concomitantly internal expression was enriched (compare ShhN in **A**, **B** & **C**). Conversely, following removal of the palmitate alone (ShhC25A & ShhC25S) surface expression was maintained **(B)** while internal expression levels were reduced to that of recombinant ligand lacking any lipid-modification (compare ShhC25A and ShhC25S to ShhNC25A in **C**). **(D)** To quantify the amount of cell-associated Shh ligand that was expressed on the surface, the MFI for internal staining was subtracted from that for total cell staining. Removal of both lipid adducts eliminates surface expression, and only 2.9% of cell-associated ShhN ($ShhN_{+pal}$) was localized to the cell surface. **(E)** Correspondingly, surface staining with 5E1-Alexa 647 in untransfected cells (GFP^-) was only measureable for recombinant Shh with cholesterol modification (Shh, ShhC25A, & ShhC25S). Control cells were mock transfected, and MFI is shown relative to control. Experiments were done in replicates of two or more and representative images are shown. NS, not significant ($p>0.05$); ***, $p<0.001$ (± s.e.m.) compared to Shh transfected cells.

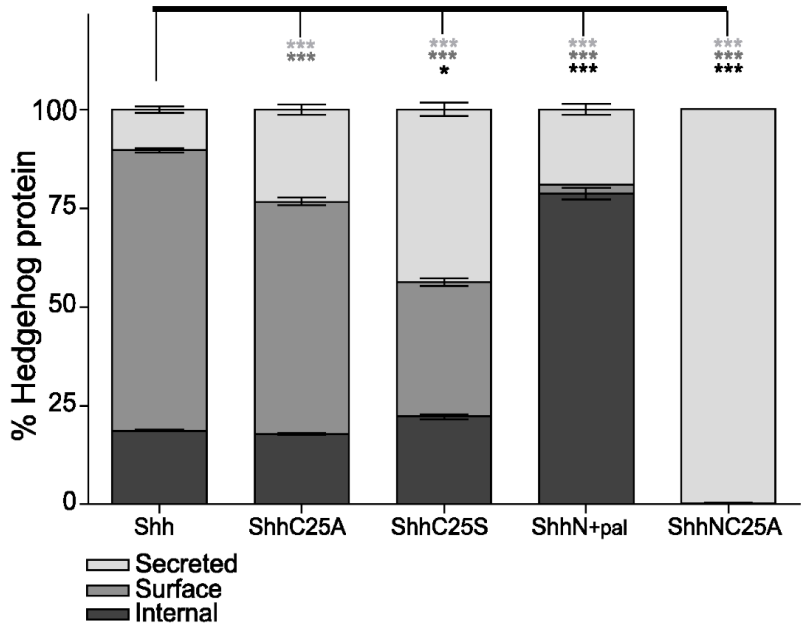

Figure 13. Quantification of the contributions of the lipid moieties to cellular distribution of Shh. Shown are integrated data from ELISA and flow cytometric measurements of recombinant forms of Shh expressed inside cells, on the cell surface, or secreted in the culture medium. The proportion of cell associated and secreted Shh protein for each recombinant expression construct was determined by ELISA measurements of cell lysate and conditioned medium in cells transfected with two fold increments of 62.5-500 ng cDNA (Figure 9B). From the same culture wells, the percentage of Shh protein expressed on the surface and within cells was determined by flow cytometric measurements (Figure 12). To determine the proportion of surface protein expression, the quantity of cell associated Shh was multiplied by the percentage expressed on the cell surface as calculated in Figure 12D. The remaining cell associated Shh protein represents the internal proportion for each recombinant construct. ***, $p<0.001$; *, $p<0.05$ (± s.e.m.)

(Figure 11V-11X) and surface localization of ligand predominated (Figure 11G-11L). These results support mathematical modeling studies that postulate that cholesterol is the predominant lipid determinant for cell surface association (Saha and Schaffer 2006). Notably, surface staining in GFP-negative cells was measurable only for cholesterol modified Shh ligands (Figure 12E). The mean fluorescence indices (MFI) for ShhC25A and ShhC25S surface staining were higher than for Shh in GFP-negative cells as a consequence of the higher levels of cholesterol modified ligand in the culture media under these conditions (Figure 9B). Furthermore, the enhanced surface MFI of ShhC25A with respect to ShhC25S is consistent with the greater hydrophobicity of alanine compared to serine (Taylor et al. 2001).

Lipid modifications dictate cell concentration and signaling potency of Shh ligand.

The evaluation of 5E1 staining in GFP-negative cells supports a predominant role for cholesterol modification in the association of recombinant Shh ligand with target cells. To directly test the influence of the lipid modifications on ligand association with receiving cells, NIH3T3 fibroblasts were exposed to varying quantities of recombinant Shh protein, and the corresponding amounts of cell-associated ligand was measured by ELISA (Figure 14). By this assay, the highest degrees of cellular association were observed following incubation with fully lipid-modified Shh. Removal of both lipid adducts (ShhNC25S) greatly diminished recovery of ligand in the cell lysate and $ShhN_{+pal}$ and ShhC25S demonstrated equivalent dose-dependent cellular association. Collectively, these

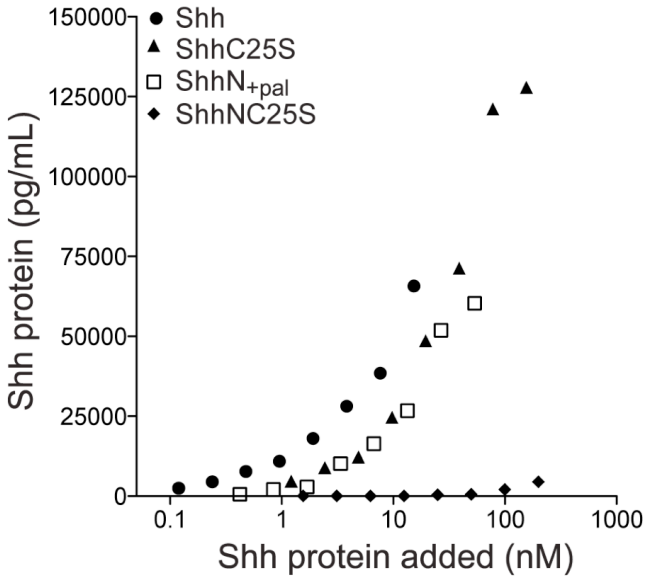

Figure 14. Lipid modification enhances Shh association with receiving cells. NIH3T3 cells were incubated at 37 ºC for 42 hours with medium containing various concentrations of recombinant Shh protein. After extensive washes, the cells were lysed and analyzed by ELISA. The highest levels of protein were recovered from cell lysates following incubation with Shh-conditioned medium. Recovery of ligand was greatly diminished when both lipid adducts were removed (ShhNC25A), and restored with either cholesteryl (ShhC25S) or palmitoyl ($ShhN_{+pal}$) modification alone. Experiments were performed in replicates of four, and representative data are shown.

data provide direct evidence that the lipid modifications are essential for association with target cells.

There are conflicting reports regarding the roles of lipid modification and ligand signaling. The signaling potency of Shh ligand devoid of cholesteryl and palmitoyl adducts in C3H10T1/2 cells can be enhanced by the introduction of a wide variety of hydrophobic modifications (Taylor et al. 2001). Conversely, several studies have reported that removal of either the cholesteryl or palmitoyl adduct abolishes ligand multimerization and signal response in NIH3T3 fibroblasts (Zeng et al. 2001; Chen et al. 2004; Goetz et al. 2006). We analyzed NIH3T3 cells, which have been used most commonly for Hh signaling assays (Taipale et al. 2000; Zeng et al. 2001; Cooper et al. 2003; Chen et al. 2004; Goetz et al. 2006), and found that signal response was greatly reduced in cloned and high-passage lines (Figure 15). As reported, removal of either lipid adduct eliminates the detection of multimeric Shh protein complexes (Figure 16). However, using low-passage and highly responsive NIH3T3 fibroblasts, measurable signaling was retained by each of the recombinant forms of Shh ligand (Figures 17 and 18), and thus multimerization is not required to generate a signal response. To directly test the effect of multimerization on signaling, conditioned medium from HEK293T cells transiently transfected with Shh was subjected to size exclusion chromatography. Purified multimer and monomer elusion fractions were then pooled and Gli reporter activity was measured. Our data suggest that signal potency of Shh conditioned medium does not reside in the multimeric fraction. Instead, multimer and monomer have roughly equivalent

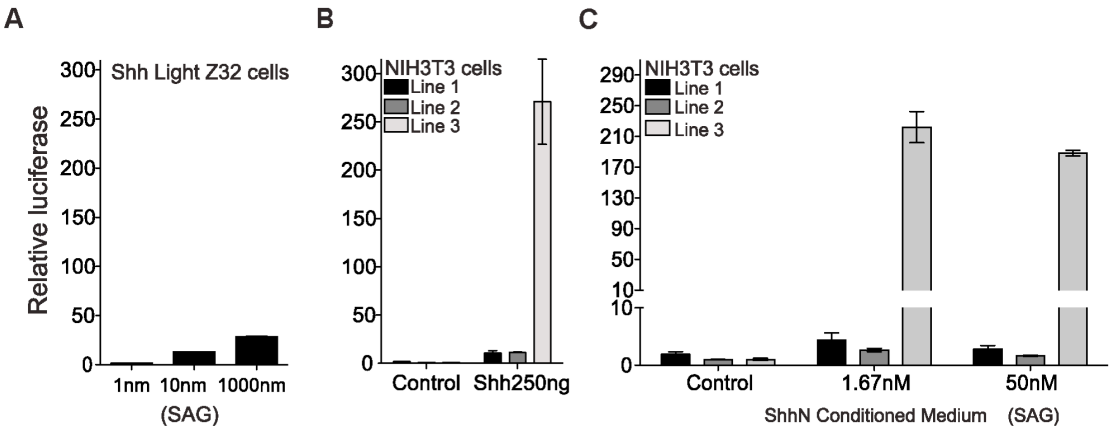

Figure 15. Variable signaling responses among lines of NIH3T3 fibroblasts. **(A)** NIH3T3 cells stably transfected with Gli-reporter and LacZ (Shh LIGHT Z3 cells) {Cooper, 2003 #34} exhibited a dose dependent, but low response to Smoothened Agonist (SAG). **(B-C)** Three different NIH3T3 cell lines transiently transfected with Gli-reporter and LacZ demonstrated marked differences in signaling competency with pathway activation by co-transfection with Shh **(B)**, the addition of ShhN conditioned medium, or SAG **(C)**. Shh LIGHT Z32 cells and lines 1 and 2 were maintained and passaged over long periods of time. Line 3 was newly purchased from ATCC and expanded in culture over one passage. Fresh aliquots of cryopreserved cells from line 3 were used in all of the experiments in this study. Experiments were performed in replicates of three (± s.d.).

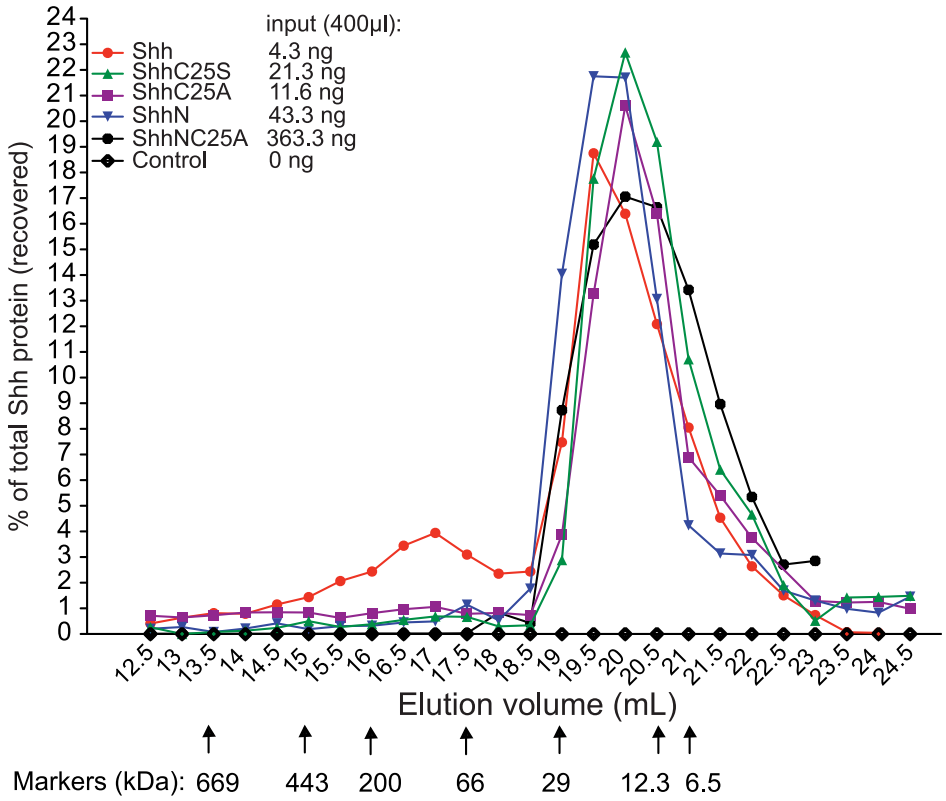

Figure 16. Both lipid adducts are required for multimerization. HEK293T cells were transfected to express Shh, ShhC25A, ShhC25S, ShhN, or ShhNC25A, and then cultured in serum-free media for 48 hours. Conditioned media (400 µL containing 4.3 ng to 363.3 ng of recombinant Shh) was then subjected to size exclusion chromatography. Collected fractions were then analyzed by ELISA, and the percentage of recombinant Shh protein in each fraction relative to the total amount eluted is shown. Recombinant protein was detected in the high molecular weight fractions (elution volumes 15ml to 18ml, estimated mass 450kDa to 50kDa) only in the Shh-conditioned medium, thus both lipid adducts are needed for multimer formation.

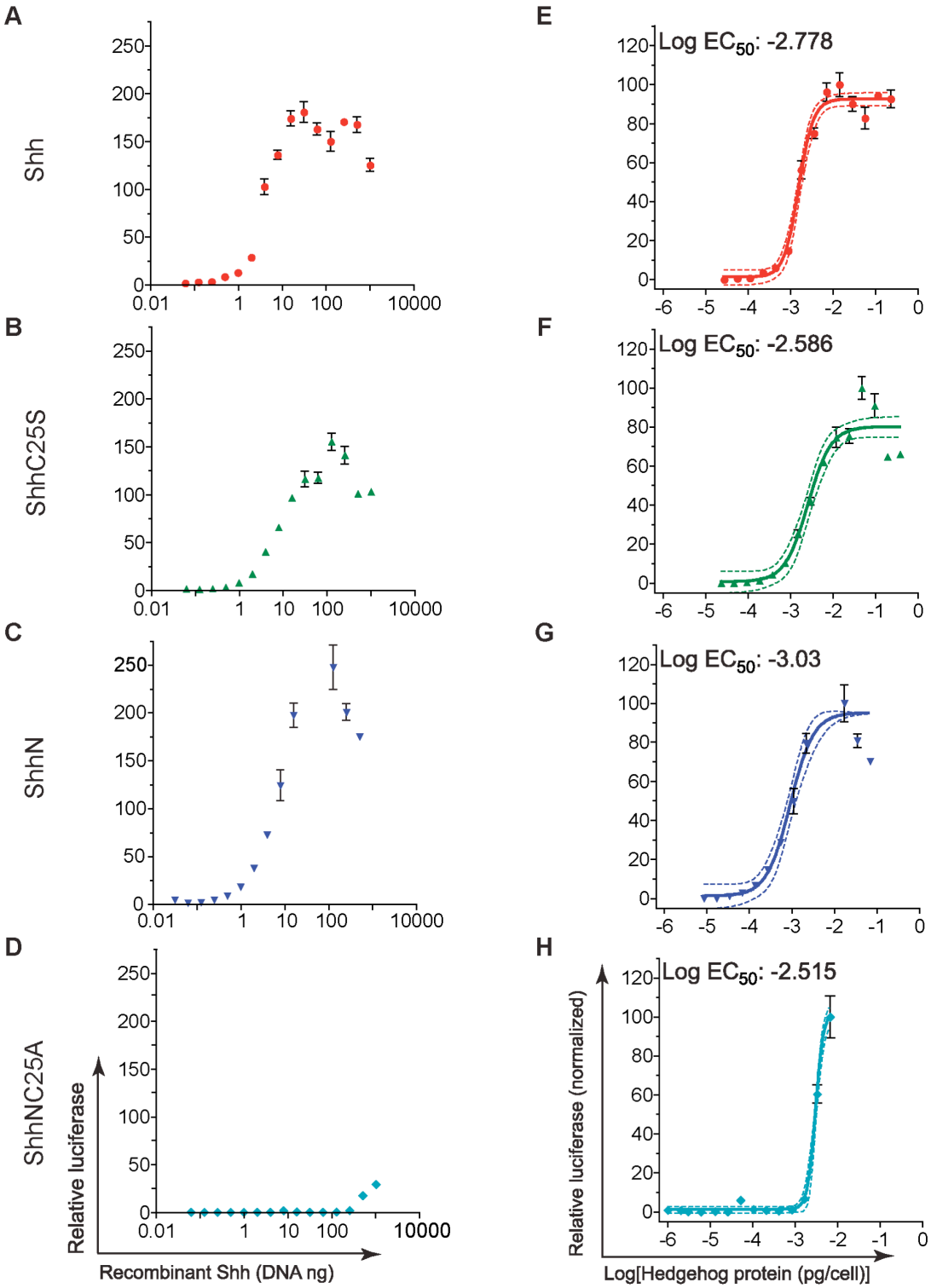

Figure 17. Figure legend on following page.

Figure 17. Shh signaling potency is directly related to cellular concentration of ligand. NIH3T3 fibroblasts were co-transfected with expression plasmids for recombinant Shh (Shh, ShhC25S, ShhN, or ShhNC25S), EGFP, Gli-reporter (8xGli-luciferase) and LacZ, changed to low-serum medium for 40 hours, and then analyzed for chemiluminescence. **(A–D)** Shown are relative luciferase values as a function of transfected recombinant Shh cDNA. ShhNC25A signaling was significantly reduced in comparison to Shh, ShhC25S, and ShhN. **(E–H)** Analysis of relative luciferase activity as a function of recombinant ligand expressed per transfected cell (pg/cell) revealed that all of recombinant forms of Shh signaled with equal potency. Solid line denotes non-linear regression and the dotted lines denote confidence intervals of 95%. Experiments were performed in replicates of three (± s.e.m.).

signaling potency (Figure 19). (See Appendix section A2.1 and figures A1, A2, and A7 for further discussion.)

In order to determine whether levels of cell-associated ligand correlate with signal response, parallel wells of low-passage and highly responsive NIH3T3 fibroblasts co-transfected with expression vectors for recombinant Shh, GLI-reporter, and EGFP were assayed. In one set of wells, relative GLI-reporter activity was measured and in the other set the concentration of recombinant ligand was determined within GFP-positive cells. When signaling activity was expressed relative to transfected DNA for recombinant Shh, signaling levels were comparable for Shh, ShhC25S, and ShhN and markedly reduced for ShhNC25S (Figure 17A-17D). Yet, when expressed relative to the cellular quantity of ligand, the half-maximal effective concentrations (EC_{50}) for each of the recombinant ligands, including ShhNC25S, were nearly identical (Figure 17E-17H and Table 1). The concentrations of recombinant variants of Shh protein recovered from the culture medium was well below the respective EC_{50} calculated in conditioned medium signaling assays, indicating that signaling was mediated by cell-associated ligand in the transfection assays (see Figure 18 and compare Table 1 and Table 2). (See Appendix section A2.1 and figures A4-A6 for discussion of Shh(n-5)). These data strongly support a direct relationship between signaling potency and cellular concentration of ligand.

When signaling was measured for ligand delivered exogenously to NIH3T3 fibroblasts, the maximal signaling level was highest with Shh and diminished by removal of one or both of the lipid adducts

Recombinant Shh	Cell transfection		Conditioned Media	
	EC_{50} (pg/cell)	Relative to Shh	EC_{50} (nM)	Relative to Shh
Shh	0.0017	1	0.81	1
ShhC25A	0.0077	4.5	5.04	6.2
ShhC25S	0.0026	1.6	7.71	9.5
ShhN	0.00093	0.6	ND	ND
ShhNC25A	ND	ND	311	384
ShhNC25S	0.0031	1.8	104.1	128.5

Table 1. Relative signaling potencies of recombinant forms of Shh ligand. The half maximal effective concentration (EC_{50}) of Shh and recombinant variants lacking one or both lipid modifications was determined in signaling assays with NIH3T3 fibroblasts that were either transfected with recombinant Shh, or to which Shh conditioned medium was added exogenously. ND, not determined.

Transfected DNA (ng)	500	250	125	62.5
Shh (nM)	0.044	0.035	0.029	0.0085
ShhC25S (nM)	0.59	0.23	0.14	0.11
ShhN (nM)	0.17	0.078	0.03	0.012
ShhNC25S (nM)	0.92	0.43	0.23	0.11

Table 2. Concentration of recombinant Shh in culture medium from signaling assays in transfected NIH3T3 fibroblasts. Shown is the amount of recombinant Shh protein measured by ELISA in the culture medium from transfected NIH3T3 fibroblasts. The concentrations of recombinant Shh protein recovered in the culture media are well below the EC_{50} measured for each type of variant when added exogenously to NIH3T3 cells.

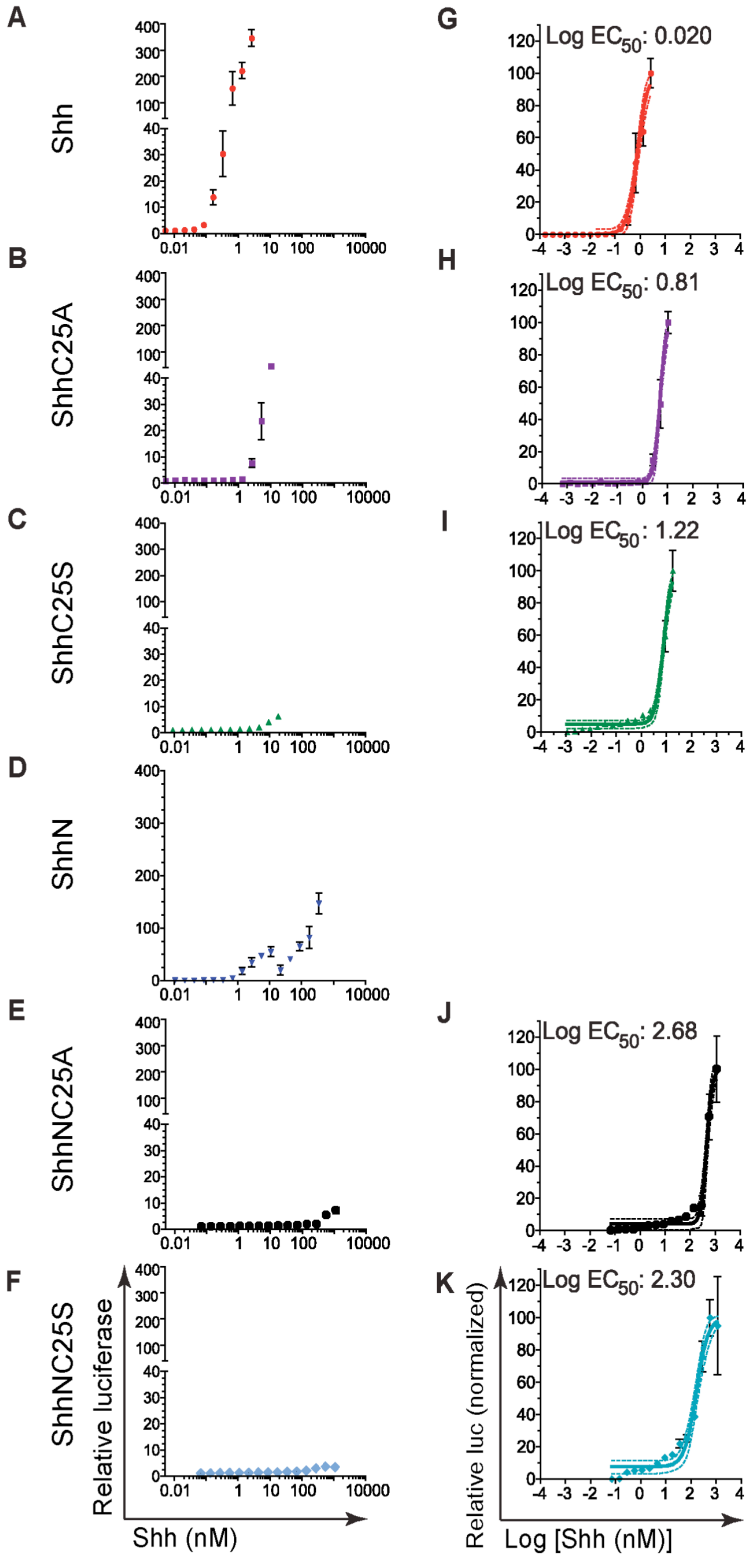

Figure 18. Figure legend on following page.

Figure 18. Lipid modification enhances signaling potency of Shh. NIH3T3 fibroblasts were co-transfected with Gli-reporter and LacZ, and changed to low-serum medium containing Shh, ShhC25A, ShhC25S, ShhN, ShhNC25A, or ShhNC25S protein. **(A–F)** Shown are relative luciferase values as a function of Shh protein (nM) added. **(G–K)** Normalized relative luciferase measurement of the Log EC_{50} for each variant of recombinant Shh revealed decreased signaling potency following removal of one or both lipid adducts. An EC_{50} could not be calculated for ShhN-conditioned medium because of the complex signaling curve **(D)**. Solid lines denote non-linear regression, and the dotted lines denote confidence intervals of 95%. Experiments were performed in replicates of three (± s.e.m.)

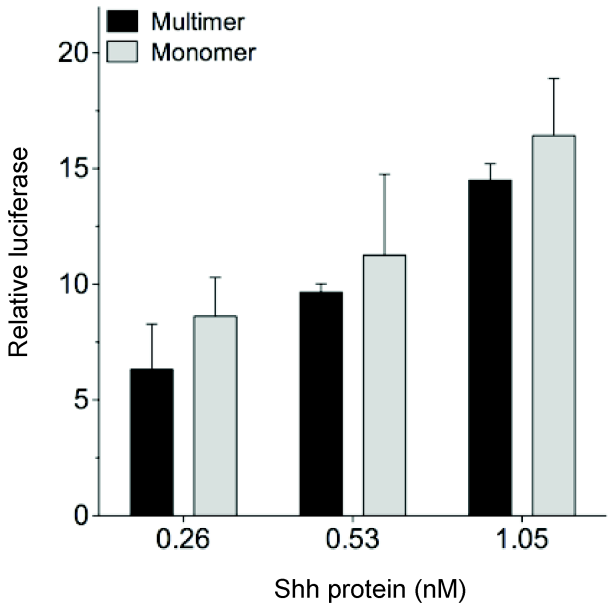

Figure 19. Multimeric and monomeric forms of Shh signal with similar potency. Conditioned medium from HEK293T cells transfected with Shh were cultured in serum-free medium for 48 hours. Conditioned medium (600 µL containing 753 ng of recombinant Shh) was subjected to size exclusion chromatography using a Superose 12 10/300 GL column, and purified elution fractions containing Shh multimer and monomer were pooled, dialyzed in DMEM, and quantified by ELISA. Shh signaling was measured by chemiluminescence in triplicate wells of NIH3T3 cells transfected with Gli-reporter (8xGli-luciferase). $p>0.05$ (± s.e.m.)

(ShhC25A>ShhN>ShhNC25A; Figure 18A-18E). The complex signaling curve measured for ShhN negated the ability to calculate an EC_{50} in this instance, possibly because of the presence of two species of ligand ($ShhN_{+pal}$ and $ShhN_{-pal}$). However, separation of $ShhN_{+pal}$ from $ShhN_{-pal}$ in ShhN conditioned medium by hydrophobic interaction chromatography revealed that $ShhN_{+pal}$ elution fraction contained the highest signaling potency (Figure 10). Furthermore, the EC_{50} calculated for Shh, ShhC25A, and ShhNC25A correlate directly with measurements of their cell-association properties (Figure 14), supporting the conclusion that the lipid modifications regulate Shh ligand association with receiving cells and dictate signaling potency.

2.4 Discussion

Hedgehog proteins are among several secreted signaling proteins that are covalently modified by lipid moieties (Reviewed in (Steinhauer and Treisman 2009)). Hedgehog family members are the only proteins that are known to be modified by cholesterol (Porter et al. 1996b), and this discovery cultivated attention on the influences of lipids on morphogen signaling (Reviewed in (Eaton 2008)). The influences of the lipid modification on ligand release and association with multivalent particles have been well characterized (Lee et al. 1994; Porter et al. 1995; Zeng et al. 2001; Feng et al. 2004; Panakova et al. 2005). The roles of the lipid adducts in signal response have been less well defined, however, in part due to constraints of *in vivo* model systems to distinguish effects on tissue distribution from signal potency (Lewis et al. 2001; Chen et al. 2004; Li et al. 2006; Huang et al. 2007) and of *in vitro* systems with poorly responsive cell lines and qualitative assays of ligand concentration (Zeng et al. 2001; Chen et al. 2004; Goetz et al. 2006). Utilizing highly responsive NIH3T3 fibroblasts and quantitative assays to integrate measurements of recombinant Shh concentration, cellular localization, and signaling, we demonstrate that the membrane-anchoring properties of cholesterol and palmitate govern the cellular reception of Shh and that signaling potency correlates directly with cellular concentration of Shh ligand. In conjunction with prior studies, these findings illustrate complementary functions of the lipid modifications to attenuate release and enhance reception of Shh signal.

Our studies indicate that either lipid moiety is sufficient to enhance cellular association and increase signaling potency. Cholesterol modification, however, tethers ligand to the plasma membrane while palmitoylation alone is not sufficient for retention on the cell surface. These distinct properties identified in our *in vitro* assays may explain opposing and seemingly puzzling effects on limb patterning observed in prior *in vivo* studies following expression of Shh lacking either the palmitoyl or cholesteryl adduct in the zone of polarizing activity (ZPA). In the mouse limb bud, digit number is reduced by targeted deletion of *Skinny Hedgehog* (*Skn*) to abrogate Shh palmitoylation, the finding interpreted to indicate a requirement for a multimeric Shh protein complex in long range signaling (Chen et al. 2004). Long range signaling, however, is enhanced by removal of the Shh processing domain to eliminate cholesterol modification, indicating that cholesterol restricts the long-range movement of Shh protein across the limb bud (Li et al. 2006). In both instances, removal of either cholesterol or palmitate disrupts Shh multimerization (Zeng et al. 2001; Chen et al. 2004). Therefore, our data suggest that the defects in digit specification in $Skn^{-/-}$ limb buds (Chen et al. 2004) are consistent with Shh protein secreted from the ZPA with reduced potency, resulting from absence of palmitoylation, and restricted long-range movement, due to cholesterylation. Conversely, in limb buds engineered to express ShhN in the ZPA (Li et al. 2006), ligand with reduced potency is distributed more broadly due to the absence of cholesterol anchorage to implement low-threshold signaling in the anterior limb bud. Collectively, these observations support a model whereby multimeric or multivalent Shh complexes

are not strictly required for Shh signaling, but rather represent a mechanism for delivering soluble and potent lipidated ligand over a range of cells during tissue patterning.

In the absence of Shh ligand, Ptc1 functions to inhibit the pathway by suppressing the activity of the transmembrane protein Smoothened (Smo) (Taipale et al. 2002). Upon binding with Shh, Ptc1 inactivation allows Smo to initiate signaling (Marigo et al. 1996; Stone et al. 1996; Fuse et al. 1999) through the Gli family of transcription factors (Reviewed in (Ingham and McMahon 2001)). In vertebrates, primary cilia appear to be the principal site where Shh signaling is regulated by reciprocal subcellular localizations of Ptc1 and Smo (Huangfu and Anderson 2005; Rohatgi et al. 2007). According to this model, Ptc1 localized to the base of primary cilia inhibits the lateral transport of Smo, and binding of Shh to Ptc1 activates signaling by reciprocal movement of Ptc1 out of the cilium and Smo into the cilium (Rohatgi et al. 2007; Milenkovic et al. 2009). Ptc1 function and the dynamics of its subcellular localization are not fully understood. Sub-stoichiometric levels of Ptc1 suffice to regulate Smo, and the levels of free Ptc1 protein determine the degree of pathway activity as well as the amount of Shh ligand required for pathway stimulation (Taipale et al. 2002). Ptc1 expression is increased by pathway activation (Goodrich et al. 1997). In NIH3T3 fibroblasts, endogenous Ptc1 is barely detectable by immunofluorescence, and upon pathway activation becomes highly enriched in primary cilia (Rohatgi et al. 2007). Against this background, our data may clarify the observation in cell-based assays that lipophilic modification of Shh enhances signaling potency without

affecting binding affinity for Ptc1 (Pepinsky et al. 1998; Williams et al. 1999; Taylor et al. 2001). Notably, binding assays were performed with cells transfected with a Ptc1 construct truncated at the carboxy-terminal domain to enhance surface expression (Stone et al. 1996; Pepinsky et al. 1998; Williams et al. 1999; Taylor et al. 2001). We measured a profound reduction in signaling potency and corresponding curtailment in cellular association of unmodified Shh (ShhNC25S and ShhNC25A), suggesting that anchorage of Shh ligand to target cells by lipid modification is critical for access to Ptc1 and other receptor complex proteins. This concept raises the intriguing notion that the lipid modification may also serve to create a reservoir of membrane-associated ligand to maintain durable signaling as cellular levels of Ptc1 are increased. As such, the tethering of Shh ligand to receiving cells could directly influence the temporal and spatial gradients of Shh signaling (Briscoe et al. 2001; Harfe et al. 2004; Dessaud et al. 2007).

CHAPTER III

GENERATION OF VISUALIZABLE SHH AND CREATION OF SHH-EGFP TRANSGENIC ZEBFRAFISH

3.1 Introduction

Within a developing organism, discrete cellular centers secrete diffusible signals that specify cell fate within neighboring cells. These factors are thought to signal in a concentration dependent manner and are called morphogens (Roelink et al. 1995). Shh is secreted from midline structures in the ventral neural tube (VNT), the notochord, and adjacent floorplate, and is among several signaling morphogens to pattern a field of progenitor cells within the neural ectoderm, neighboring mesoderm, and endoderm (Krauss et al. 1993; Roelink et al. 1994; Roelink et al. 1995; Teleman et al. 2001). Proper ligand distribution is thus essential to obtain a full range of graded responses, and so it is notable that during protein biogenesis the secreted signaling domain of Shh is covalently modified by cholesterol and palmitate adducts (Porter et al. 1996b; Pepinsky et al. 1998). Determining the detailed roles of the lipid modifications in Shh cellular packaging and handling is paramount to understanding Shh long-range signaling.

To aid our studies on Shh protein propagation and reception, as described in Chapter II, and to learn how a morphogen with unique biochemical properties is trafficked and patterns neural tissues, we generated a visualizable form of the ligand to use in cell culture studies and in generation of a transgenic zebrafish model. Using the Gal4-UAS system to drive tissue specific Shh expression, we

created transgenic lines of zebrafish containing genomic sequences that regulate Shh-EGFP temporal and spatial expression within the notochord and floor plate. We also generated transgenic lines of Hh protein lacking a palmitoyl or cholesteryl adduct (zShhC24S-EGFP and zShhN-EGFP respectively).

When we started this project, a Shh gradient had never been visualized *in vivo*. Since then, however, studies in murine and *Drosophila* have both visualized fluorescently labeled Hh in the neural tube or imaginal wing disc (Torroja et al. 2004; Chamberlain et al. 2008). These studies and others confirm the existence of a Shh gradient in the VNT and demonstrate that Shh is concentrated in large puncta in an apical region of ventral midline cells over the notochord (Huang et al. 2007; Chamberlain et al. 2008). Furthermore, live imaging by confocal microscopy demonstrates that fluorescently labeled Shh colocalizes with the cilium, concentrating at the base. Hh is also observed associating with microtubules (Chamberlain et al. 2008).

Nonetheless, we generated transgenic zebrafish effector lines (*Tg*[*UAS-zShh-EGFP*] and *Tg*[*UAS-zShhC24S-EGFP*]) and driver lines (*Tg*[*arB/C-Shh:Gal4-VP16*]) that specifically drive Shh expression in the notochord and floor plate. The optical clarity of zebrafish embryos allows for real-time fluorescence imaging of individual cell behaviors, making them more advantages than murine models for these sorts of experiments. We planned to determine the contribution of the palmitoyl adduct on ventral neural tube patterning and ligand distribution. We hypothesized that disruption of ventral neural tube patterning, but not the propagation of GFP-tagged ligand, by expression of ShhC24S-EGFP in the floor

plate of wild-type zebrafish embryos, would constitute strong evidence that the palmitoyl adduct is required for cell non-autonomous response.

Though we were not able to complete these studies and have since determined that the palmitoyl adduct is involved in cellular reception and Shh internalization (Chapter II), these transgenic lines can still be used to further understand the role of the palmitoyl adduct *in vivo*. Furthermore, in zebrafish, the primary cilium is influential in early development and its absence affects maximal Shh signaling (Aanstad et al. 2009; Huang and Schier 2009). It would be interesting to examine the role of the lipid adducts on Shh trafficking in the context of the primary cilium.

3.2 Materials and Methods

Cell culture and transfection

Co-transfection assays: NIH3T3 mouse embryonic fibroblasts were cultured in 6-well plates and co-transfected (FuGene® 6, Roche) with one of the four recombinant Shh fusion constructs (ShhN51-EGFP, ShhK66-EGFP, ShhK69-EGFP, or ShhA193-EGFP), a Gli-reporter (pGL3-8xGli-luciferase) (Sasaki et al. 1997; Cooper et al. 2003), and pCMV-LacZ, (a transfection control with a 9:1 ratio of Gli-reporter:LacZ). Twelve hours later, cells were changed to low-serum medium (0.5% calf serum) and cultured for an additional forty hours (Taipale et al. 2000; Taipale et al. 2002). Cells were then used in chemiluminescent signaling assays. Luciferase activity was normalized to β-galactosidase activity and data are shown relative to control vector (EGFP).

Co-plating assays: In these studies, NIH3T3 cells were transfected with one of the four recombinant Shh fusion constructs (ShhN51-EGFP, ShhK66-EGFP, ShhK69-EGFP, or ShhA193-EGFP) and co-plated with Shh Light Z32 cells (cells stably transfected with Gli-reporter and LacZ), changed to low-serum medium, incubated at 37˚C for approximately 40 hours, and then analyzed by chemiluminescent signaling assays. Luciferase activity was normalized to β-galactosidase activity and data are shown relative to control vector (EGFP).

Shh signaling assays

Chemiluminescence (Dual-Light® Luciferase and ß-Galactosidase Reporter Gene Assay System) was measured in lysed (Passive Lysis Buffer; Promega) NIH3T3 cells as directed by the manufacturer (FLUOstar Omega, BMG Labtech) .

Western blot analysis

NIH3T3 mouse embryonic fibroblasts were transiently transfected with a Shh fluorescently labeled (FL) construct and following 24 hours in culture, cell lysates were immunoprecipitated with an anti-GFP monoclonal antibody, separated by SDS-PAGE and probed with either an anti-GFP polyclonal antibody (1:1000) (used in Figure 22) or an anti-Shh antibody (JH134 1:1000) (not shown).

In situ RNA hybridization

In situ hybridization was performed as described (Hauptmann and Gerster 2000). Previously described RNA probes, *shh* (Krauss et al. 1993) were also used. Images were collected as demonstrated (Park et al. 2004).

Molecular cloning

Zebrafish Shha (zShh/Shha) coding sequence was obtained from zShh T7TS vector (Ekker et al. 1995) and EGFP coding region was isolated from pEGFP-C1 (Clontech). A non-helical oligopeptide linker (NH), APAETKAEPMT (George and Heringa 2002), was inserted between zShh and EGFP sequences.

After rigorous functional studies demonstrating that Shh-NH-EGFP was both processed correctly and retained signaling capabilities, EGFP was added in between zShh Ala 192 and Ala 193. Two unique restriction enzyme sites, Nhe I and Xho I, were introduced flanking NH-EGFP sequence and between zShh A192 and A193 and were used to insert NH-EGFP in frame into the coding region of zShh (Figure 24). UAS-GFPpA fragment was obtained from UG (Koster and Fraser 2001) as described in (Inbal et al. 2006). Using pT2-UAS-GFP-γ-Cry-GM2 described in (Inbal et al. 2006), GFP was released and zShh-NH-EGFP construct described above was inserted between UAS and pA using Kpn I and Apa I restriction sites. pT2-arB/C-Shh:Gal4-VP16 uses ar-B and ar-C intronic enhancer regulatory sequences to control zShh temporal and spatial expression within the floor plate and notochord (Muller et al. 1999) (Figure 24). Gal4-VP16 coding sequence was obtained and inserted as described (Inbal et al. 2006).

Generation of pT2-UAS-zShhNH-EGFPγ-Cry-GM2 and pT2-Gal4VP16-arB/C-zShhγ-Cry-GM2 transgenic zebrafish

Transgenesis was performed using the Sleeping Beauty transposon system and transgenes were cloned into the pT2/γ-Cry-GM2 vector (Davidson et al. 2003). DNA constructs were co-injected with SB10 transposase capped RNA into 1-cell stage embryos and raised to adulthood. Transgenic lines were generated as described (Inbal et al. 2006).

Immunohistochemistry and live imaging

Embryos were fixed in 4% paraformaldehyde in phosphate-buffered saline and both live and fixed tissue were imaged using Zeiss LSM 510 laser scanning inverted microscope and processed using ImageJ. Rabbit polyclonal alpha-GFP antibody at 1:500 (Torrey Pines Biolabs) and Cy2 conjugated goat anti-rabbit antibody at 1:150 (Abcam).

3.3 Results

Generation of Shh-EGFP chimeric proteins

To gain mechanistic insight into how the Shh lipid modifications affect its cellular packaging, handling and trafficking, we generated a visualizable form of the ligand. Fourteen putative sites to insert enhanced green fluorescent protein (EGFP) were chosen based on the protein structure of Shh (Hall et al. 1995) as well as mutagenesis studies performed that altered the Ptc binding domain (Fuse et al. 1999). EGFP was inserted at surface residues to minimize protein-folding errors. For each site, EGFP sequences were introduced in frame into full length Shh cDNA to retain the autoprocessing domain and allow for full lipid modification. These recombinant Shh-EGFP fusion constructs were tested and screened for the ability to undergo autoprocessing and signaling.

Determining Shh-EGFP signaling and autoprocessing

Using two distinct Shh signaling assays, a co-plating and a co-transfection assay, we measured whether Shh-EGFP was able to retain both autocrine and paracrine signaling. Four of the fourteen Shh-EGFP constructs, (ShhN51-EGFP, ShhK66-EGFP, ShhR69-EGFP, and ShhA193-EGFP) (Figure 20), retained Shh signaling. In the co-transfection assay, using NIH3T3 mouse embryonic fibroblasts, recombinant Shh-EGFP fusion construct was co-transfected with CMV promoter driven LacZ (a transfection control), and a Shh reporter construct (pGL3-8xGli-luciferase) that drives luciferase expression upon pathway activation

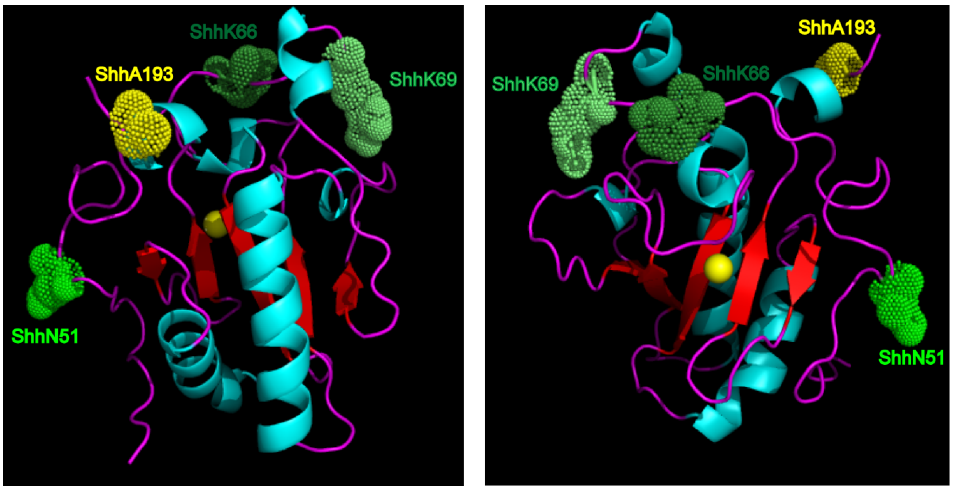

Figure 20. *Mus musculus* structure of Shh indicating EGFP insertion sites used to generate fluorescently conjugated Shh constructs. Shown are two different structural orientations illustrating four sites (ShhN51, ShhK66, ShhK69, and ShhA193) where EGFP was inserted. All four of the recombinant DNA fusion constructs retained signaling.

(Taipale et al. 2002). This assay tests Shh biogenesis and Ptc receptor binding (Figure 21 A and B). All recombinant Shh-EGFP constructs retained autocrine signaling, thus presumably they were able to bind Ptc. In the co-plating assay, NIH3T3 cells transfected with one of four Shh-EGFP constructs, were coplated with mouse embryonic fibroblast cells that stably express the Shh reporter construct and LacZ (Light Z32). This second assay, in addition to Ptc receptor binding and Hedgehog biogenesis, also more readily measures secretion and reception (Figure 21 A and C). ShhA193-EGFP retained robust signaling capacity in both assays. We did not control for protein concentration in this assay and cannot definitively make any conclusions about the various levels of Shh signaling. Due to the drastic differences in signaling, the results from the co-plating assay are interesting nonetheless. The mutant Shh fusion constructs in which EGFP was added in proximity to the amino terminus of the signaling domain, showed diminished signaling, even though all bound to Ptc with equal affinity. This aberration in signaling could simply be because Light Z32 cells are not very responsive to Shh (discussed in detail in Chapter II), the local concentration was not sufficient resulting in diminished Shh cellular association and signaling, or they were not processed or secreted efficiently. Additionally, these amino terminal Shh-EGFP constructs may have diminished binding to heparin sulfate proteoglycans (HSPG). HSPGs influence Shh signaling and trafficking and are thought to interact with Shh via the Cardin-Weintraub (C-W) domain (a region on the Shh amino terminus) that binds heparin (Rubin et al. 2002; Chan et al. 2009). Perhaps conformational changes altering the C-W

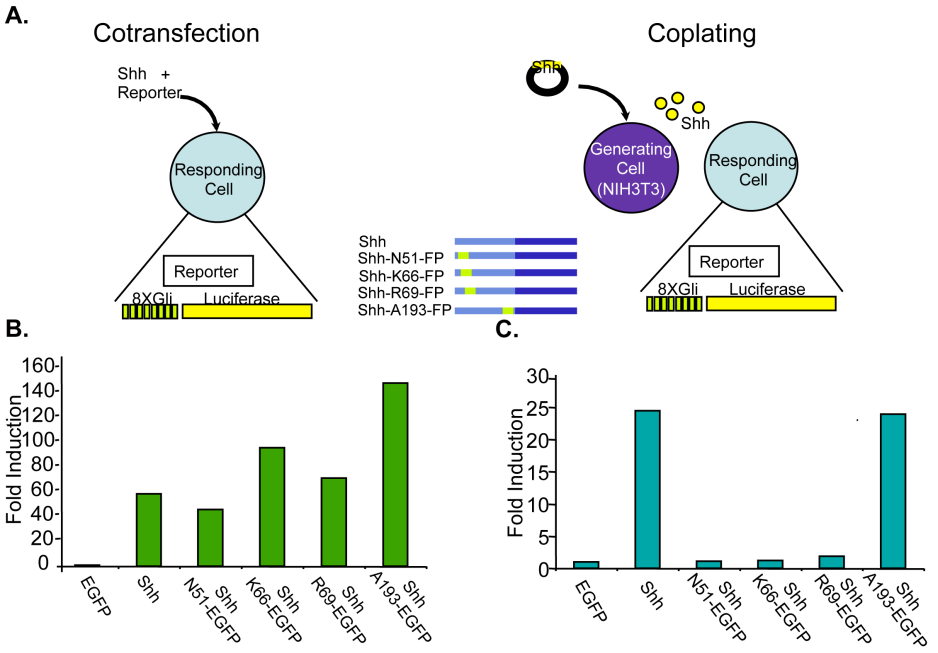

Figure 21. Cell-based Shh signaling assays. (A) Schematic of signaling assays in NIH3T3 fibroblasts. In one assay, cells transfected with Shh (Hh-generating cell; black circle) are coplated with cells stably transfected with Gli-reporter and LacZ. In a cotransfection assay, a Shh expression construct is cotransfected with Gli-luciferase reporter and CMV promotor driven LacZ control into a Hh-responsive cell (shaded circle). **(B)** and **(C)**, Luciferase activity normalized to ß-galactosidase activity in response to control vector (EGFP) and Shh expression in coplating **(B)** and cotransfection assays **(C)**.

region are preventing Shh from interacting with HSPGs. Thus, these amino terminal recombinant Shh-EGFP fusion constructs may not be trafficked effectively resulting in diminished signaling.

The fusion constructs were also screened in transfected cells for the ability to undergo autoprocessing. NIH3T3 cells were transiently transfected with one of the Shh-EGFP constructs for 24 hours and then lysed. The whole cell lysate was co-immunoprecipitated with a monoclonal α-GFP antibody, separated on a polyacrylamide gel, and then transferred, and probed with a polyclonal α-GFP antibody. The fully processed form of Shh-FL is 45 kD, while the unprocessed precursor protein is 80 kD. Unlike the other Shh-FL constructs generated, ShhA193-EGFP was completely processed, showing a band at only 45 kD. In contrast, ShhR69-EGFP was only partly processed. Thus, the ShhA193-EGFP undergoes correct biogenesis, processing, receptor binding, secretion, and reception (Figure 22). We used ShhA193-EGFP for our future studies and also created Shh-EGFP constructs lacking a palmitoyl adduct (Figure A11), a cholesterol adduct, and an unmodified recombinant form of Shh. As we were interested in generating a Shh-EGFP zebrafish model, these mutational studies were not pursued further.

Generation and identification of transgenic zebrafish

Based on the assays described earlier, ShhA193-EGFP is fully processed and signals efficiently. To confirm its signaling capacity *in vivo*, ShhA193-EGFP capped mRNA was injected into a one cell stage of an *olig2*:DsRED zebrafish

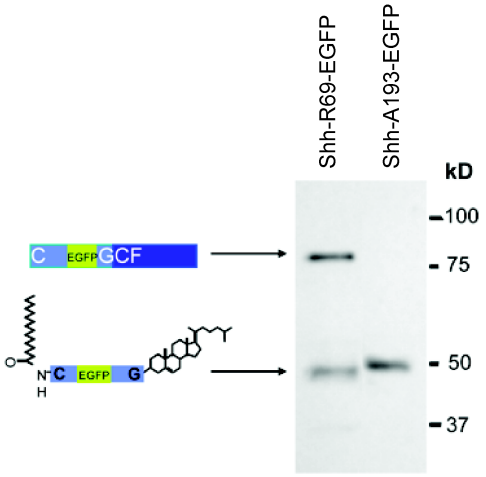

Figure 22. Evaluation of Shh-FL auto-processing. The processed amino-terminal Shh-EGFP fusion product (Mr = 50 kD) can be visualized for both ShhR69-EGFP and ShhA193-EGFP transfections. The presence of unprocessed ShhR69-EGFP precursor protein (Mr ~ 80 kD) indicates that insertion of GFP in this location reduces the autoprocessing efficiency. The apparent size difference between ShhR69-EGFP and ShhA193-EGFP appears to result from a shift in electrophoretic mobility rather than a difference in molecular weight.

embryo. These transgenic lines express dsRED within the *olig2* domain of the ventral neural tube in response to Hh signaling (Shin et al. 2003). We found that injected capped ShhA193-EGFP mRNA signals with equal potency as injected wild-type Shh mRNA and displays a phenotype similar to that of Shh overexpression; the *olig2*:dsRED domain is expanded in the spinal cord and ventral diencephalon along with a shortened tail and “u” shaped somites (Krauss et al. 1993) (Figure 23). Thus, ShhA193-EGFP signals efficiently in zebrafish.

We introduced EGFP after the corresponding alanine in zebrafish Shh (zShh) cDNA. zShh contains one less amino acid then murine Shh, so the construct used in transgenesis is zShhA192-EGFP. In generating our zebrafish lines, we used the Gal4-UAS system (Scheer and Campos-Ortega 1999) to drive tissue specific expression of the zShh-FL constructs as we anticipate that embryonic malformations produced by zShhA193-EGFP, may hinder the production of transgenic lines. The driver line was generated to express Gal4 under the power of regulatory sequences that control zShh temporal and spatial expression within the floor plate and notochord (Muller et al. 1999) (Figure 24). Effector lines were engineered to express zShh-FL fusion genes. Similar studies using GFP labeled Hh and the Gal4-UAS system have been performed successfully in *Drosophila* wing disc (Torroja et al. 2004).

The Gal4-UAS system uses two different kinds of lines, an activator and an effector line. In the activator line Gal4, a yeast regulatory protein that binds specific DNA motifs, namely Upstream Activating Sequences (UAS), activates

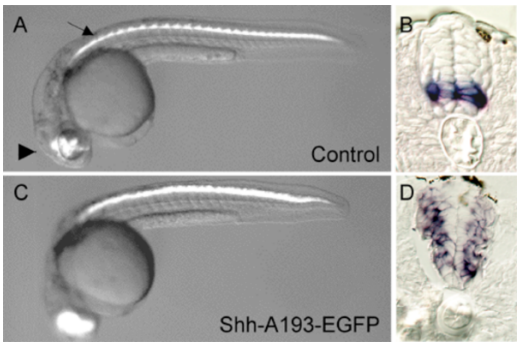

Figure 23. ShhA193-EGFP signaling in zebrafish. **(A)** and **(B)**, *olig2:*dsRED expression within the ventral diencephalon (arrowhead) and ventral spinal cord (arrow) in a transgenic zebrafish embryo, revealed by fluorescence imaging **(A)** and *in situ* hybridization **(B)**. **(C)** and **(D)**, Injection of mouse pCS2+ShhNHA193-EGFP capped mRNA at one-cell stage expands the expression domain of *olig2:*dsRED in the ventral diencephalon and spinal cord, and produces head and trunk malformation. Note that the ventral diencephalon is misshaped, the chevron contour of the somites are lost, and the tail is shortened **(C)**.

transcription of a gene to which it is fused. The effector gene is silent unless crossed to the activator line (Fischer et al. 1988; Sadowski et al. 1988). We will be using Gal4-VP16 in our studies. Gal4 is fused to a portion of the herpes simplex virus protein VP16 resulting in a more potent transcriptional activator than Gal4 alone (Sadowski et al. 1988). The driver line we generated expresses Gal4 under the control of zShh regulatory sequences that have been characterized by Uwe Strähle, and control notochord and floor plate expression. These enhancers direct expression in both mouse and zebrafish indicating that regulation in these tissues is conserved (Muller et al. 1999). The effector lines express UAS linked to a zShh-FL fusion construct. Crossing the driver line with the effector line will produce embryos that temporally regulate expression of zShh-FL within the notochord and floor plate (Figure 24).

As a method of transgenesis, we are using the Sleeping Beauty (SB) transposon system (Hermanson et al. 2004) that unlike plasmid injection reduces the possibility of high molecular weight extrachromosomal concatemer formation (Udvadia and Linney 2003), allows for higher germline transmission, better chromosomal integration, and more stable expression in zebrafish (Davidson et al. 2003; Hackett et al. 2005). The SB transposon system consists of a transposon vector with inverted repeat/direct repeat (IR/DR) regions flanking the gene of interest and a transposase that recognizes the ends of the IR/DR site. The transposase is used to excise the transposon from the vector and insert it into a

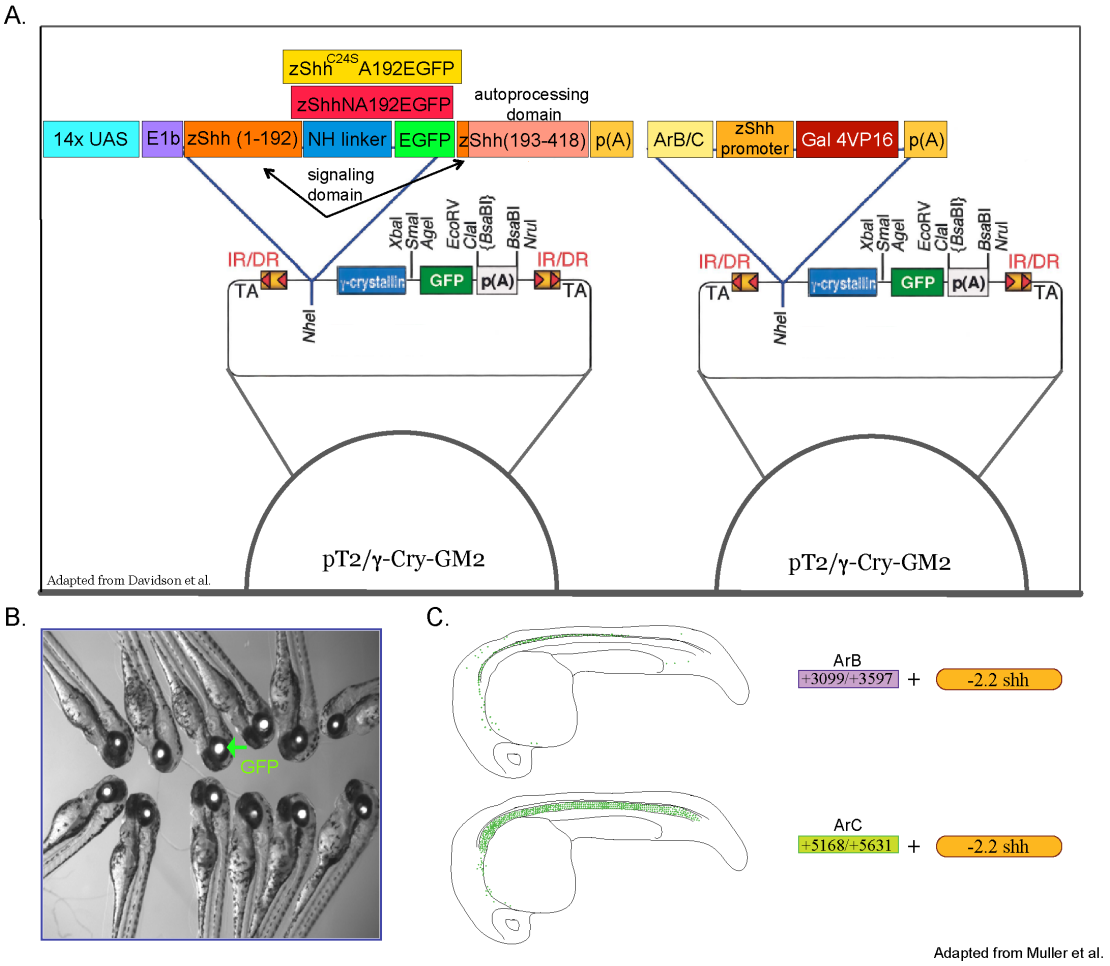

Figure 24. Schematic of method to generate transgenic zebrafish. (A) pT2 transposon contains a multicloning site (MCS), tissue specific γ-crystallin promoter linked to GFP sequences and flanking IR/DR transposon sequences. For the driver construct, Shh regulatory, promoter, Gal4VP16 and polyadenylation sequences are subcloned into pT2/ γ-Cry GM2 MCS. For the effector transposons, UAS and zShhNHEGFP sequences are subcloned into pT2/ γ-Cry GM2 MCS. **(B)** The γ-crystallin promoter linked to GFP sequences allows founder fish to be identified by GFP-positive lenses at 2 dpf. **(C)** Shown are the intronic enhancer sequences used in creation of pT2-Gal4VP16-arB/C.

DNA site in the chromosome with TA base pairs. This is a highly coordinated event; the excision step is immediately followed by an integration step (Hackett et al. 2005) resulting in incorporation of a single cassette instead of multicopy concatemers.

The transgenes were cloned into pT2/γCry-GM2 vector (Davidson et al. 2003) and 20pg of the DNA construct was injected into the cell of a 1 cell stage wild-type embryo followed immediately by injecting 200pg capped RNA encoding SB10 transposase into the yolk (Inbal et al. 2006). Injected embryos were raised to adulthood and crossed with wild-type fish. Founder lines were identified by GFP-positive lenses of their progeny at 2 dpf. Embryos with GFP positive lenses were used to generate transgenic lines. We generated eight different heterozygous lines and one homozygous *Tg*[*UAS-zShhA192-EGFP*] line which expresses fully modified zShh (Shha). We also generated two driver lines (*Tg*[*ArB/C-Shh:Gal4-VP16*]).

To determine activity of the distinct *Tg*[*UAS-zShh-EGFP*] effector lines, we used a transgenic line of zebrafish (*Tg*[*gsc:Gal4-VP16*]^{vu160}) with Gal4 expression driven by *Goosecoid* regulatory sequences. In this line, Gal4 is transiently expressed in the hatching gland, prechordal plate mesoderm, and notochord during the first 24 hours of development (Inbal et al. 2006). From this screen, we isolated a line (*Tg*[*UAS-zShh-EGFP*]^{3913}) that had the strongest EGFP expression as determined by live embryo imaging and immunohistochemistry. Comparing these results with expression patterns from *Tg*[*gsc:Gal4-VP16*]^{vu160}-/*Tg*[*UAS-EGFP*]^{vu157} (Inbal et al. 2006) progeny, suggested that zShh-EGFP

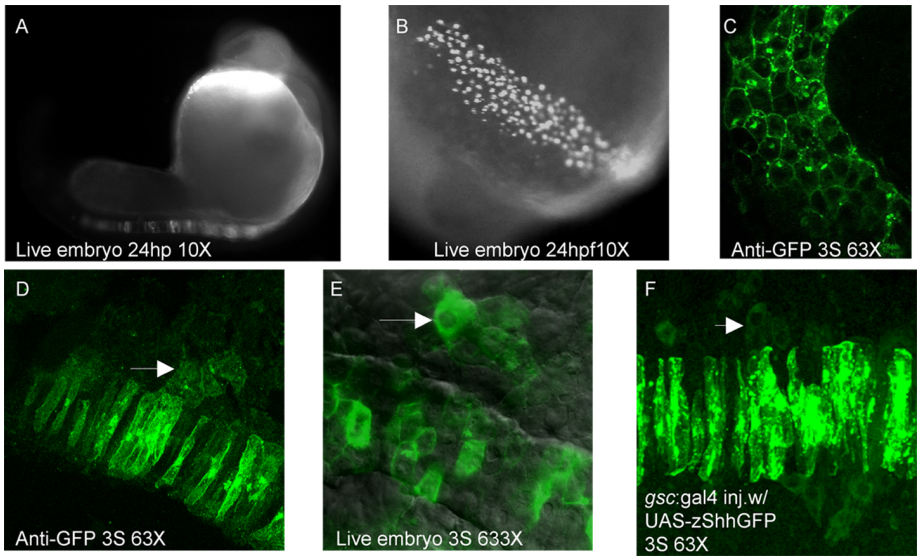

Figure 25. Characterization of zShh-EGFP expression in zebrafish. (A-E) Progeny from driver line *Tg*[*gsc:Gal4-VP16*] and effector line *Tg*[*UAS-zShh-EGFP*]. **(A** & **B**) zShh-EGFP expression at 24hpf is seen in the notochord and hatching gland. (C&D) Flatmounted embryos at 3s, immunostained with anti-GFP and visualized using Cy2 conjugated secondary antibody shows zShh-EGFP expression in the hatching gland **(C)** and in the notochord as well as some cell diameter away **(D)**. **(E)** Live embryo imaged at 3s showing zShh-EGFP expression in the notochord and in surrounding tissue. **(F)** *gsc:Gal4-VP16* embryo injected with UAS-zShh-EGFP and capped transposase mRNA shows zShh-EGFP expression in the notochord and surrounding mesoderm.

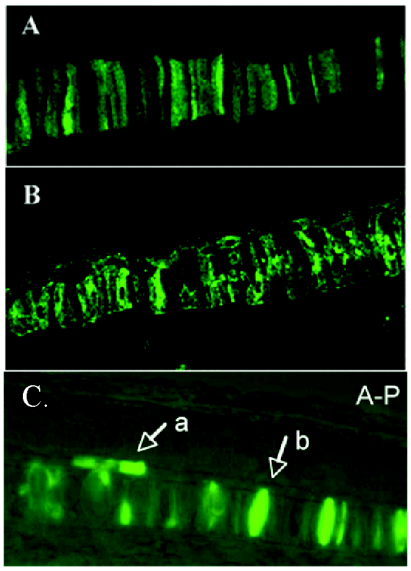

Figure 26. Visualization of EGFP or zShh-EGFP in the notochord and floor plate of a zebrafish embryo. (A) Progeny from driver line *Tg*[*gsc:Gal4*-VP16] and effector line *Tg*[*UAS-EGFP*]. **(B)** Progeny from driver line *Tg*[*gsc:Gal4*] and effector line *Tg*[*UAS-zShh-EGFP*]. **(A** & **B)** Flat mounted embryos at 3s immunostained with anti-GFP and visualized with Cy2 secondary antibody shows diffuse expression in the notochord only **(A)** while **(B)** shows more localized zShh-EGFP expression in the notochord as well outside the notochord. **(C)** *Tg*[*UAS-EGFP*] embryo injected with pT2GM2-ArB/C-Shh-Gal4-VP16 DNA and capped RNA encoding SB 10 transposase. Live embryo imaged at 1dpf showing expression in the floor plate (a) and notochord (b).

expression was specific to Shh (Figure 26). Preliminary results show zShh-EGFP protein outside the notochord, some cell diameters away from the source in both fixed and live embryos (Figure 25). We did not characterize these lines further, but it would be interesting to determine what role Shh may have in the zebrafish hatching gland. The ultimate utility of this approach, however, depends upon the ability to visualize Shh-FL diffusion from a source of localized expression (Figure 26C).

3.4 Discussion and Future Directions

We generated transgenic zebrafish effector lines (*Tg*[*UAS-zShh-EGFP*] and *Tg*[*UAS-zShhC24S-EGFP*]) and driver lines (*Tg*[*arB/C-Shh:Gal4-VP16*]) that specifically drive Shh expression in the notochord and floor plate and may be used in future studies. New lines will have to be generated as over time and after multiple generations these lines no longer express zShh-EGFP. We have frozen stocks of sperm for several effector and driver lines that can be used to restore these transgenic zebrafish via *in vitro* fertilization (Ransom and Zon 1999). The absent Shh-EGFP expression is most likely the effect of DNA methylation and transcriptional silencing. Due to the CpG-rich tandem repeat, 14xUAS is also susceptible to methylation *in vivo*; in vertebrates these repeats are often targets of methylation (Giniger et al. 1985; Giniger and Ptashne 1988). By isolating tissue specific drivers that regulate GFP expression through a multicopy UAS, Goll et al. demonstrated that over succeeding generations, GFP expression diminished or was completely repressed. This transcriptional repression is a result of methylation of the multicopy UAS. In addition, to in vitro fertilization using frozen sperm, silenced transgenes may be reactivated by augmenting Gal4-VP16 levels or by using DNA methyltransferase-1 mutant zebrafish lines (Goll et al. 2009). Nonetheless, future directions are described below and then more thoroughly in Chapter IV.

Characterization of transgenic zebrafish

All independent lines generated would be characterized to determine which driver and effector lines are most appropriate to measure zShh-EGFP diffusion by ensuring that: 1. that strong zShh-EGFP expression is driven in the floor plate and 2. expression is exclusively in the floor plate and not in the ventral neural tube. This will allow for proper measurement of zShh-EGFP as a diffusible ligand. *Tg*[*ArB/C-Shh:Gal4-VP16*] embryos as well as the progeny from *Tg*[*ArB/C-Shh:Gal4-VP16*] and *Tg*[*UAS-zShh-EGFP*] or *Tg*[*UAS-zShh*^{C24S}*EGFP*] crosses will be analyzed using immunohistochemistry, *in situ* hybridization, and live imaging at different developmental stages beginning at initial EGFP expression. Embryos from lines displaying the strongest EGFP expression using epifluoresence microscopy will be analyzed further. EGFP immunohistochemistry will be performed simultaneously to detect EGFP levels that may be too weak to be otherwise observed. Using riboprobes Gal4-VP16, Shh, Ptc, and EGFP (Thisse et al. 1993) whole mount *in situ* hybridization will be performed and then transverse sections of the spinal cord will be collected to determine *Gal4-VP16* mRNA expression profile (Inbal et al. 2006) in the neural tube and notochord (Park and Appel 2003) allowing us to demonstrate if EGFP presence is limited to the floor plate. By comparing *Gal4-VP16* mRNA expression with EGFP protein expression, we will illustrate if in fact Shh protein is being secreted. We expect an overlap between *Gal4-VP16* mRNA and EGFP protein expression, but that EGFP protein will also be present some distance away from the floor plate. Observing an overlap between *shh* mRNA and *egfp* mRNA will confirm that

EGFP can be used as a monitor of Shh presence. In addition, Ptc mRNA will be used as a read out for Hedgehog pathway activation (Chen and Struhl 1996; Briscoe et al. 2001). We expect there to be an expansion of the Ptc domain in *Tg*[*ArB/C-Shh:Gal4-VP16*]/*Tg*[*UAS-zShh-EGFP*] embryos due to Shh over expression. Using genomic DNA from adult zebrafish, all independent lines will also be characterized for transgene copy number by Southern blot analysis to ensure accurate comparisons between *Tg*[*UAS-zShh-EGFP*] and *Tg*[*UAS-zShhC24S-EGFP*] lines. We plan to start our analysis at the tailbud stage as endogenous Shh is already expressed (Strahle and Blader 1994; Ekker et al. 1995) and neural tube formation is beginning.

Measuring the extent of Shh-EGFP ligand distribution in the ventral neural tube

Live embryo and time lapse confocal imaging will be used to visualize the effects of the palmitoyl adduct on Shh gradient and long range signaling by comparing zShh-EGFP positive embryos with zShhC24S-EGFP ones while measuring the amount of EGFP expression away from the source of signal, the floor plate. Two live imaging experiments will be performed, one that will highlight the side of the embryo while the other will show a transverse section of the developing spinal cord. mRNA injections of membrane red fluorescent protein will aid in determining zShh-EGFP localization (Yin and Solnica-Krezel 2007). For the first experiment, time-lapse recordings will be collected every 5-10 minutes with focus on the midline of a dechorionated embryo oriented with dorsal to the top and anterior to the left to observe the floor plate and neural tube during and

after neural tube closure. Embryos will be mounted in 0.8% low melting point agarose in embryo media using glass bottom 35mm Petri dishes and imaged with Zeiss Axiovert 200 spinning disk confocal microscope or the LSM 510 inverted confocal microscope. Images will be captured using a 40 and 60 times oil immersion lenses and analyzed with Improvision Openlab software (Kirby et al. 2006; Yin and Solnica-Krezel 2007). In the second experiment, we will examine the neural tube in the transverse plane through the trunk at the level of the hindbrain primordium during and after the end of neuralation in order to measure the extent of zShh-EGFP versus zShhC24S-EGFP trafficking during neural tube patterning. Embryos will be transferred to 0.2% agarose in embryo media and mounted in 3% methylcellulose on a coverslip enclosed by vacuum grease (Crump et al. 2004) and data will be analyzed as described above. EGFP immunohistochemistry will be performed simultaneously to detect EGFP levels that may be too weak to be otherwise observed. This will provide an alternate way to measure zShh-EGFP distribution in the ventral neural tube.

Measuring Shh signaling and patterning

Data from the trafficking studies proposed above will be compared to antibody staining for expression markers of graded signaling and the distance of these expression domains from the floor plate will be measured. We will compare EGFP and Ptc antibody staining patterns with neural tube markers to correlate Shh graded signaling with graded distribution and patterning in the ventral neural tube. Ptc will be used as a read out for Shh pathway activation and zShh-EGFP

antibody staining pattern to evaluate extent of Shh diffusion. As a read out for proper signaling, we will use induction of ventral neural tube antibody markers Axial (zebrafish homologue of *HNF3*β and a marker for lateral and medial floor plate), Nkx2.2, a lateral floor plate and ventral interneuron 3 marker (Odenthal et al. 2000; Park et al. 2004; Schafer et al. 2005) Isl1, a motor neuron marker, suppression of Pax7, and distance of the expression domains from the floor plate (Jessell 2000). In zebrafish, *shh* is expressed in the medial and lateral floor plate while *twhh* (tiggy-winkle hedgehog, a shh related gene) is restricted to the medial floor plate (Ekker et al. 1995; Lewis and Eisen 2001; Park et al. 2004). Though Shh is needed for motor neuron induction, Twhh can compensate for motorneuron development in the absence of Shh. To avoid the effects of Twhh on our analysis of Shh, we will use antisense morpholino oligonucleotides to suppress Twhh expression (Lewis and Eisen 2001). In addition to the lines and crosses described earlier, we will use progeny from the driver line and *Tg*[*UAS-EGFP*] described earlier as a control to illustrate potential anomalies of zShh-EGFP trafficking due to linkage of EGFP. Note that zShh-EGFP positive embryos will display a Shh overexpression phenotype so we expect to observe a decrease in ventralizing phenotype in zShhC24S-EGFP positive embryos.

We hypothesize that zShhC24S-EGFP positive embryos will have an increase in Shh propagation, thus a broader range of EGFP expression, but will decrease in ventral neural tube progenitor domains and a decrease in Ptc protein levels, confirming that the palmitoyl adduct enhances cellular reception and potency. From *in vitro* studies described in Chapter II, the palmitoyl adduct also

promotes internalization, indicating that it may have an additional role in trafficking Shh, for example, to the primary cilium, to initiate a signaling event. Recently, Shh has been found to interact with several accessory proteins in Shh signal regulation. It would be interesting to determine what role, if any, the palmitoyl adduct may have in promoting association with these other binding partners (Beachy et al. 2010). Additional future directions and other possible uses for these transgenic lines are discussed further in Chapter IV. Alternate approaches to the methods described above are detailed in Appendix A2.2.

CHAPTER IV

CONCLUSIONS AND FUTURE DIRECTIONS

4.1 Summary

Sonic hedgehog (Shh) signaling is an important mechanism for regulating cell growth during embryonic development, tissue homeostasis and tumorigenesis. In responding tissues, concentration and duration of cellular contact to secreted Shh protein are essential for tissue patterning. Shh ligand is covalently modified by two lipid moieties, cholesterol and palmitate, and their hydrophobic properties govern the cellular release and formation of soluble multimeric Shh complexes. My studies were designed to gain insight into the influences of the lipid moieties on cellular reception and signal response. To implement these studies, recombinant forms of Shh ligand that were either fully lipidated or had one or both lipid adducts eliminated, were analyzed in NIH3T3 mouse embryonic fibroblasts. Quantitative measurements of recombinant Shh protein concentration, cellular localization, and signaling potency were integrated to determine the contributions of each lipid adduct on ligand cellular localization and signaling potency. Our studies demonstrate that lipid modification is required for cell reception, that either adduct is sufficient to confer cellular association, that the cholesterol adduct anchors ligand to the plasma membrane and that the palmitate adduct augments ligand internalization. We further show that, independent of the formation of multimeric Shh protein complexes, signaling

potency correlates directly with cellular concentration of Shh ligand independent of the formation of multimeric Shh protein complexes. Our findings demonstrate that lipid modification of Shh determines its cell concentration and potency, revealing complementary functions of hydrophobic modification in morphogen signaling by attenuating cellular release and augmenting reception of Shh protein in target tissues.

Additionally, to explore these questions *in vivo*, we generated a visualizable form of the Shh ligand for expression and imaging in zebrafish embryos. This fluorescent form of Shh retains autoprocessing, is lipid modified, binds Ptc, and signals effectively, both upon transfection of ligand and when Shh protein is exogenously provided to responsive cells transfected with Gli reporter. Employing this visualizable form of Shh (ShhA192-EGFP) and using the binary Gal4-UAS system to drive tissue specific Shh expression, transgenic lines of zebrafish were created containing genomic sequences that regulate Shh-EGFP temporal and spatial expression within the notochord and floor plate. We also generated transgenic lines of mutant forms of Hh protein lacking a palmitoyl or cholesteryl adduct (ShhC24S-EGFP and ShhN-EGFP respectively). The optical clarity of zebrafish embryos allows for real time visualization of individual cell behaviors. These tools will help illuminate the role of Shh lipid adducts on tissue patterning, ligand distribution, and signal potency. Furthermore, it would be interesting to explore the role of palmitate and cholesterol moieties on the ability of Hh to interact with other binding partners, such as membrane associated

proteins Gas 1, BOC, CDO, and HSPGs or even with organelles like primary cilia.

4.2 A Discussion of Two Opposing Models

Diametrically opposing views of the lipid modifications and Hedgehog signaling

In direct contrast to our findings, Ohlig et al. recently presented an intriguing model whereby the lipid modifications must be cleaved in order to shed Shh ligand from producing cells and render the multimeric conformation competent for signaling (Ohlig et al. 2011). This article builds upon previous work from the same group suggesting that a disintegrin and metalloprotease (ADAM) mediates shedding of Shh from its lipid adducts resulting in a soluble and secreted form of Shh protein (Dierker et al. 2009). According to the model, the palmitoyl adduct is required for ADAM-mediated removal of 8-10 amino acids from the amino terminus of the Shh ligand. In the absence of proteolysis, these amino terminal sequences occupy the Ptc binding site of adjacent Shh ligands in the multimer and inhibit signaling (Figure 27).

The foundation of the model is based upon the authors' observations that removal of the palmitate (ShhC25S) allowed for Shh multimerization and release in the absence of ADAM-mediated proteolysis of amino-terminal Shh sequences. Furthermore they found that the ShhC25S multimer demonstrated markedly reduced signaling in C3H10T1/2 osteoblast precursor cells. To test the model,

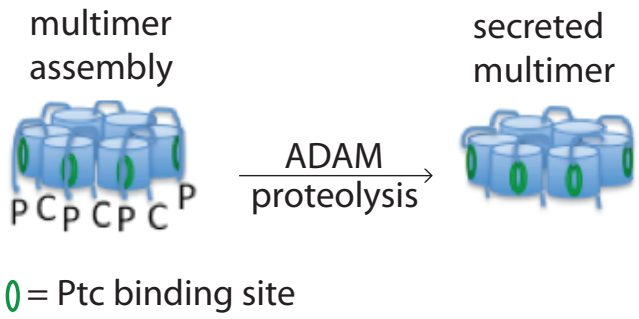

adapted from Ohlig et al. 2011

Figure 27. The palmitoyl adduct is required for multimeric Shh shedding. The palmitoyl adduct is needed for ADAM-mediated removal of amino acid residues from the amino terminus of Shh ligand. In the absence of proteolysis, these amino terminal sequences occupy the Ptc binding site and inhibit Shh signaling.

the authors found that monomeric ligand that had not undergone ADAM-mediated proteolysis (ShhNC25S and ShhN) signaled with full potency in a chick chondrocyte differentiation assay. They hypothesize that since these mutant forms are only monomeric, the palmitoyl adduct is no longer needed to mediate proteolysis and unblock the Shh Ptc binding site required for signaling. Thus, they concluded that the multimeric form of Shh is not required for signaling per se, but that there was a strict requirement for removal of amino terminal sequences in order for multimeric Shh to signal.

This model is diametrically opposed to our findings that the lipid adducts are critical for cellular response to Shh ligand (see Chapter II and Figure 28). The details of our experiments and those conducted by Ohlig et al. deserve closer inspection. Our studies employed quantitative methods for determining both the exact concentrations of Shh protein that cells were exposed to, and for measuring the degree of signal response. Additionally, we employed highly responsive cells, a Gli-luciferase reporter, and carefully measured a dose response for each form of recombinant Shh. In the studies performed by Ohlig et al., recombinant Shh quantity for the C3H10T1/2 cell signaling assays was estimated by western blot analysis. This qualitative approach is quite different from our quantification of Shh ligand by ELISA. As such, very different concentrations of recombinant Shh may have been compared for signaling assays in the Ohlig et al. studies. For example, we determined by ELISA that removal of lipid adducts resulted in either a 2.5-fold or a 10-fold increase in secreted ligand for ShhC25S and ShhNC25S, respectively. Additionally,

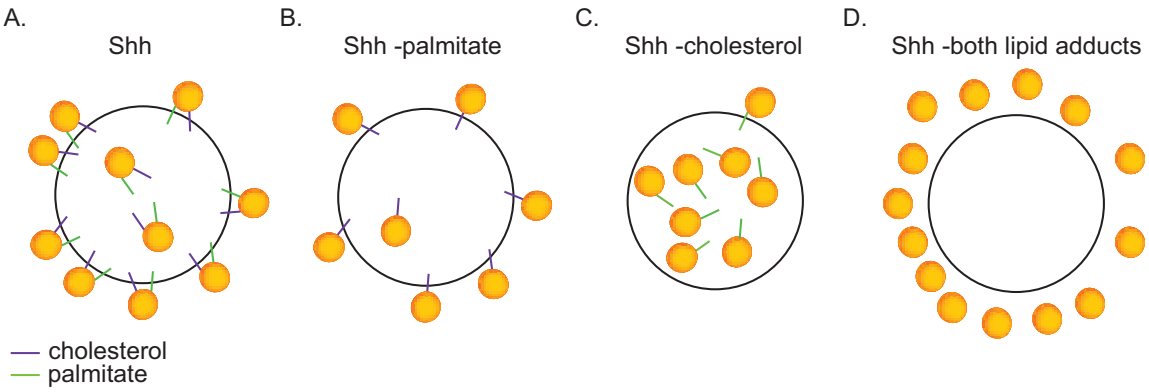

Figure 28. The Shh lipid adducts are required for cellular association and consequently signaling. (A) Both cholesterol and palmitate confer the highest degree of surface association. **(B)** Cholesterol enhances Shh cell surface association. **(C)** Palmitate augments Shh internalization. **(D)** In the absence of either lipid adduct, Shh is not readily able to associate with the cell resulting in significantly diminished Shh signaling capability. See Chapter II for more detailed discussion.

C3H10T1/2 osteoblast precursor cells are far less responsive than NIH3T3 mouse embryonic fibroblasts and employ alkaline phosphatase production to indicate Shh signaling. Alkaline phosphatase production reflects C3H10T1/2 cell differentiation in response to Shh signaling, and represents a qualitative threshold response. Thus, important differences in signaling potency may not be apparent when using C3H10T1/2 cells. Furthermore, all of the signaling assays in the Ohlig et al. study employed a single dose of recombinant Shh ligand instead of a dose response curve. Finally, the most crucial signaling assay of monomeric Shh (ShhNC25S) to support the model for ADAM-mediated processing was performed using a chick chondrocyte differentiation assay. This assay utilizes a biphasic readout of signaling (presence or absence of collagenX) and is thus qualitative. Furthermore, in this particular instance the chondrocytes were incubated with an unknown amount of recombinant ShhNC25S protein (a 1:1 ratio of conditioned medium to DMEM). These differences in methodology and data interpretation are critical. If we had used threshold or biphasic signaling responses as readouts for our studies, we may have concluded that all recombinant forms of Shh signal with equal potency. Yet, by generating a dose response curve with a linear signaling readout and precisely quantifying concentrations of Shh protein, we were able to tease out important difference that would have otherwise been missed. That being said, in addition to NIH3T3 cells, we also employed C3H10T1/2 cells in our studies and the signaling results with quantified amounts of recombinant Shh protein mirrored the results of our luciferase based assays in NIH3T3 cells. We found that ShhNC25S did not signal

nearly as well as Shh and in fact only minimal signaling was detected after subjecting C3H10T1/2 cells to ShhNC25S protein for over 100 hours (Figure A9).

According to the model proposed by Ohlig et al., the multimeric form of ShhC25S fails to signal because the Ptc binding site of one Shh ligand is occupied by amino terminal sequences of an adjacent Shh ligand. If so, signal response to ShhC25S should remain the same regardless of the amount of recombinant ShhC25S protein added to cells. They did not perform this experiment which would have effectively tested their model. Had I reviewed the manuscript, I would have asked for this critical experiment.

4.3 Outstanding Questions

David versus Goliath: Potency of the elusive Shh multimeric complex versus the enigmatic Shh monomer

The multimeric form of Shh is not required for Hedgehog signaling, but is thought to be more potent than Shh monomer (Chen et al. 2004; Goetz et al. 2006). Shh multimeric complexes may be the primary biologically relevant form of Shh *in vivo* and could be involved in trafficking and packaging Shh for delivery to the cellular membrane (Steinhauer and Treisman 2009). Our data indicate that fully lipidated Shh ligand should signal with equal potency regardless of whether it is presented to receiving cells in a multimeric or monomeric conformation; it is the number of Shh ligands delivered to the cell that is imperative. In support, we have found that the signaling potency of Shh conditioned medium from transiently transfected cells does not appear to be concentrated in the 10-20% of

Shh protein that is in a multimeric conformation. Moreover, several studies (Zeng et al. 2001; Chen et al. 2004; Goetz et al. 2006) including ours established that both lipid adducts are required for multimerization and that neither cholesterol nor palmitate is required for Hh binding to Ptc (Fuse et al. 1999; Williams et al. 1999). Further complicating the notion of multimerization is a study that differentiated between medium (66-669 kDa) and large size (>669 kDa) multimers and proposed that both lipid moieties are needed for large multimers, but that either lipid adduct is sufficient for the formation of mid-sized multimers. Active Shh signaling, however, is limited to either large multimeric complexes or mid-sized multimers created from the palmitoyl adduct alone (Feng et al. 2004). Our preliminary data suggest that monomer and multimer have equal potency, but this has not been conclusively illustrated (Figures 16, 19, A1 and A2; Appendix A.1.1). I propose the following to resolve the discrepancies between previous works and to confirm that Shh multimerization does not affect signal potency.

We, and other groups (Zeng et al. 2001; Goetz et al. 2006), have shown that the majority of Shh isolated from conditioned medium from stably transfected Shh cell lines (e.g. HEK293 cells containing an ecdysone-inducible Shh expression construct (Cooper et al. 1998)) is in the multimeric fraction. Generation of stably-transfected cells for all of the recombinant forms of Shh analyzed in this manuscript would be required to enhance the multimer to monomer ratio and rigorously test for the presence or absence of multimeric Shh following removal of one or both of the lipid moieties as well as to compare the signaling potency of multimeric and monomeric Shh. Following size exclusion

chromatography, elusion fractions would be used in Gli-reporter based chemiluminescent signaling assays. Monoclonal anti-Shh 5E1 antibody purification columns may also be employed to concentrate Shh protein fractions (Ericson et al. 1996; Feng et al. 2004). All the recombinant forms of Shh previously discussed bind to 5E1 conjugated protein G beads with equal affinity (Figure A8). Additionally, Shh responsiveness in Light 2 cells (NIH3T3 embryonic fibroblasts stably transfected with Gli responsive Firefly luciferase and constitutive *Renilla* luciferase) can be enhanced by altering culture conditions; DMEM supplemented with Ham's F12 Nutrient Mixture (Invitrogen) resulted in four times greater signaling when compared to standard culture conditions (Figure A7). This increase in sensitivity may allow low levels of signaling to be more detectable and may uncover otherwise unapparent differences or confirm similarities between multimeric and monomeric signaling capacity.

Further examining Shh multimeric complexes and the role of Dispatched on multimer secretion

Hedgehog multimerization studies have only been analyzed using size exclusion gel filtration chromatography on Shh secreted into culture medium from either transfected cells or posterior limb buds (Zeng et al. 2001; Chen et al. 2004; Goetz et al. 2006). Speculation deems that Shh multimerization occurs on the cell surface (Zeng et al. 2001), but we do not know whether Shh is secreted as multimer via Dispatched1 (Disp1 or mDispA), or whether it is secreted as a monomer, multimerizes on the cell surface, and is then released by Disp1. Disp1 mediates secretion of lipid modified Shh and also plays a role in long range

signaling (Burke et al. 1999; Caspary et al. 2002; Kawakami et al. 2002; Ma et al. 2002). Though, Disp1 is not required to generate a Shh response, the range of Hh distribution from its site of synthesis is decreased in *Disp1-/-* tissue even if Shh is correctly produced and secreted using Disp1 expressing cells. Therefore, Disp1 is not only important in expressing cells, but may be involved in spreading and distributing Shh. This role for Disp1 in mediating Shh transport supports the notion that it may enhance Shh multimerization that inadvertently may augment long range signaling (Etheridge et al. 2010). It would be exciting to observe multimerization in action on the surface of live cells and to investigate further the mechanistic roles of Disp1.

Using flow cytometry in combination with fluorescence resonance energy transfer (FRET) may allow detection of Shh multimerization on the surface of live cells. NIH3T3 cells co-transfected with three separate Shh fluorescent constructs, conjugated to cyan fluorescently protein (CFP), yellow fluorescent protein (YFP) or mRFP (monomeric red fluorescent protein) would be subject to 2-step FRET analysis using flow cytometry. Favorable geometric orientation and close proximity of the proteins and fluorophores are necessary for favorable FRET. These fluorophores share significant spectral overlap and due to their small size tend not to greatly alter the geometry of the protein they are linked to or the interaction between the chromophores themselves, making them good contenders for FRET. The efficiency of energy transfer from donor to acceptor chromophore is based on the Förster equation and is inversely proportional to the sixth power of the distance separating the two chromophores. Thus, even a

slight decrease in the distance between fluorophores results in substantial decrease in FRET (Dye 2005). If Shh undergoes multimerization, light energy that excites Shh-CFP fusion protein (donor) would be transferred to Shh-YFP (acceptor) indicating that the two proteins interacted. Trimerization would take this a step further resulting in mRFP fluorescence; energy transferred to Shh-YFP would then also be transferred to Shh-mRFP. Due to excitation and emission overlaps, CFP-YFP FRET and YFP-mRFP FRET are more efficient than direct CFP-mRFP FRET. In addition, measuring CFP and CFP-YFP FRET quenching would be another indicator of 2-step FRET (Dye 2005; He et al. 2005). ShhC25S or ShhN fluorescently labeled constructs would serve as controls as they associate with the cell surface, but do not multimerize. Fluorescence microscopy would further validate the flow cytometry results as well as provide additional cellular localization data (Banning et al. 2010). Furthermore, to test the role of Disp on Shh surface multimerization and secretion, the experiments described above could be repeated using transfected *mDispA -/-* mouse embryonic fibroblasts (MEF) (Ma et al. 2002).

A model for lipid adducts in Shh signal regulation

Our studies demonstrate that, though both the Shh palmitate and cholesterol moieties can each confer cellular association, it is the cholesterol adduct that anchors ligand to the surface of the plasma membrane and the palmitate adduct that augments ligand internalization. Assume: 1. We are only considering what happens to Shh once it reaches the cell, 2. Shh ligand

internalization implies that Shh is being degraded and thus has just partaken in a signaling event and 3. Shh signaling is principally mediated via primary cilia. Based on these assumptions we propose the following model: The cholesterol adduct anchors Shh to the cellular membrane, holding Shh at the surface until it is required for signaling. The palmitoyl adduct is involved in trafficking Shh to the cilium and participating in a signaling event prior to ligand internalization. In the absence of cholesterol forcefully tethering Shh to the membrane, Shh is vigorously shuttled to the cilium to undergo signaling and is then degraded. In the presence of cholesterol alone, fewer Shh ligands traffic to the cilium resulting in less Smo association with the cilium, and diminished signal response. We further propose that other Shh binding partners that positively regulate the pathway may be involved in trafficking Shh to the cilium to generate a Shh signaling event. We suggest that the palmitoyl adduct may enhance Shh interaction with these other binding partners and could facilitate binding to Shh (Figure 29). In the following sections we propose methods and provide additional background required to test this hypothesis.

Shh lipid adducts and the primary cilium

To initially test our hypothesis and determine the role of the Hh lipid adducts on trafficking, we would transfect mouse embryonic fibroblasts, such as NIH3T3 cells, with the fluorescent labeled (FL) Shh constructs we generated (ShhA193-FL, ShhNA193-FL, and ShhC25SA193-FL). Assuming that we are able to visualize Shh-FL on cilium type structures, we would then confirm that

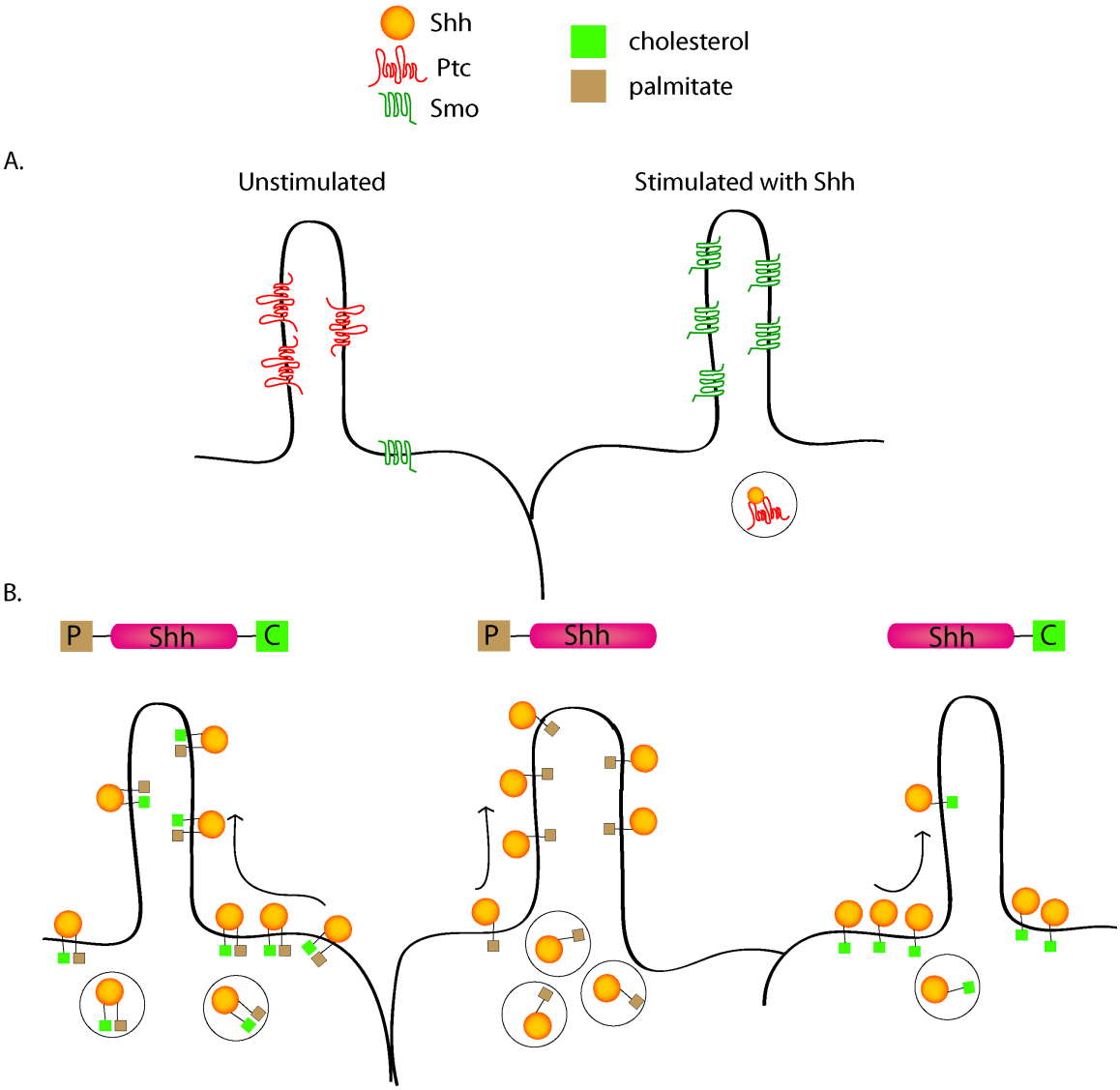

Figure 29. A model for lipid adducts in Shh signal regulation. (A) In the absence of Shh ligand, Ptc is concentrated in the primary cilium. Inactivation of Ptc by Hh enables Smo to accumulate in ciliary membranes. **(B)** Shown is a possible model based on our studies, suggesting that the cholesterol adduct anchors Shh to the cellular membrane; holding Shh at the surface until it is required for signaling. On the other hand, the palmitoyl adduct is involved in trafficking Shh to the cilium resulting in a signal response before the ligand is internalized for degradation. In the absence of cholesterol forcefully tethering Shh to the membrane, Shh is rapidly shuttled to the cilium to undergo signaling and is then degraded; not only is the concentration of Shh in the cilium greater, but the rate at which it is trafficked increases. In the presence of cholesterol alone, fewer Shh ligands traffic to the cilium at a slower rate resulting in less Smo association with the cilium, and diminished signal response.

Shh is in fact present on cilium by using primary cilia specific markers Inversin and Pericentrin. Inversin marks primary cilia and is not involved in Hh signaling. Additionally, Pericentrin localizes around the basal body and is found at the base of primary cilia. Observing co-localization between Shh-FL and fluorescently labeled versions of these cilia specific markers would serve as a proof of principle (Rohatgi et al. 2007). Next, using fluorescence recovery after photobleaching (FRAP) (Reviewed in (Lippincott-Schwartz et al. 2003)), we will be able to selectively photobleach the primary cilium with a high-intensity laser and measure the rate of recovery occurring as Shh-FL returns to the previously bleached cilium. Fluorescence recovery would be a measure of Shh-FL trafficking to the cilium. Analysis of fluorescence recovery by quantifying the time of non-bleached Shh-FL to return to photobleached area would allow us to differentiate between the roles of the palmitate and cholesterol Shh adducts. We hypothesize that Shh lacking the palmitoyl moiety would require more time to reach and be less concentrated at the cilium, while Shh lacking the cholesterol adduct would be trafficked at a faster rate and have a higher concentration on the cilium than wild-type Shh.

Another way to examine a Shh signaling event is to observe an increase of Smo localization to the primary cilia. In the absence of Hh ligand, Ptc is concentrated in cilia (Huangfu and Anderson 2005; Rohatgi et al. 2007) and acts catalytically to suppress the activity of Smoothened (Smo) (Taipale et al. 2002). Inactivation of Ptc by Hh binding removes Ptc from the cilium, enabling Smo to accumulate in ciliary membranes (Rohatgi et al. 2007; Milenkovic et al. 2009).

This accumulation is followed by a secondary process converting Smo to an active state (Rohatgi and Scott 2008; Rohatgi et al. 2009). We propose using Smo accumulation in the cilium as a readout for Shh signaling. We would also employ pharmacological reagents allowing us to differentiate between the various states of Smo and confirm that Smo is in fact in a signaling state and not just merely on the cilium (Rohatgi et al. 2009). NIH3T3 fibroblasts, transfected with fluorescently labeled Smo (Smo-FL) would be subject to real time fluorescent imaging upon the addition of unlabeled wild-type and mutant (ShhN and ShhC25S) Shh protein. We hypothesize that in the absence of the palmitoyl adduct, less Smo would localize to the cilia at a slower rate (fluorescence intensity may also be diminished suggesting less Smo on the cilium) while in the absence of the cholesteryl adduct, Smo would reach the cilium faster and be more concentrated in cilia. In zebrafish, primary cilia also play a role in Shh signal transduction (Huang and Schier 2009), thus these studies may be pursued further using our transgenic zebrafish models. We may be able to visually observe the spatial distribution of Shh and determine whether the palmitoyl adduct has a function in modulating signaling via the primary cilium.

Shh lipid adducts in spatial and temporal gradients

In the neural tube, Shh is secreted from localized sources, specifically the notochord and floor plate, and patterns the ventral neural tube in both a concentration and temporal dependent manner (Roelink et al. 1995; Dessaud et al. 2007). The importance of Shh exposure as well as duration is also apparent in

the limb bud where Shh is involved in posterior digit formation (Harfe et al. 2004). *Ex vivo* experiments suggest that when neural plate explants are immersed for short periods of time in either high or low concentrations of Shh protein, they generate similar levels of Gli and transcriptional responses. Over time though, Gli expression decreases as Ptc is upregulated and cells desensitize to the continuous Shh signal. This leads to a conversion of Shh concentration to a specific period of Gli activity and more ventral target genes are expressed (Jeong and McMahon 2005; Stamataki et al. 2005; Dessaud et al. 2007). Changes in the concentration of or the duration of Shh exposure may have similar effects on transcription responses, as reducing either results in a decreases in intracellular Gli as cellular identity requires Gli activity to be maintained above a particular threshold (Reviewed in (Ribes and Briscoe 2009)).

Shh signaling data described in Chapter II were collected at a specific time point, and thus we were unable to determine the effect of lipid adducts on Shh signaling or localization over time. Preliminary data from experiments examining osteoblast differentiation in C3H101/2 cells (osteoblast differentiation requires a specific threshold of Shh signaling (Kinto et al. 1997)) did not demonstrate a novel role for Shh lipid adducts on temporal kinetics of signaling (Figure A9, Appendix 2.1 for further discussion of these results). Osteoblast differentiation, however, does not allow for a readout of graded Shh threshold responses. More precise measurements will be obtained by repeating this experiment and observing differentiation (by examining transcription expression profiles, Figure 3) in chick neural plate explants incubated over time with quantified amounts of

Shh protein. Two possible experiments could be performed. In the first, neural plate explants will be subjected to the same concentration of Shh protein over different time intervals. If the palmitoyl adduct is involved in shuttling Shh to cilia, then Shh in the absence of the cholesterol adduct would impart a particular cell fate faster than wild-type Shh. On the other hand, in the absence of the palmitoyl adduct it would take longer to attain that same cellular fate. This potential difference between lipid adducts may be more evident by examining cell types that require more Shh to differentiate. In the second experiment, neural plate explants would be subjected to Shh protein for the same duration and then analyzed. If the palmitoyl moiety enhances Shh localization to the cilium, signaling may proceed at a faster rate. Therefore, over the same period of time, Shh lacking the cholesterol adduct may result in a lower threshold response or a more dorsal neuronal phenotype. While, in the absence of the palmitoyl moiety, higher threshold response would be achieved. As described above, tissue exposed to Shh protein for long periods of time eventually becomes sensitized and Shh ligand no longer influences differentiation (Dessaud et al. 2007). In the absence of Shh lipid adducts, the time for cells to reach this level of sensitization and differentiate could increase if palmitate enhances signaling and affects Shh potency.

Shh binding partners and the Shh palmitoyl adduct

Additionally, we propose that other Shh binding partners that positively regulate the pathway may be involved in trafficking Shh to the cilium to generate

a Shh signaling event. We suggest that the palmitoyl adduct may enhance Shh interaction with these other binding partners and could facilitate binding to Shh. Accessory proteins, CDO, BOC and Gas1 directly bind Shh and either CDO/BOC or Gas1 in addition to Ptc are required for Shh mediated differentiation and proliferation. These additional binding partners, however, are not required for Shh to bind Ptc (Allen et al. 2011; Izzi et al. 2011). Ptc is thought to mediate Shh endocytosis (Incardona et al. 2000). Furthermore, we demonstrate that the Shh palmitoyl adduct enhances surface association and may also modulate Shh ligand internalization. Collectively, this suggests a role for the palmitoyl adduct in facilitating interactions with CDO, BOC, and Gas1. This interaction could occur after Shh binds Ptc and binding CDO/BOC could facilitate Shh concentration in the cilium. Megalin (Lrp2), another Shh binding protein, is involved in Shh endocytosis, which is inhibited by heparin (McCarthy et al. 2002), suggesting that Shh signaling may also be modulated by glypican heparin chains; once Shh is no longer required on the cell surface, Megalin, in the absence of heparin, internalizes excess Shh. The palmitoyl adduct may be involved in Shh binding to Megalin or in Shh endocytosis.

Preliminary observations using fluorescent microscopy show internalization and colocalization of ShhA193-ECFP with Ptc-EYFP in signal receiving cells (Figure A10, Appendix A2.1). This method and these studies may be used to answer questions regarding the role of the palmitoyl adduct in Shh interaction with Ptc, Megalin and other binding partners. In addition, fluorescent protein subcellular localization markers and antibody staining could be used to

characterize the cellular compartments in which Shh-FL and ShhC25S-FL are localized. Follow up experiments could include examination of protein localization within isolated membranes such as lipid rafts and organelles like primary cilia or cytonemes. The role of the Shh palmitoyl adduct in Hh interaction with other proteins may be further explored using standard methods to over-express or knock down gene function of Shh binding partners in transgenic zebrafish lines *Tg*[*UAS-zShhC24S-EGFP*] and *Tg*[*UAS-zShh-EGFP*] as previously described.

In conclusion, the studies described in this thesis highlight the importance of the cholesteryl and palmitoyl adducts on Shh trafficking, localization, and signaling *in vitro* and provide an *in vivo* model for continued analysis.

APPENDIX

A1.1 Isolation of multimeric and monomeric Shh fractions and their role in Hh signaling.

The multimeric form of Shh is not required for Hedgehog signaling, but is thought to be more potent than Shh monomer (Chen et al. 2004; Goetz et al. 2006). Our data suggests that monomer and multimer Shh may have equal potency, but more rigorous analysis is required. The technical issues we encountered and other supporting figures are described below and in figures A1 and A2. See Chapter IV and figure A7 for alternate methods and further analysis.

Our data do not indicate that the signaling potency of Shh conditioned medium from transiently transfected cells resides in the multimeric fraction (which represents 10-20% of total Shh protein by either Superose 12 or Superose 6 HPLC). Instead, our data are more consistent with multimer and monomer having roughly equivalent signaling potency. Low relative abundance of multimeric Shh has impeded rigorous testing of the contribution of multimerization on signaling potency.

We have analyzed Shh conditioned medium from transiently transfected cells on a Superose 12 column and found that the yield of multimeric Shh protein is lower than that of a Superose 6 column (Figure A1). Previous studies have been performed using Superose 12 or Superdex 200 that is better for low molecular weight separation HPLC columns (Zeng et al. 2001; Chen et al. 2004; Goetz et al. 2006). We also analyzed the effects of detergent concentration

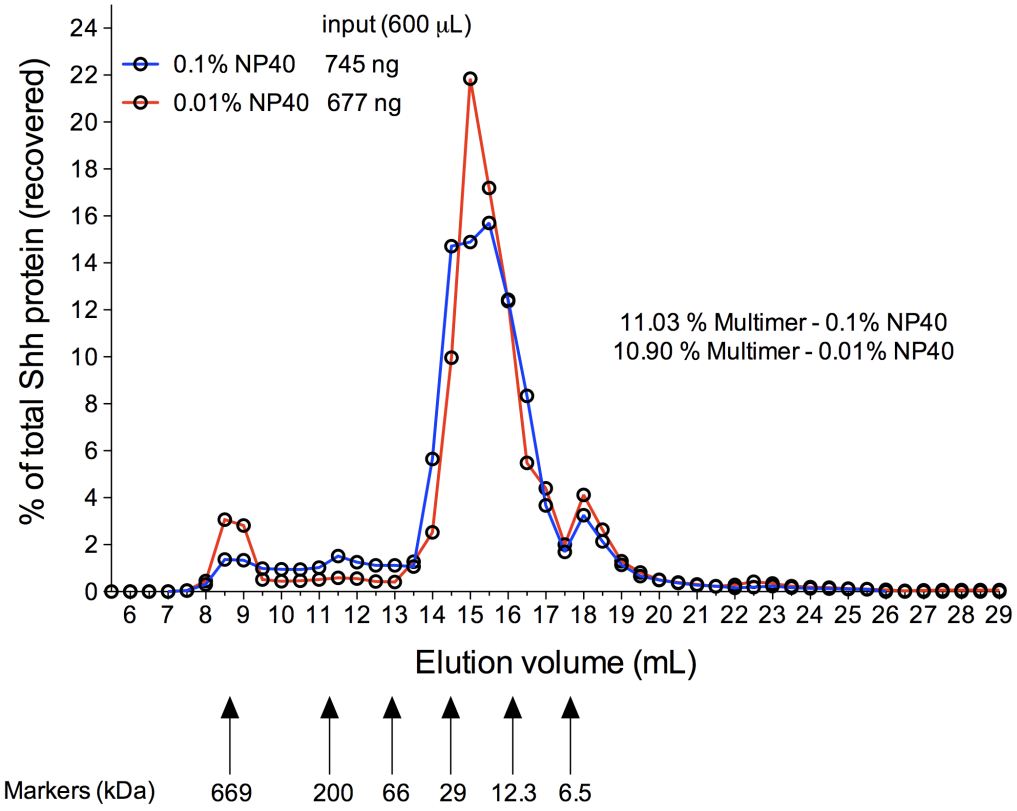

Figure A1. HEK293T cells transiently transfected with Shh and fractionated on a size exclusion column. Conditioned medium from HEK293T cells transfected with recombinant Shh was concentrated (Amicon® Ultra-15 centrifugation filter; Millipore) and analyzed by HPLC (High Performance Liquid Chromatography) at 4°C using the Amersham Biosciences ÄKTA Purifier P-900 (GE Healthcare Life Sciences). Conditioned medium was fractionated using a Superose 12 10/300 GL column (GE Healthcare Life Sciences) equilibrated in PBS with either 0.1% or 0.01% NP-40. The 0.5 mL elution fractions were collected and analyzed by ELISA. The column void volume is 7 mL. Regardless of detergent concentration the percentage of multimeric Shh isolated with the Superose 12 column was approximately 11%. In contrast, the percentage of multimeric Shh isolated with the Superose 6 column was 22%.

and determined that the yield of multimeric Shh in the conditioned medium we have generated is not enhanced by detergent concentration used to equilibrate the Superose 12 column (0.0001-0.1% Nonidet P-40. We conclude that, as reported (Goetz et al. 2006) the ratio of multimer to monomer is low in transiently transfected cells.

Figure 19 contains the data from our best experiment and suggests that both forms of Shh protein signal with equal potency. Measurable Shh signaling (Gli reporter activity) was also detected using approximately 200 kDa mid-size multimers (0.5 mL elution volume fractions 10-12) (Figure A1 and data not shown), however due to low protein concentration in these fractions quantitative dose response analysis could not be performed. This is the only experiment, out of a total of 5 independent experiments, for which we achieved detectable signaling, albeit at 1/10 of maximum levels for unfractionated conditioned media. The two next best experiments, shown in Figure A2, illustrate the technical challenges we faced in purifying sufficient quantities of multimeric and monomeric Shh protein for signaling assays.

To perform the signaling assay illustrated in Figure 19, for example, 1.7 liters of Shh-conditioned medium was concentrated for purification of multimeric and monomeric Shh protein by size exclusion chromatography. Shown in Figure A2 are the results of 2 other experiments to illustrate the technical limitations and important caveats. Shh-conditioned medium was concentrated to approximately 18 nM as determined by ELISA and was not dialyzed prior to use in a signaling assay (Figure A2(A)). The signaling curve for the conditioned medium

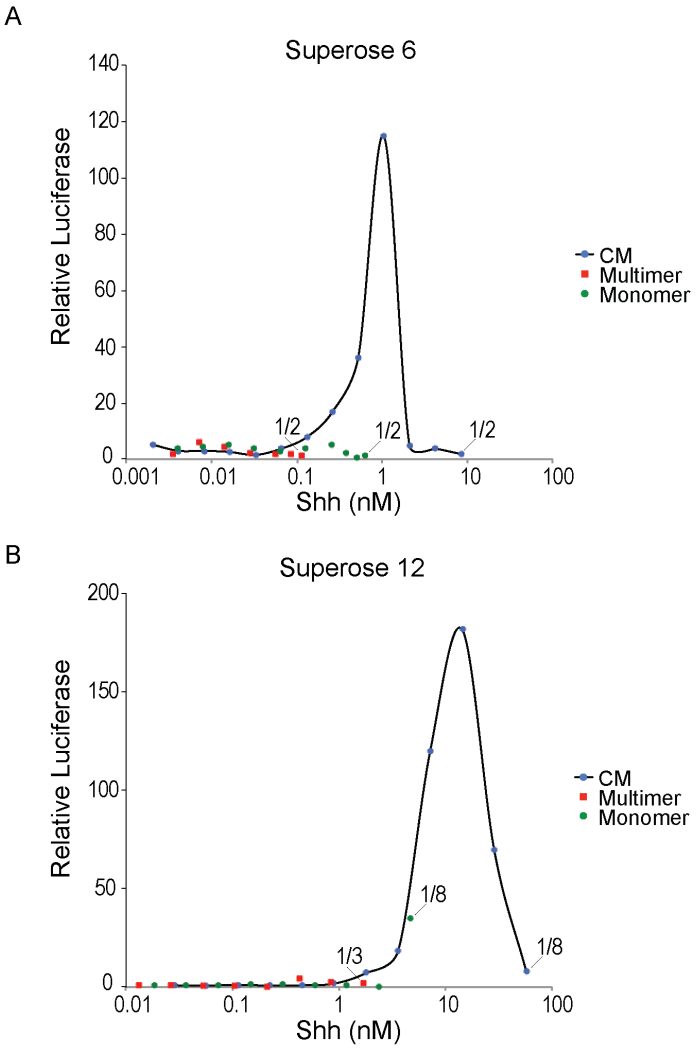

Figure A2. Shh signaling assays using multimer and monomer fractions of Shh protein separated on a size exclusion column. Shown are two experiments comparing the signaling potency of concentrated conditioned medium (CM) from HEK293T cells transfected with recombinant Shh and the multimeric and monomeric fractions of Shh protein following purification with either a Superose 6 **(A)** or Superose 12 **(B)** column. Shh signaling was measured by chemiluminescence in triplicate wells of NIH3T3 cells transfected with Gli-reporter (8xGli-luciferase) and β-galactosidase. Shown are the averaged relative luciferase values for 2-fold dilutions of each Shh protein preparation with the starting dilution labeled for each tracing. **(A)** The Shh-conditioned medium was not dialyzed and the multimeric and monomeric Shh fractions were dialyzed in DMEM before the signaling assay. **(B)** All of the multimer, monomer, and CM preparations were dialyzed before the signaling assay.

demonstrates that serial dilution was required to eliminate the presence of an inhibitory substance in the concentrated medium and that the EC_{50} for this assay was ~0.8 nM. The Shh multimer and monomer fractions purified from a Superose 6 column were then dialyzed and analyzed for signaling potency at 2-fold serial dilutions. The yield of monomer and multimer, however, appear to have been too low to obtain signaling competent Shh protein after serial dilution. Shh-conditioned medium was concentrated to approximately 96 nM as determined by ELISA (Figure A2(B)). After dialysis, however, the concentration by ELISA was 461 nM. ELISA readings of the HPLC fractions also differed before and after dialysis, but to a lesser extent, indicating that dialysis can affect the results of the ELISA assay for both fractionated and unfractionated conditioned medium. The signaling curve for this batch of concentrated conditioned medium revealed that serial dilution was still required to eliminate the presence of an inhibitory substance despite dialysis and that the EC_{50} for this assay was ~6.3 nM based on the ELISA reading after dialysis. The Shh multimer and monomer fractions purified from the Superose 12 column were dialyzed and analyzed for signaling potency at 2-fold serial dilutions (starting at 1 to 8 for the monomer and 1 to 3 for the multimer fractions) (Figure A2). Again, however, the yield of monomer and multimer appear to have been too low to adequately compare signaling potency. Based on the results of numerous experiments, it is clear that the low relative abundance of multimeric Shh in our conditioned medium and the accumulation of an inhibitory factor during concentration precluded rigorous testing of the signaling potency of multimeric versus monomeric Shh. See Chapter IV for

further discussion and future experimentation.

A2.1 Additional discussion of figures

Figure A3: Shh signaling in the chick neural tube

Though this experiment yielded no results, it offers an additional method to the zebrafish studies proposed in Chapter III. By simply electroporating Shh-EGFP in to the chick neural tube, we were unable to differentiate between cells that were electroporated with Shh-EGFP and those that received it as a result of Shh trafficking (A3 A and B). We created a bicistronic vector, pCIG-Shh-EGFP-IRES-dsRED, to differentiate between electroporated cells and cells that exogenously received Shh. Electroporated cells will express dsRed in the nucleus and EGFP, while cells receiving Shh-EGFP will only express EGFP. This provides a "localized" source of Shh. We would be able to measure the range of Shh-EGFP and ShhC25S-EGFP and correlate distribution with signaling by examining transcription factor expression profiles in the VNT.

Figure A4, A5, and A6: Shh(n-5) cellular distribution and signaling

Shh(n-5) has similar cellular localization to ShhC25S and ShhC25A, all of which lack the Shh palmitoyl adduct. Its EC_{50} is 0.09 pg/cell which is significantly higher than all the other recombinant Shh constructs used in this study. Thus, its inefficient signaling may be due to a conformational change that prevents it from interacting with other Shh regulatory proteins like HSPGs or CDO. As mentioned

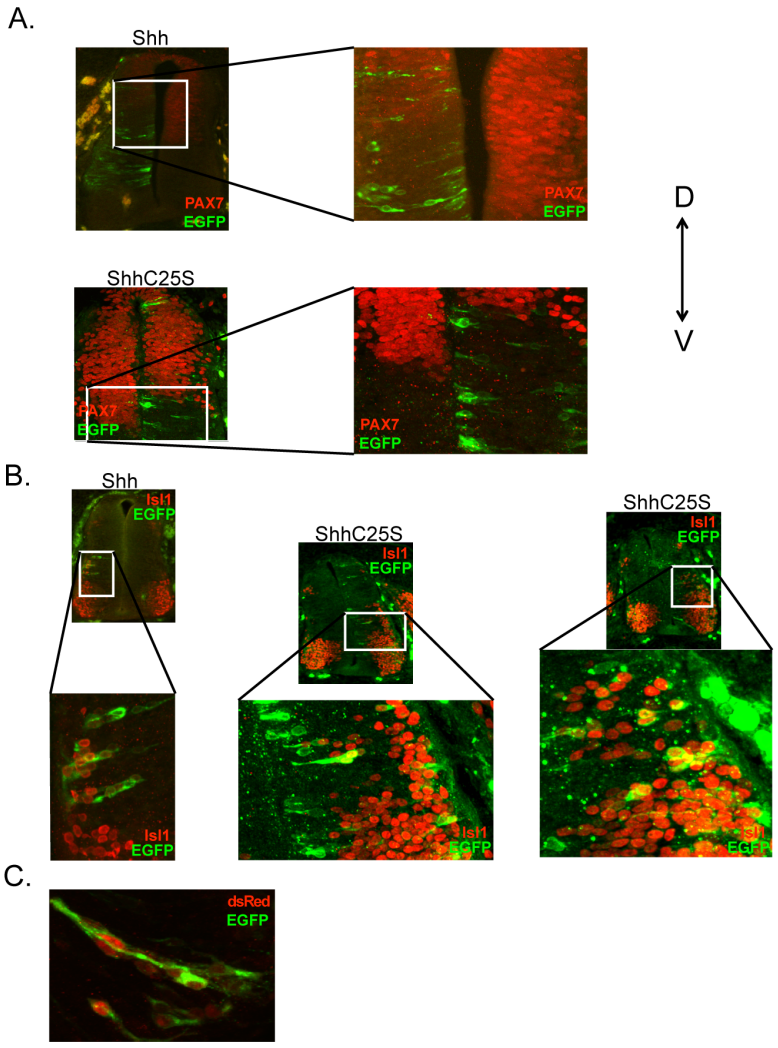

Figure A3. Shh-EGFP and ShhC25S-EGFP both signal in the chick neural tube. **(A** & **B)** Chick embryos at approximately Hamburger-Hamilton (HH) stage 10 were electroporated into one side of the developing neural tube (NT) with either recombinant Shh-EGFP or ShhC25S-EGFP. Embryos were collected at HH 19 to 21, the NT was isolated, fixed, OCT embedded and frozen at -80 degrees C. 20µm sections were cut and processed for immunofluorescence analysis. Cells, electroporated with recombinant Shh are EGFP positive. **(A)** Shh overexpression, reduced Pax 7 (DSHB Pax7 1:500; goat anti-mouse Alexa 555) staining in the electroporated dorsal NT compared to the non-electroporated control side. **(B)** Shh overexpression, increased the range of Isl1 expression (DSHB Isl1 1:1000; goat anti-mouse Alexa 555) staining in the electroporated ventral NT compared to the non-electroporated control side. **(C)** Chick embryos electroporated with pCIG-Shh-EGFP-IRES-dsRED.

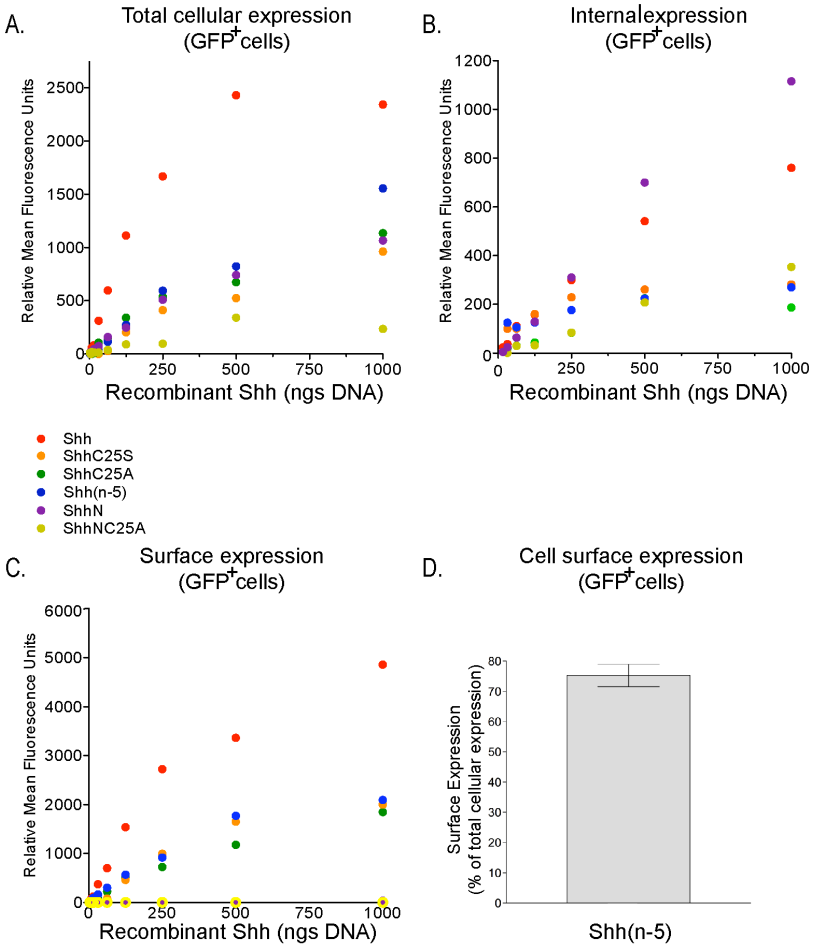

Figure A4. Cellular distribution of Shh(n-5) is comparable to ShhC25A and Shh25S. (A–C) Figure 12 with the addition of Shh(n-5). Shh(n-5) behaves in a similar fashion to ShhC25A and ShhC25S. Distinct influences of the cholesterol and palmitate modifications on Shh cellular localization were revealed by quantification of mean fluorescence indices (MFI) for 5E1-Alexa 647 staining of NIH3T3 fibroblasts co-transfected with recombinant Shh (0.06 ng to 1000 ng) and EGFP (1050 ng). See figure 12 for more details. Following removal of the palmitate alone (Shh(n-5), ShhC25A & ShhC25S) surface expression was maintained **(C)** while internal expression levels were reduced to that of recombinant ligand lacking any lipid-modification (compare ShhC25A/S and Shh(n-5) to ShhNC25A in **B**). **(D)** To quantify the amount of cell-associated Shh ligand that was expressed on the surface, the MFI for internal staining was subtracted from that for total cell staining. Control cells were mock transfected, and MFI is shown relative to control. Again the percentage of Shh(n-5) on the cell surface is comparable to ShhC25A and ShhC25S (compare Figure A4D and 12D).

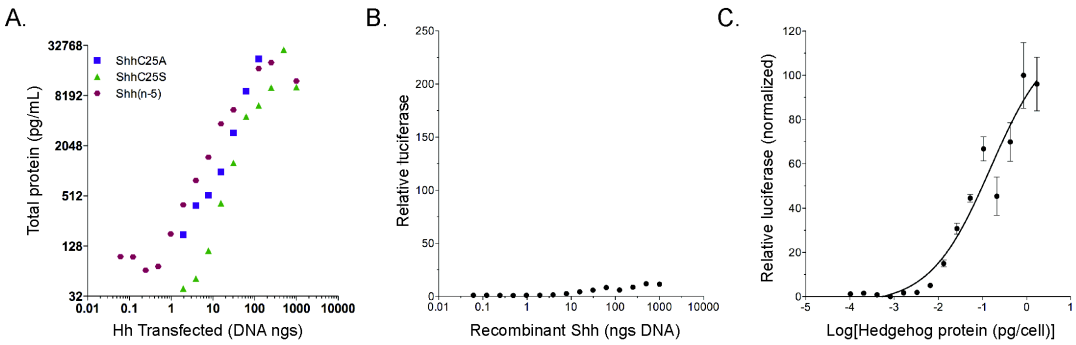

Figure A5. Shh(n-5) signaling potency is significantly less than ShhC25A and ShhC25S, even though all lack the palmitoyl adduct. (A) Each of the constructs conferred dose dependent and similar expression levels of recombinant Shh protein. Shown are the sums of protein measurements in cell lysate and culture medium from NIH3T3 cells transfected with a range of cDNA for constructs in which Shh palmitoylation is abolished (ShhC25S, ShhC25A and Shh(n-5)). **(B** & **C)** NIH3T3 fibroblasts were co-transfected with expression plasmids for recombinant Shh (Shh, ShhC25S, ShhN, or ShhNC25S), EGFP, Gli-reporter (8xGli-luciferase) and LacZ, changed to low-serum medium for 40 hours, and then analyzed for chemiluminescence. **(B)** Shown is the relative luciferase value as a function of transfected recombinant Shh(n-5) cDNA. Shh(n-5) signaling was significantly reduced in comparison to ShhC25S and ShhC25A. **(C)** Analysis of relative luciferase activity as a function of recombinant ligand expressed per transfected cell (pg/cell). Though the cellular distribution of Shh(n-5) is comparable to ShhC25S and ShhC25A, its EC_{50} (0.090) is markedly higher. Thus, the significant reduction in signal potency is due to the amino terminal deletion and is attributed to more than just a loss of the palmitoyl adduct.

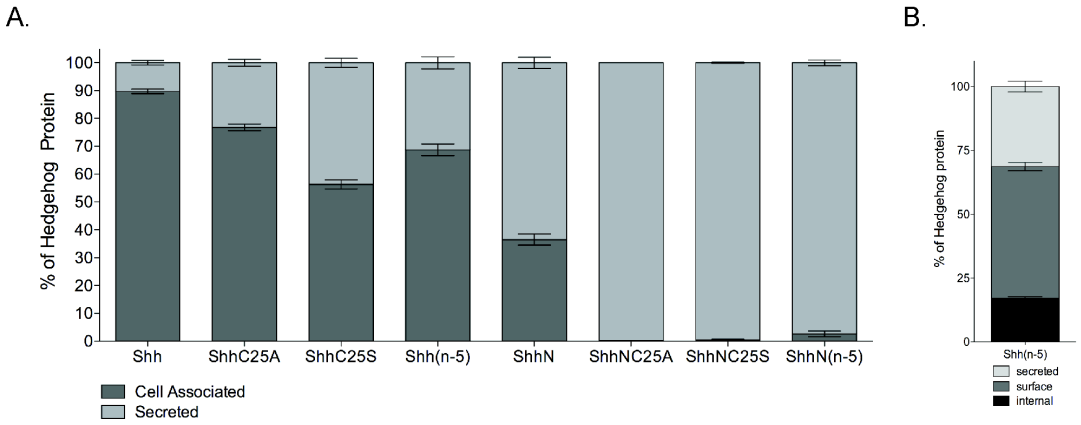

Figure A6. Cellular distribution of Shh(n-5) is comparable to other mutant recombinant Shh constructs lacking the palmitoyl adduct. (A) As described (Figure 9B), precise quantification of recombinant Shh protein concentrations in either the cell lysate or culture medium revealed both cholesterol and palmitate modifications confer cellular association. Shown are the averages of Shh protein measurements from cells transfected with cDNA (62.5 ng to 500 ng in two fold increments). Shown here is Shh(n-5) and ShhN(n-5) which were omitted from figure 9B. Shh(n-5) is not modified by palmitate and is lacking amino acid residues C25 to R29. Shh protein, measured in lysates from cells expressing Shh(n-5) resulted in approximately 68% of protein secreted. This is comparable to results from ShhC25A and ShhC25S (Figure 9B). Less than 5% of ShhN(n-5) protein is cell associated which is consistent with data from ShhNC25A and ShhNC25S; all three of these recombinant Shh proteins are not lipid modified. **(B)** Shown are integrated data from ELISA and flow cytometric measurements of recombinant form of Shh(n-5) expressed inside cells, on the cell surface, or secreted in the culture medium. Protein distribution within the cell is comparable to ShhC25A and ShhC25S, that also lack a palmitoyl adduct (Figure 13).

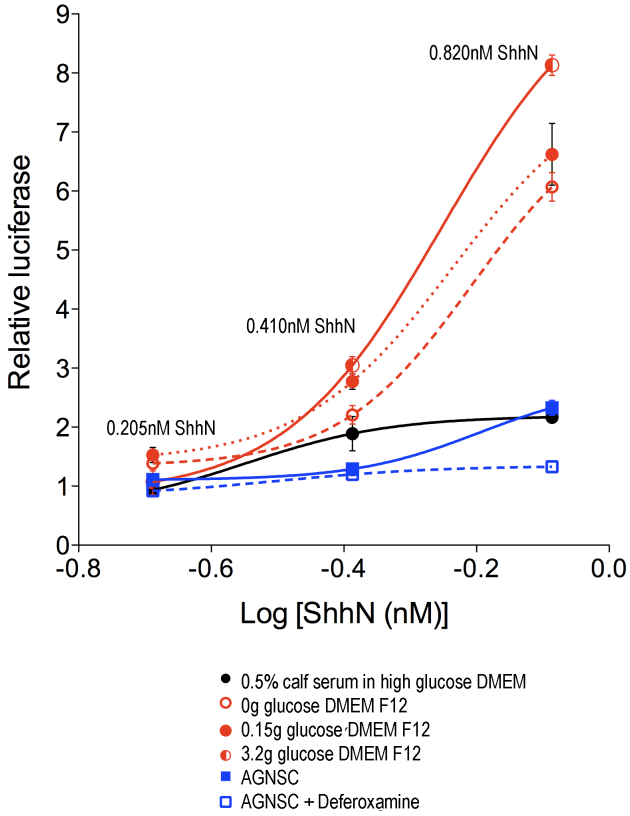

Figure A7. DMEM-F12 medium enhances Gli-reporter based Shh signaling assays. Light 2 cells (a clonal NIH 3T3 cell line stably incorporating Gli-dependent firefly luciferase and constitutive *Renilla* luciferase reporters) were incubated for 38 hours with three different concentrations of ShhN conditioned medium (0.21, 0.41, and 0.82 nM) in 0.5% calf serum in either high glucose DMEM, DMEM-F12, or adherent glioma neural stem cell medium (AGNSC). Shown are relative firefly luciferase values, normalized to *Renilla* luciferase, as a function of Shh protein (nM) added. Using DMEM-F12 markedly enhances Shh signaling.

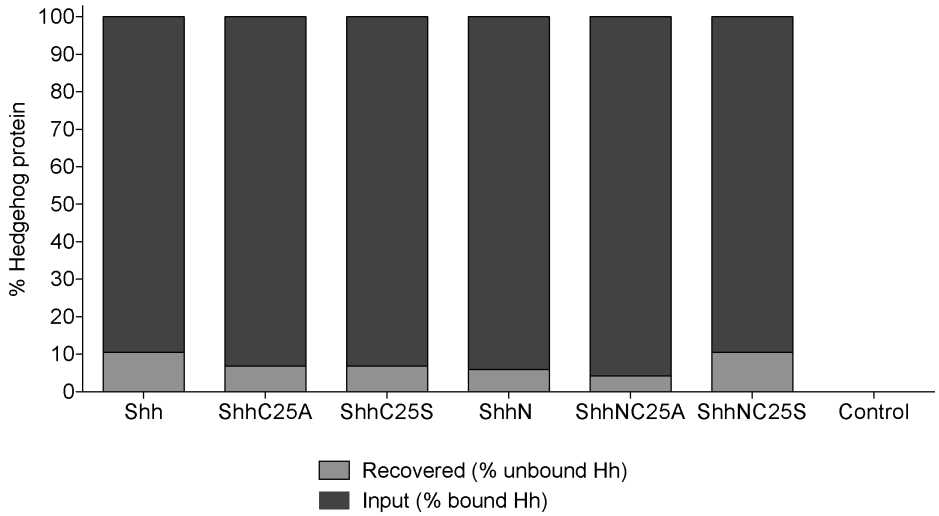

Figure A8. Shh conditioned medium from recombinant wild-type and mutant Shh bind to 5E1 conjugated beads with similar affinity. Conditioned medium was collected from HEK293T cells transfected with recombinant Shh constructs (Shh, ShhC25A, ShhC25S, ShhN, ShhNC25A, and ShhNC25S) and control (untransfected). Shh conditioned medium was quantified via ELISA. The same concentration of Shh protein and the same volume of conditioned medium (DMEM was added to supplement the volume where needed) was purified using a 5E1 Affi-Gel affinity matrix column. Shown is the percent of Hh protein that bound to the column and what was recovered after passing the medium through the column. The unbound Shh protein was quantified by ELISA and subtracted from the input concentration to determine Each of the recombinant Shh constructs bound 5E1 with similar affinities.

earlier the five amino acid deletion may interfere with the ability of heparin (from HSPGs) to correctly associate with the C-W domain with in Shh.

Figure A9: The role of Shh lipid adducts in Shh temporal expression

These data support the results from Shh signaling assays described in Chapter II Figure 17.

Figure A10 - Fluorescence imaging studies

By live-cell imaging we have detected ShhA193-EGFP within transfected cells and also in neighboring cells. These studies were performed in another Shh-responsive cell line, C3H10T1/2 mouse embryonic fibroblasts (Pepinsky et al. 1998), that are larger than NIH3T3 cells and have more extensive membrane projections. Fluorescent protein subcellular localization markers in live cells and antibody staining in fixed cells may be used to characterize the cellular compartments in which the various Shh-fluorescent protein molecules are localized. ShhA193-ECFP was transfected (Fugene, Roche) into one plate of cells and Ptc-EYFP was transfected into another. On the following day, both cultures were harvested, washed with PBS and coplated on a poly-lysine coated coverslip and subsequently imaged at 37˚C in a live-cell imaging chamber (Bioptechs FCS2). By this method, extensive co-localization of ShhA193-ECFP and Ptc-EYFP can be observed in vesicular compartments. Because, the cells were transfected in separate culture plates, we believe that the ShhA193-ECFP was delivered from adjacent cells in the co-culture. To confirm this observation a

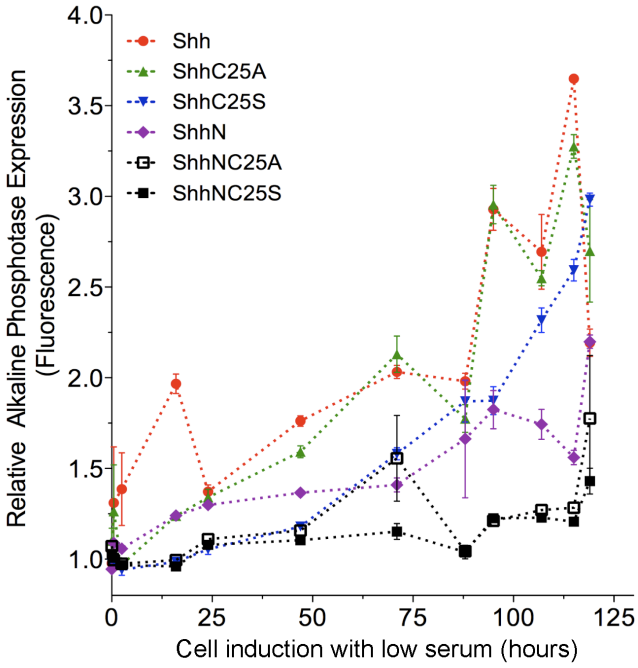

Figure A9. Role of Shh lipid adducts in osteoblast differentiation. NIH3T3 fibroblasts were transfected with equal amounts of expression plasmids for recombinant Shh (Shh, ShhC25A, ShhC25S, ShhN, ShhNC25A, or ShhNC25S), changed to low-serum medium at different time points (cell exposure to low serum medium is shown in the figure), lysed simultaneously at 120 hours, and then analyzed for alkaline phosphotase (AP) via fluorescence. Shown are relative AP levels as a function of induction time.

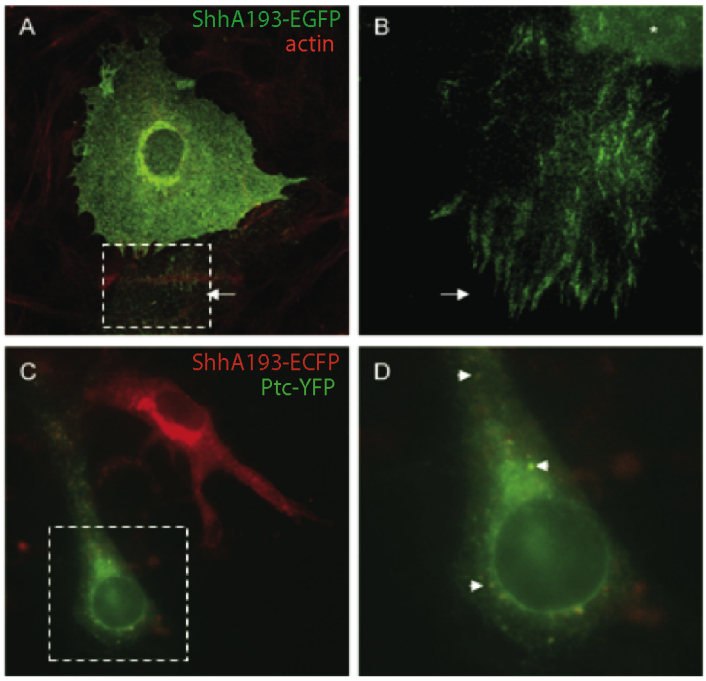

Figure A10. Images of Shh and Ptc fused to fluorescent proteins. (A & **B)** ShhA193-EGFP expression in C3H101/2 cells stained with an antibody against EGFP. Note that staining can also be detected in both transfected cells (asterisk in B) and neighboring cells (arrows in A and B). Double labeling with actin is shown in A (red staining). **(C&D)** Live cell imaging of ShhA193-ECFP (pseudocolored red) and Ptc-YFP (pseudocolored green) in separately transfected and then coplated cells. Arrowheads indicate co-localization of Shh and Ptc.

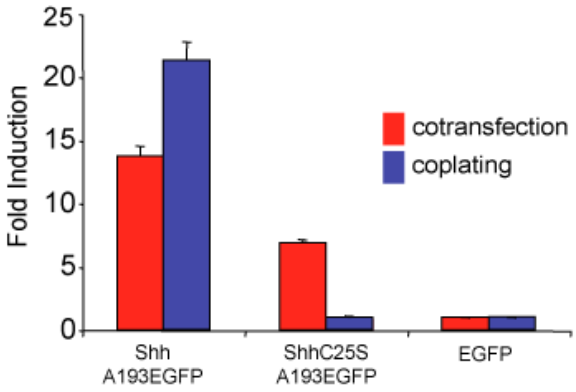

Figure A11. ShhC25SA193-EGFP retains Shh signaling. ShhA193-EGFP and ShhC25SA193-EGFP both retain the ability to signal and bind Ptc. These constructs were used to generate zebrafish transgenic lines. Note: signaling cannot be compared as protein levels were not quantified and a less responsive NIH3T3 cell line was used. See Chapter II for discussion on signaling capacity of Shh versus ShhC25S.

bicistronic vector that expresses both Ptc-EYFP and nuclear-localized dsRED fluorescent protein should be used. These findings are consistent with a second activity of Ptc to sequester Hh proteins through receptor-mediated endocytosis (Chen and Struhl 1996; Incardona et al. 2000).

Shh lipid adducts and association with cytonemes

Additional studies described below are inspired by generation of Shh-FL proteins and preliminary results from Figure A10. Cytonemes, thin actin based filaments, that project from cells in a purposely oriented and specifically distributed manner are thought to be involved in morphogen trafficking and long range cellular communication (Reviewed in (Bryant 1999)). From *in vitro* experiments using wing disc fragments, cytonemes on imaginal wing discs are induced by tissue fragments containing the signaling center associated with the anterior-posterior boundary. Additionally, formation of cytonemes are dependent on attractive signals such as Hh and fibroblast growth factor (FGF). It appears that cytonemes are not limited to *Drosophila* and have been observed in cultured limb buds subjected to FGF and in chick embryo cells (Ramirez-Weber and Kornberg 1999; Roy et al. 2011). Viruses also use cytonemes and similar cellular projections to spread from cell to cell. Viral pathogens use these filopodial type bridges mediated by ligand receptors to transfer surface associated complexes and cytoplasmic content between cells (Reviewed in (Sherer and Mothes 2008)).

Cytonemes are particularly interesting when considering a lipid modified morphogen and how it may be secreted and handled in the context of long range

signaling (Reviewed in (Teleman et al. 2001)). Intriguing is the possibility that distant cells may be in contact via cytonemes with Hh generating cells. If cytonemes, or other cellular extensions, are involved in Shh signaling, then they could transport Shh or a downstream signaling component. Graded activity of the Shh pathway could be accounted for by time- or transport-dependent decay of the intermediate as it cycles back to the cell body. Cytonemes are destroyed by fixatives like formaldehyde and methanol (Reviewed in (Bryant 1999)), and therefore live-imaging of Shh-FP molecules or electron microscopy are well suited for these types of studies.

Preliminary results, by live-cell imaging and antibody staining, demonstrate detection of ShhA193-EGFP within transfected cells and also in neighboring, untransfected cells (Figure A10). These studies were performed in another Shh-responsive cell line, C3H10T1/2 mouse embryonic fibroblasts (Pepinsky et al. 1998), that are larger than NIH3T3 cells and have more extensive membrane projections. One interesting observation is that ShhA193-EGFP can be detected in neighboring cells in structures that resemble focal adhesions (arrows in Figure A10 A and B). This observation may relate to the previously reported finding that C3H10T1/2 cells attach readily to ShhN coated plates, but not to plates coated with amino-terminal truncated ShhN, indicating that the amino-terminus may promote cell-extracellular matrix contact (Williams et al. 1999). Shh association and trafficking via cytonemes would be interesting to pursue further. Additionally, filopodia type structures are visible during zebrafish gastrulation (Besser et al. 2007). It would be fascinating to determine if

cytonemes are in fact present in zebrafish, if they serve a purpose in gradient formation or morphogen trafficking, and what role, if any, the Hh lipid adducts play.

Figure A12: Shh protein is detectable in human cerebrospinal fluid

In mice embryos, Shh was detected in the circulating embryonic cerebrospinal fluid (CSF) (Huang et al. 2010). It is of interest to determine whether human adult CSF also contains Shh and whether the presence of absence correlates with diseases known to have a role for Shh. If, for example, patients with Shh responsive gliomas (Ehtesham et al. 2007), show elevated Shh levels, this could provide physicians with another diagnostic tool to determine a disease state. Current methods (ELISA) are only barely able to detected Shh protein levels within the CSF. Concentrating Shh protein by affinity chromatography using 5E1 anti-Shh antibody may help increase detection by ELISA.

A2.2 – Alternative zebrafish experiments

Alternate approaches to visualizing Shh-EGFP

Our main concern is inadequate levels of zShh-EGFP expression, which will hinder use of live embryo imaging techniques. To compensate, we have described immunohistochemistry experiments that will use EGFP antibody detection instead. With this technique we still may not be able to visualize zShh-

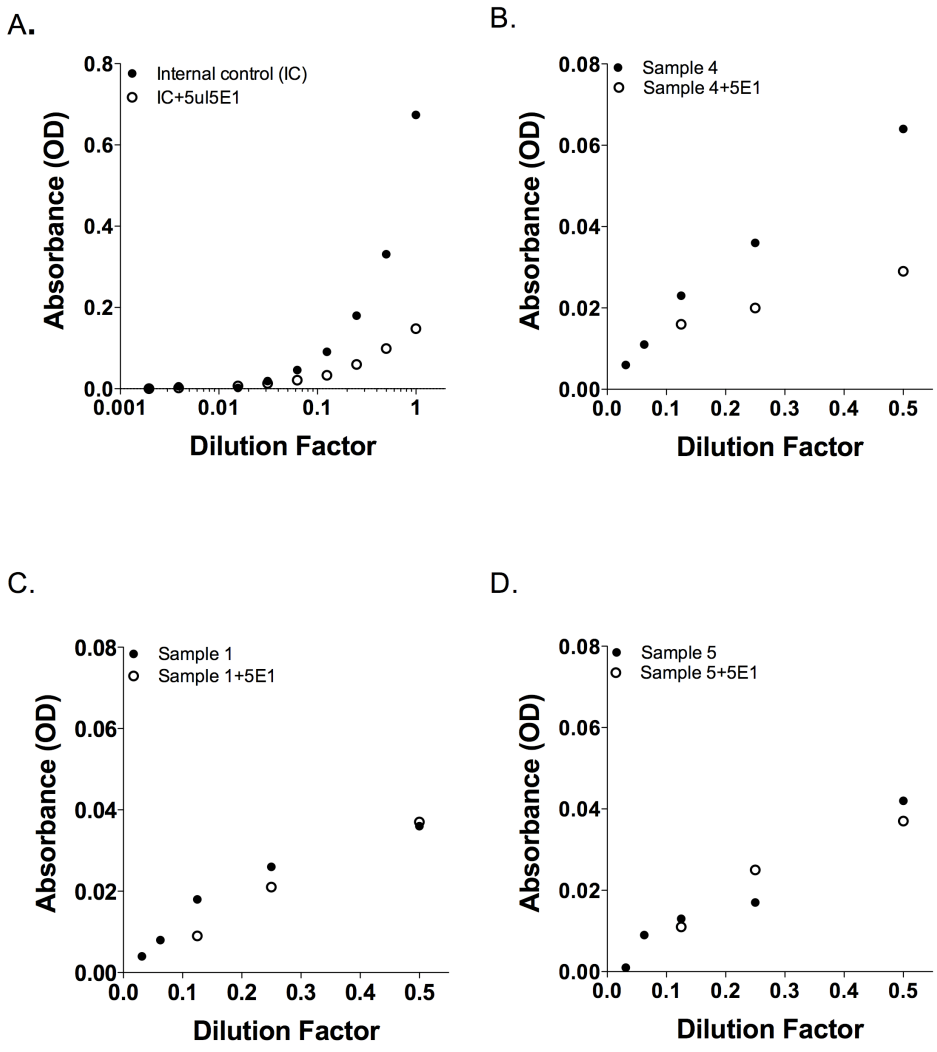

Figure A12. Shh protein is detectable in human cerebrospinal fluid. We examined human CSF in three samples and control (purified Shh protein). Each sample was analyzed over several dilutions by ELISA (filled circle). To determine specificity of Shh signal, Shh protein was pre-incubated with excess 5E1 anti-Shh monoclonal antibody prior to ELISA (open circle). **(A)** As expected, in the control sample (purified Shh protein), Shh was detected and neutralized with the 5E1. **(B)** In sample 4 (CSF from a patient with Multiple Sclerosis), Shh protein can be measured above background and is also diminished upon 5E1 incubation. (**C** & **D**) Either no Shh protein is present or protein amounts are below the level of detection. Sample 5 is from a patient with optic neuritis and otherwise normal CSF.

EGFP in structures away from the source of signal. As an alternative, we will use Tyramide Signal Amplification system (Perkin Elmer) that uses the catalytic activity of horseradish peroxidase and fluorescent tyramide substrates to generate reactive tyramide species that covalently bind to the enzyme activity site in order to increase detection sensitivity. Shh is a diffusible ligand, therefore we may lose Shh protein while fixing the embryo during washing steps, thus a more stringent fixing method that uses ethanol, paraformaldehyde and acetic acid may be required. In addition, *Tg*[*UAS-zShh-EGFP*] and *Tg*[*UAS-zShh*^{C24S}*EGFP*] lines may have sufficient amounts of endogenous Shh present to compensate for any abnormality in hedgehog signaling, thus we may not be able to observe changes in markers of graded signaling. Therefore, generating these lines in *syu*^{t4} (Schauerte et al. 1998; Park et al. 2004) background would be useful.

REFERENCES

Aanstad, P., Santos, N., Corbit, K.C., Scherz, P.J., Trinh le, A., Salvenmoser, W., Huisken, J., Reiter, J.F., and Stainier, D.Y. 2009. The extracellular domain of Smoothened regulates ciliary localization and is required for high-level Hh signaling. *Curr Biol* **19**(12): 1034-1039.

Abe, Y., Kita, Y., and Niikura, T. 2008. Mammalian Gup1, a homolog of Saccharomyces cerevisiae glycerol uptake/transporter 1, acts as a negative regulator for N-terminal palmitoylation of Sonic hedgehog. *FEBS J* **275**(2): 318-331.

Allen, B.L., Song, J.Y., Izzi, L., Althaus, I.W., Kang, J.S., Charron, F., Krauss, R.S., and McMahon, A.P. 2011. Overlapping roles and collective requirement for the coreceptors GAS1, CDO, and BOC in SHH pathway function. *Dev Cell* **20**(6): 775-787.

Allen, B.L., Tenzen, T., and McMahon, A.P. 2007. The Hedgehog-binding proteins Gas1 and Cdo cooperate to positively regulate Shh signaling during mouse development. *Genes Dev* **21**(10): 1244-1257.

Banning, C., Votteler, J., Hoffmann, D., Koppensteiner, H., Warmer, M., Reimer, R., Kirchhoff, F., Schubert, U., Hauber, J., and Schindler, M. 2010. A flow cytometry-based FRET assay to identify and analyse protein-protein interactions in living cells. *PLoS One* **5**(2): e9344.

Beachy, P.A., Hymowitz, S.G., Lazarus, R.A., Leahy, D.J., and Siebold, C. 2010. Interactions between Hedgehog proteins and their binding partners come into view. *Genes Dev* **24**(18): 2001-2012.

Belloni, E., Muenke, M., Roessler, E., Traverso, G., Siegel-Bartelt, J., Frumkin, A., Mitchell, H.F., Donis-Keller, H., Helms, C., Hing, A.V., Heng, H.H., Koop, B., Martindale, D., Rommens, J.M., Tsui, L.C., and Scherer, S.W. 1996. Identification of Sonic hedgehog as a candidate gene responsible for holoprosencephaly. *Nat Genet* **14**(3): 353-356.

Berman, D.M., Karhadkar, S.S., Maitra, A., Montes De Oca, R., Gerstenblith, M.R., Briggs, K., Parker, A.R., Shimada, Y., Eshleman, J.R., Watkins, D.N., and Beachy, P.A. 2003. Widespread requirement for Hedgehog ligand stimulation in growth of digestive tract tumours. *Nature* **425**(6960): 846-851.

Bernfield, M., Gotte, M., Park, P.W., Reizes, O., Fitzgerald, M.L., Lincecum, J., and Zako, M. 1999. Functions of cell surface heparan sulfate proteoglycans. *Annu Rev Biochem* **68**: 729-777.

Besser, J., Leito, J.T., van der Meer, D.L., and Bagowski, C.P. 2007. Tip-1 induces filopodia growth and is important for gastrulation movements during zebrafish development. *Dev Growth Differ* **49**(3): 205-214.

Bitgood, M.J., Shen, L., and McMahon, A.P. 1996. Sertoli cell signaling by Desert hedgehog regulates the male germline. *Curr Biol* **6**(3): 298-304.

Bosanac, I., Maun, H.R., Scales, S.J., Wen, X., Lingel, A., Bazan, J.F., de Sauvage, F.J., Hymowitz, S.G., and Lazarus, R.A. 2009. The structure of SHH in complex with HHIP reveals a recognition role for the Shh pseudo active site in signaling. *Nat Struct Mol Biol* **16**(7): 691-697.

Briscoe, J., Chen, Y., Jessell, T.M., and Struhl, G. 2001. A hedgehog-insensitive form of patched provides evidence for direct long-range morphogen activity of sonic hedgehog in the neural tube. *Mol Cell* **7**(6): 1279-1291.

Briscoe, J., Pierani, A., Jessell, T.M., and Ericson, J. 2000. A homeodomain protein code specifies progenitor cell identity and neuronal fate in the ventral neural tube. *Cell* **101**(4): 435-445.

Bryant, P.J. 1999. Filopodia: fickle fingers of cell fate? *Curr Biol* **9**(17): R655-657.

Buglino, J.A. and Resh, M.D. 2008. Hhat is a palmitoylacyltransferase with specificity for N-palmitoylation of Sonic Hedgehog. *J Biol Chem* **283**(32): 22076-22088.

Bumcrot, D.A., Takada, R., and McMahon, A.P. 1995. Proteolytic processing yields two secreted forms of sonic hedgehog. *Mol Cell Biol* **15**(4): 2294-2303.

Burke, R., Nellen, D., Bellotto, M., Hafen, E., Senti, K.A., Dickson, B.J., and Basler, K. 1999. Dispatched, a novel sterol-sensing domain protein dedicated to the release of cholesterol-modified hedgehog from signaling cells. *Cell* **99**(7): 803-815.

Capurro, M.I., Xu, P., Shi, W., Li, F., Jia, A., and Filmus, J. 2008. Glypican-3 inhibits Hedgehog signaling during development by competing with patched for Hedgehog binding. *Dev Cell* **14**(5): 700-711.

Caspary, T., Garcia-Garcia, M.J., Huangfu, D., Eggenschwiler, J.T., Wyler, M.R., Rakeman, A.S., Alcorn, H.L., and Anderson, K.V. 2002. Mouse Dispatched homolog1 is required for long-range, but not juxtacrine, Hh signaling. *Curr Biol* **12**(18): 1628-1632.

Chamberlain, C.E., Jeong, J., Guo, C., Allen, B.L., and McMahon, A.P. 2008. Notochord-derived Shh concentrates in close association with the apically positioned basal body in neural target cells and forms a dynamic gradient during neural patterning. *Development* **135**(6): 1097-1106.

Chamoun, Z., Mann, R.K., Nellen, D., von Kessler, D.P., Bellotto, M., Beachy, P.A., and Basler, K. 2001. Skinny hedgehog, an acyltransferase required for palmitoylation and activity of the hedgehog signal. *Science* **293**(5537): 2080-2084.

Chan, J.A., Balasubramanian, S., Witt, R.M., Nazemi, K.J., Choi, Y., Pazyra-Murphy, M.F., Walsh, C.O., Thompson, M., and Segal, R.A. 2009. Proteoglycan interactions with Sonic Hedgehog specify mitogenic responses. *Nat Neurosci* **12**(4): 409-417.

Chang, B.E., Blader, P., Fischer, N., Ingham, P.W., and Strahle, U. 1997. Axial (HNF3beta) and retinoic acid receptors are regulators of the zebrafish sonic hedgehog promoter. *EMBO J* **16**(13): 3955-3964.

Chang, T.Y., Chang, C.C., Ohgami, N., and Yamauchi, Y. 2006. Cholesterol sensing, trafficking, and esterification. *Annu Rev Cell Dev Biol* **22**: 129-157.

Charron, F., Stein, E., Jeong, J., McMahon, A.P., and Tessier-Lavigne, M. 2003. The morphogen sonic hedgehog is an axonal chemoattractant that collaborates with netrin-1 in midline axon guidance. *Cell* **113**(1): 11-23.

Chen, M.H., Li, Y.J., Kawakami, T., Xu, S.M., and Chuang, P.T. 2004. Palmitoylation is required for the production of a soluble multimeric Hedgehog protein complex and long-range signaling in vertebrates. *Genes Dev* **18**(6): 641-659.

Chen, X., Tukachinsky, H., Huang, C.H., Jao, C., Chu, Y.R., Tang, H.Y., Mueller, B., Schulman, S., Rapoport, T.A., and Salic, A. 2011. Processing and turnover of the Hedgehog protein in the endoplasmic reticulum. *J Cell Biol* **192**(5): 825-838.

Chen, Y. and Struhl, G. 1996. Dual roles for patched in sequestering and transducing Hedgehog. *Cell* **87**(3): 553-563.

Chiang, C., Litingtung, Y., Lee, E., Young, K.E., Corden, J.L., Westphal, H., and Beachy, P.A. 1996. Cyclopia and defective axial patterning in mice lacking Sonic hedgehog gene function. *Nature* **383**(6599): 407-413.

Chuang, P.T. and McMahon, A.P. 1999. Vertebrate Hedgehog signalling modulated by induction of a Hedgehog-binding protein. *Nature* **397**(6720): 617-621.

Cohen, M.M., Jr. 2002. Malformations of the craniofacial region: evolutionary, embryonic, genetic, and clinical perspectives. *Am J Med Genet* **115**(4): 245-268.

Cooper, M.K., Porter, J.A., Young, K.E., and Beachy, P.A. 1998. Teratogen-mediated inhibition of target tissue response to Shh signaling. *Science* **280**(5369): 1603-1607.

Cooper, M.K., Wassif, C.A., Krakowiak, P.A., Taipale, J., Gong, R., Kelley, R.I., Porter, F.D., and Beachy, P.A. 2003. A defective response to Hedgehog signaling in disorders of cholesterol biosynthesis. *Nat Genet* **33**(4): 508-513.

Crump, J.G., Maves, L., Lawson, N.D., Weinstein, B.M., and Kimmel, C.B. 2004. An essential role for Fgfs in endodermal pouch formation influences later craniofacial skeletal patterning. *Development* **131**(22): 5703-5716.

Currie, P.D. and Ingham, P.W. 1996. Induction of a specific muscle cell type by a hedgehog-like protein in zebrafish. *Nature* **382**(6590): 452-455.

Davidson, A.E., Balciunas, D., Mohn, D., Shaffer, J., Hermanson, S., Sivasubbu, S., Cliff, M.P., Hackett, P.B., and Ekker, S.C. 2003. Efficient gene delivery and gene expression in zebrafish using the Sleeping Beauty transposon. *Dev Biol* **263**(2): 191-202.

Day, E.S., Wen, D., Garber, E.A., Hong, J., Avedissian, L.S., Rayhorn, P., Shen, W., Zeng, C., Bailey, V.R., Reilly, J.O., Roden, J.A., Moore, C.B., Williams, K.P., Galdes, A., Whitty, A., and Baker, D.P. 1999. Zinc-dependent structural stability of human Sonic hedgehog. *Biochemistry* **38**(45): 14868-14880.

DeCamp, D.L., Thompson, T.M., de Sauvage, F.J., and Lerner, M.R. 2000. Smoothened activates Galphai-mediated signaling in frog melanophores. *J Biol Chem* **275**(34): 26322-26327.

Desbordes, S.C. and Sanson, B. 2003. The glypican Dally-like is required for Hedgehog signalling in the embryonic epidermis of Drosophila. *Development* **130**(25): 6245-6255.

Dessaud, E., Yang, L.L., Hill, K., Cox, B., Ulloa, F., Ribeiro, A., Mynett, A., Novitch, B.G., and Briscoe, J. 2007. Interpretation of the sonic hedgehog morphogen gradient by a temporal adaptation mechanism. *Nature* **450**(7170): 717-720.

Dierker, T., Dreier, R., Petersen, A., Bordych, C., and Grobe, K. 2009. Heparan sulfate-modulated, metalloprotease-mediated sonic hedgehog release from producing cells. *J Biol Chem* **284**(12): 8013-8022.

Dorus, S., Anderson, J.R., Vallender, E.J., Gilbert, S.L., Zhang, L., Chemnick, L.G., Ryder, O.A., Li, W., and Lahn, B.T. 2006. Sonic Hedgehog, a key development gene, experienced intensified molecular evolution in primates. *Hum Mol Genet* **15**(13): 2031-2037.

Dye, B.T. 2005. Flow cytometric analysis of CFP-YFP FRET as a marker for in vivo protein-protein interaction. *Clinical and Applied Immunology Reviews* **5**: 307-324.

Eaton, S. 2008. Multiple roles for lipids in the Hedgehog signalling pathway. *Nat Rev Mol Cell Biol* **9**(6): 437-445.

Echelard, Y., Epstein, D.J., St-Jacques, B., Shen, L., Mohler, J., McMahon, J.A., and McMahon, A.P. 1993. Sonic hedgehog, a member of a family of putative signaling molecules, is implicated in the regulation of CNS polarity. *Cell* **75**(7): 1417-1430.

Ehtesham, M., Sarangi, A., Valadez, J.G., Chanthaphaychith, S., Becher, M.W., Abel, T.W., Thompson, R.C., and Cooper, M.K. 2007. Ligand-dependent activation of the hedgehog pathway in glioma progenitor cells. *Oncogene* **26**(39): 5752-5761.

Ekker, S.C., Ungar, A.R., Greenstein, P., von Kessler, D.P., Porter, J.A., Moon, R.T., and Beachy, P.A. 1995. Patterning activities of vertebrate hedgehog proteins in the developing eye and brain. *Curr Biol* **5**(8): 944-955.

Epstein, D.J., McMahon, A.P., and Joyner, A.L. 1999. Regionalization of Sonic hedgehog transcription along the anteroposterior axis of the mouse central nervous system is regulated by Hnf3-dependent and -independent mechanisms. *Development* **126**(2): 281-292.

Ericson, J., Morton, S., Kawakami, A., Roelink, H., and Jessell, T.M. 1996. Two critical periods of Sonic Hedgehog signaling required for the specification of motor neuron identity. *Cell* **87**(4): 661-673.

Ericson, J., Rashbass, P., Schedl, A., Brenner-Morton, S., Kawakami, A., van Heyningen, V., Jessell, T.M., and Briscoe, J. 1997. Pax6 controls progenitor cell identity and neuronal fate in response to graded Shh signaling. *Cell* **90**(1): 169-180.

Etheridge, L.A., Crawford, T.Q., Zhang, S., and Roelink, H. 2010. Evidence for a role of vertebrate Disp1 in long-range Shh signaling. *Development* **137**(1): 133-140.

Feng, J., White, B., Tyurina, O.V., Guner, B., Larson, T., Lee, H.Y., Karlstrom, R.O., and Kohtz, J.D. 2004. Synergistic and antagonistic roles of the Sonic hedgehog N- and C-terminal lipids. *Development* **131**(17): 4357-4370.

Fischer, J.A., Giniger, E., Maniatis, T., and Ptashne, M. 1988. GAL4 activates transcription in Drosophila. *Nature* **332**(6167): 853-856.

Fuse, N., Maiti, T., Wang, B., Porter, J.A., Hall, T.M., Leahy, D.J., and Beachy, P.A. 1999. Sonic hedgehog protein signals not as a hydrolytic enzyme but as an apparent ligand for patched. *Proc Natl Acad Sci U S A* **96**(20): 10992-10999.

Gallet, A., Rodriguez, R., Ruel, L., and Therond, P.P. 2003. Cholesterol modification of hedgehog is required for trafficking and movement, revealing an asymmetric cellular response to hedgehog. *Dev Cell* **4**(2): 191-204.

Geng, X., Speirs, C., Lagutin, O., Inbal, A., Liu, W., Solnica-Krezel, L., Jeong, Y., Epstein, D.J., and Oliver, G. 2008. Haploinsufficiency of Six3 fails to activate Sonic hedgehog expression in the ventral forebrain and causes holoprosencephaly. *Dev Cell* **15**(2): 236-247.

George, R.A. and Heringa, J. 2002. An analysis of protein domain linkers: their classification and role in protein folding. *Protein Eng* **15**(11): 871-879.

Giniger, E. and Ptashne, M. 1988. Cooperative DNA binding of the yeast transcriptional activator GAL4. *Proc Natl Acad Sci U S A* **85**(2): 382-386.

Giniger, E., Varnum, S.M., and Ptashne, M. 1985. Specific DNA binding of GAL4, a positive regulatory protein of yeast. *Cell* **40**(4): 767-774.

Goetz, J.A., Singh, S., Suber, L.M., Kull, F.J., and Robbins, D.J. 2006. A highly conserved amino-terminal region of sonic hedgehog is required for the formation of its freely diffusible multimeric form. *J Biol Chem* **281**(7): 4087-4093.

Goll, M.G., Anderson, R., Stainier, D.Y., Spradling, A.C., and Halpern, M.E. 2009. Transcriptional silencing and reactivation in transgenic zebrafish. *Genetics* **182**(3): 747-755.

Goodrich, L.V., Jung, D., Higgins, K.M., and Scott, M.P. 1999. Overexpression of ptc1 inhibits induction of Shh target genes and prevents normal patterning in the neural tube. *Dev Biol* **211**(2): 323-334.

Goodrich, L.V., Milenkovic, L., Higgins, K.M., and Scott, M.P. 1997. Altered neural cell fates and medulloblastoma in mouse patched mutants. *Science* **277**(5329): 1109-1113.

Guerrero, I. and Chiang, C. 2007. A conserved mechanism of Hedgehog gradient formation by lipid modifications. *Trends Cell Biol* **17**(1): 1-5.

Hackett, P.B., Ekker, S.C., Largaespada, D.A., and McIvor, R.S. 2005. Sleeping beauty transposon-mediated gene therapy for prolonged expression. *Adv Genet* **54**: 189-232.

Hahn, H., Wicking, C., Zaphiropoulous, P.G., Gailani, M.R., Shanley, S., Chidambaram, A., Vorechovsky, I., Holmberg, E., Unden, A.B., Gillies, S., Negus, K., Smyth, I., Pressman, C., Leffell, D.J., Gerrard, B., Goldstein, A.M., Dean, M., Toftgard, R., Chenevix-Trench, G., Wainwright, B., and Bale, A.E. 1996. Mutations of the human homolog of Drosophila patched in the nevoid basal cell carcinoma syndrome. *Cell* **85**(6): 841-851.

Hall, T.M., Porter, J.A., Beachy, P.A., and Leahy, D.J. 1995. A potential catalytic site revealed by the 1.7-A crystal structure of the amino-terminal signalling domain of Sonic hedgehog. *Nature* **378**(6553): 212-216.

Hall, T.M., Porter, J.A., Young, K.E., Koonin, E.V., Beachy, P.A., and Leahy, D.J. 1997. Crystal structure of a Hedgehog autoprocessing domain: homology between Hedgehog and self-splicing proteins. *Cell* **91**(1): 85-97.

Han, C., Belenkaya, T.Y., Wang, B., and Lin, X. 2004. Drosophila glypicans control the cell-to-cell movement of Hedgehog by a dynamin-independent process. *Development* **131**(3): 601-611.

Harfe, B.D. 2011. Keeping up with the zone of polarizing activity: New roles for an old signaling center. *Dev Dyn* **240**(5): 915-919.

Harfe, B.D., Scherz, P.J., Nissim, S., Tian, H., McMahon, A.P., and Tabin, C.J. 2004. Evidence for an expansion-based temporal Shh gradient in specifying vertebrate digit identities. *Cell* **118**(4): 517-528.

Hauptmann, G. and Gerster, T. 2000. Multicolor whole-mount in situ hybridization. *Methods Mol Biol* **137**: 139-148.

He, L., Wu, X., Simone, J., Hewgill, D., and Lipsky, P.E. 2005. Determination of tumor necrosis factor receptor-associated factor trimerization in living cells by CFP->YFP->mRFP FRET detected by flow cytometry. *Nucleic acids research* **33**(6): e61.

Hermanson, S., Davidson, A.E., Sivasubbu, S., Balciunas, D., and Ekker, S.C. 2004. Sleeping Beauty transposon for efficient gene delivery. *Methods Cell Biol* **77**: 349-362.

Huang, P. and Schier, A.F. 2009. Dampened Hedgehog signaling but normal Wnt signaling in zebrafish without cilia. *Development* **136**(18): 3089-3098.

Huang, X., Litingtung, Y., and Chiang, C. 2007. Region-specific requirement for cholesterol modification of sonic hedgehog in patterning the telencephalon and spinal cord. *Development* **134**(11): 2095-2105.

Huang, X., Liu, J., Ketova, T., Fleming, J.T., Grover, V.K., Cooper, M.K., Litingtung, Y., and Chiang, C. 2010. Transventricular delivery of Sonic hedgehog is essential to cerebellar ventricular zone development. *Proc Natl Acad Sci U S A* **107**(18): 8422-8427.

Huangfu, D. and Anderson, K.V. 2005. Cilia and Hedgehog responsiveness in the mouse. *Proc Natl Acad Sci U S A* **102**(32): 11325-11330.

Inbal, A., Topczewski, J., and Solnica-Krezel, L. 2006. Targeted gene expression in the zebrafish prechordal plate. *Genesis* **44**(12): 584-588.

Incardona, J.P., Lee, J.H., Robertson, C.P., Enga, K., Kapur, R.P., and Roelink, H. 2000. Receptor-mediated endocytosis of soluble and membrane-tethered Sonic hedgehog by Patched-1. *Proc Natl Acad Sci U S A* **97**(22): 12044-12049.

Ingham, P.W. and McMahon, A.P. 2001. Hedgehog signaling in animal development: paradigms and principles. *Genes Dev* **15**(23): 3059-3087.

Ingham, P.W., Nakano, Y., and Seger, C. 2011. Mechanisms and functions of Hedgehog signalling across the metazoa. *Nat Rev Genet* **12**(6): 393-406.

Izzi, L., Levesque, M., Morin, S., Laniel, D., Wilkes, B.C., Mille, F., Krauss, R.S., McMahon, A.P., Allen, B.L., and Charron, F. 2011. Boc and Gas1 each form distinct Shh receptor complexes with Ptch1 and are required for Shh-mediated cell proliferation. *Dev Cell* **20**(6): 788-801.

Jacob, J. and Briscoe, J. 2003. Gli proteins and the control of spinal-cord patterning. *EMBO Rep* **4**(8): 761-765.

Jaillon, O., Aury, J.M., Brunet, F., Petit, J.L., Stange-Thomann, N., Mauceli, E., Bouneau, L., Fischer, C., Ozouf-Costaz, C., Bernot, A., Nicaud, S., Jaffe, D., Fisher, S., Lutfalla, G., Dossat, C., Segurens, B., Dasilva, C., Salanoubat, M., Levy, M., Boudet, N., Castellano, S., Anthouard, V., Jubin, C., Castelli, V., Katinka, M., Vacherie, B., Biemont, C., Skalli, Z., Cattolico, L., Poulain, J., De Berardinis, V., Cruaud, C., Duprat, S., Brottier, P., Coutanceau, J.P., Gouzy, J., Parra, G., Lardier, G., Chapple, C., McKernan, K.J., McEwan, P., Bosak, S., Kellis, M., Volff, J.N., Guigo, R., Zody, M.C., Mesirov, J., Lindblad-Toh, K., Birren, B., Nusbaum, C., Kahn, D., Robinson-Rechavi, M., Laudet, V., Schachter, V., Quetier, F., Saurin, W., Scarpelli, C., Wincker, P., Lander, E.S., Weissenbach, J., and Roest Crollius, H. 2004. Genome duplication in the teleost fish Tetraodon nigroviridis reveals the early vertebrate proto-karyotype. *Nature* **431**(7011): 946-957.

Jeong, J. and McMahon, A.P. 2005. Growth and pattern of the mammalian neural tube are governed by partially overlapping feedback activities of the hedgehog antagonists patched 1 and Hhip1. *Development* **132**(1): 143-154.

Jeong, Y., El-Jaick, K., Roessler, E., Muenke, M., and Epstein, D.J. 2006. A functional screen for sonic hedgehog regulatory elements across a 1 Mb interval identifies long-range ventral forebrain enhancers. *Development* **133**(4): 761-772.

Jeong, Y., Leskow, F.C., El-Jaick, K., Roessler, E., Muenke, M., Yocum, A., Dubourg, C., Li, X., Geng, X., Oliver, G., and Epstein, D.J. 2008. Regulation of a remote Shh forebrain enhancer by the Six3 homeoprotein. *Nat Genet* **40**(11): 1348-1353.

Jessell, T.M. 2000. Neuronal specification in the spinal cord: inductive signals and transcriptional codes. *Nat Rev Genet* **1**(1): 20-29.

Jiang, J. and Hui, C.C. 2008. Hedgehog signaling in development and cancer. *Dev Cell* **15**(6): 801-812.

Johnson, R.L., Rothman, A.L., Xie, J., Goodrich, L.V., Bare, J.W., Bonifas, J.M., Quinn, A.G., Myers, R.M., Cox, D.R., Epstein, E.H., Jr., and Scott, M.P. 1996. Human homolog of patched, a candidate gene for the basal cell nevus syndrome. *Science* **272**(5268): 1668-1671.

Kavran, J.M., Ward, M.D., Oladosu, O.O., Mulepati, S., and Leahy, D.J. 2010. All mammalian Hedgehog proteins interact with cell adhesion molecule, down-regulated by oncogenes (CDO) and brother of CDO (BOC) in a conserved manner. *J Biol Chem* **285**(32): 24584-24590.

Kawakami, T., Kawcak, T., Li, Y.J., Zhang, W., Hu, Y., and Chuang, P.T. 2002. Mouse dispatched mutants fail to distribute hedgehog proteins and are defective in hedgehog signaling. *Development* **129**(24): 5753-5765.

Kim, M.S., Saunders, A.M., Hamaoka, B.Y., Beachy, P.A., and Leahy, D.J. 2011. Structure of the protein core of the glypican Dally-like and localization of a region important for hedgehog signaling. *Proc Natl Acad Sci U S A* **108**(32): 13112-13117.

Kinto, N., Iwamoto, M., Enomoto-Iwamoto, M., Noji, S., Ohuchi, H., Yoshioka, H., Kataoka, H., Wada, Y., Yuhao, G., Takahashi, H.E., Yoshiki, S., and Yamaguchi, A. 1997. Fibroblasts expressing Sonic hedgehog induce osteoblast differentiation and ectopic bone formation. *FEBS Lett* **404**(2-3): 319-323.

Kirby, B.B., Takada, N., Latimer, A.J., Shin, J., Carney, T.J., Kelsh, R.N., and Appel, B. 2006. In vivo time-lapse imaging shows dynamic oligodendrocyte progenitor behavior during zebrafish development. *Nat Neurosci* **9**(12): 1506-1511.

Koster, R.W. and Fraser, S.E. 2001. Tracing transgene expression in living zebrafish embryos. *Dev Biol* **233**(2): 329-346.

Krauss, S., Concordet, J.P., and Ingham, P.W. 1993. A functionally conserved homolog of the Drosophila segment polarity gene hh is expressed in tissues with polarizing activity in zebrafish embryos. *Cell* **75**(7): 1431-1444.

Lee, J.D., Kraus, P., Gaiano, N., Nery, S., Kohtz, J., Fishell, G., Loomis, C.A., and Treisman, J.E. 2001. An acylatable residue of Hedgehog is differentially required in Drosophila and mouse limb development. *Dev Biol* **233**(1): 122-136.

Lee, J.D. and Treisman, J.E. 2001. Sightless has homology to transmembrane acyltransferases and is required to generate active Hedgehog protein. *Curr Biol* **11**(14): 1147-1152.

Lee, J.J., Ekker, S.C., von Kessler, D.P., Porter, J.A., Sun, B.I., and Beachy, P.A. 1994. Autoproteolysis in hedgehog protein biogenesis. *Science* **266**(5190): 1528-1537.

Lee, J.J., von Kessler, D.P., Parks, S., and Beachy, P.A. 1992. Secretion and localized transcription suggest a role in positional signaling for products of the segmentation gene hedgehog. *Cell* **71**(1): 33-50.

Lettice, L.A., Heaney, S.J., Purdie, L.A., Li, L., de Beer, P., Oostra, B.A., Goode, D., Elgar, G., Hill, R.E., and de Graaff, E. 2003. A long-range Shh enhancer regulates expression in the developing limb and fin and is associated with preaxial polydactyly. *Hum Mol Genet* **12**(14): 1725-1735.

Lewis, K.E. and Eisen, J.S. 2001. Hedgehog signaling is required for primary motoneuron induction in zebrafish. *Development* **128**(18): 3485-3495.

Lewis, P.M., Dunn, M.P., McMahon, J.A., Logan, M., Martin, J.F., St-Jacques, B., and McMahon, A.P. 2001. Cholesterol modification of sonic hedgehog is required for long-range signaling activity and effective modulation of signaling by Ptc1. *Cell* **105**(5): 599-612.

Li, Y., Zhang, H., Litingtung, Y., and Chiang, C. 2006. Cholesterol modification restricts the spread of Shh gradient in the limb bud. *Proc Natl Acad Sci U S A* **103**(17): 6548-6553.

Lippincott-Schwartz, J., Altan-Bonnet, N., and Patterson, G.H. 2003. Photobleaching and photoactivation: following protein dynamics in living cells. *Nat Cell Biol* **Suppl**: S7-14.

Lum, L., Yao, S., Mozer, B., Rovescalli, A., Von Kessler, D., Nirenberg, M., and Beachy, P.A. 2003. Identification of Hedgehog pathway components by RNAi in Drosophila cultured cells. *Science* **299**(5615): 2039-2045.

Ma, Y., Erkner, A., Gong, R., Yao, S., Taipale, J., Basler, K., and Beachy, P.A. 2002. Hedgehog-mediated patterning of the mammalian embryo requires transporter-like function of dispatched. *Cell* **111**(1): 63-75.

Mann, R.K. and Beachy, P.A. 2004. Novel lipid modifications of secreted protein signals. *Annu Rev Biochem* **73**: 891-923.

Marigo, V., Davey, R.A., Zuo, Y., Cunningham, J.M., and Tabin, C.J. 1996. Biochemical evidence that patched is the Hedgehog receptor. *Nature* **384**(6605): 176-179.

Maun, H.R., Wen, X., Lingel, A., de Sauvage, F.J., Lazarus, R.A., Scales, S.J., and Hymowitz, S.G. 2010. Hedgehog pathway antagonist 5E1 binds hedgehog at the pseudo-active site. *J Biol Chem* **285**(34): 26570-26580.

Mavromatakis, Y.E., Lin, W., Metzakopian, E., Ferri, A.L., Yan, C.H., Sasaki, H., Whisett, J., and Ang, S.L. 2010. Foxa1 and Foxa2 positively and negatively regulate Shh signalling to specify ventral midbrain progenitor identity. *Mech Dev* **128**(1-2): 90-103.

McCarthy, R.A., Barth, J.L., Chintalapudi, M.R., Knaak, C., and Argraves, W.S. 2002. Megalin functions as an endocytic sonic hedgehog receptor. *J Biol Chem* **277**(28): 25660-25667.

McLellan, J.S., Yao, S., Zheng, X., Geisbrecht, B.V., Ghirlando, R., Beachy, P.A., and Leahy, D.J. 2006. Structure of a heparin-dependent complex of Hedgehog and Ihog. *Proc Natl Acad Sci U S A* **103**(46): 17208-17213.

McLellan, J.S., Zheng, X., Hauk, G., Ghirlando, R., Beachy, P.A., and Leahy, D.J. 2008. The mode of Hedgehog binding to Ihog homologues is not conserved across different phyla. *Nature* **455**(7215): 979-983.

Milenkovic, L., Scott, M.P., and Rohatgi, R. 2009. Lateral transport of Smoothened from the plasma membrane to the membrane of the cilium. *J Cell Biol* **187**(3): 365-374.

Mohler, J. and Vani, K. 1992. Molecular organization and embryonic expression of the hedgehog gene involved in cell-cell communication in segmental patterning of Drosophila. *Development* **115**(4): 957-971.

Motoyama, J., Takabatake, T., Takeshima, K., and Hui, C. 1998. Ptch2, a second mouse Patched gene is co-expressed with Sonic hedgehog. *Nat Genet* **18**(2): 104-106.

Muenke, M. and Beachy, P.A. 2000. Genetics of ventral forebrain development and holoprosencephaly. *Curr Opin Genet Dev* **10**(3): 262-269.

Muller, F., Chang, B., Albert, S., Fischer, N., Tora, L., and Strahle, U. 1999. Intronic enhancers control expression of zebrafish sonic hedgehog in floor plate and notochord. *Development* **126**(10): 2103-2116.

Nusse, R. 2003. Wnts and Hedgehogs: lipid-modified proteins and similarities in signaling mechanisms at the cell surface. *Development* **130**(22): 5297-5305.

Nusslein-Volhard, C. and Wieschaus, E. 1980. Mutations affecting segment number and polarity in Drosophila. *Nature* **287**(5785): 795-801.

Odenthal, J., van Eeden, F.J., Haffter, P., Ingham, P.W., and Nusslein-Volhard, C. 2000. Two distinct cell populations in the floor plate of the zebrafish are induced by different pathways. *Dev Biol* **219**(2): 350-363.

Ogden, S.K., Fei, D.L., Schilling, N.S., Ahmed, Y.F., Hwa, J., and Robbins, D.J. 2008. G protein Galphai functions immediately downstream of Smoothened in Hedgehog signalling. *Nature* **456**(7224): 967-970.

Ohlig, S., Farshi, P., Pickhinke, U., van den Boom, J., Hoing, S., Jakuschev, S., Hoffmann, D., Dreier, R., Scholer, H.R., Dierker, T., Bordych, C., and Grobe, K. 2011. Sonic hedgehog shedding results in functional activation of the solubilized protein. *Dev Cell* **20**(6): 764-774.

Oro, A.E., Higgins, K.M., Hu, Z., Bonifas, J.M., Epstein, E.H., Jr., and Scott, M.P. 1997. Basal cell carcinomas in mice overexpressing sonic hedgehog. *Science* **276**(5313): 817-821.

Panakova, D., Sprong, H., Marois, E., Thiele, C., and Eaton, S. 2005. Lipoprotein particles are required for Hedgehog and Wingless signalling. *Nature* **435**(7038): 58-65.

Park, H.C. and Appel, B. 2003. Delta-Notch signaling regulates oligodendrocyte specification. *Development* **130**(16): 3747-3755.

Park, H.C., Shin, J., and Appel, B. 2004. Spatial and temporal regulation of ventral spinal cord precursor specification by Hedgehog signaling. *Development* **131**(23): 5959-5969.

Paulsen, I.T., Brown, M.H., and Skurray, R.A. 1996. Proton-dependent multidrug efflux systems. *Microbiol Rev* **60**(4): 575-608.

Pepinsky, R.B., Rayhorn, P., Day, E.S., Dergay, A., Williams, K.P., Galdes, A., Taylor, F.R., Boriack-Sjodin, P.A., and Garber, E.A. 2000. Mapping sonic hedgehog-receptor interactions by steric interference. *J Biol Chem* **275**(15): 10995-11001.

Pepinsky, R.B., Zeng, C., Wen, D., Rayhorn, P., Baker, D.P., Williams, K.P., Bixler, S.A., Ambrose, C.M., Garber, E.A., Miatkowski, K., Taylor, F.R., Wang, E.A., and Galdes, A. 1998. Identification of a palmitic acid-modified form of human Sonic hedgehog. *J Biol Chem* **273**(22): 14037-14045.

Perrimon, N. and Bernfield, M. 2000. Specificities of heparan sulphate proteoglycans in developmental processes. *Nature* **404**(6779): 725-728.

Piddock, L.J. 2006. Multidrug-resistance efflux pumps - not just for resistance. *Nat Rev Microbiol* **4**(8): 629-636.

Porter, J.A., Ekker, S.C., Park, W.J., von Kessler, D.P., Young, K.E., Chen, C.H., Ma, Y., Woods, A.S., Cotter, R.J., Koonin, E.V., and Beachy, P.A. 1996a. Hedgehog patterning activity: role of a lipophilic modification mediated by the carboxy-terminal autoprocessing domain. *Cell* **86**(1): 21-34.

Porter, J.A., von Kessler, D.P., Ekker, S.C., Young, K.E., Lee, J.J., Moses, K., and Beachy, P.A. 1995. The product of hedgehog autoproteolytic cleavage active in local and long-range signalling. *Nature* **374**(6520): 363-366.

Porter, J.A., Young, K.E., and Beachy, P.A. 1996b. Cholesterol modification of hedgehog signaling proteins in animal development. *Science* **274**(5285): 255-259.

Ramirez-Weber, F.A. and Kornberg, T.B. 1999. Cytonemes: cellular processes that project to the principal signaling center in Drosophila imaginal discs. *Cell* **97**(5): 599-607.

Ransom, D.G. and Zon, L.I. 1999. Collection, storage, and use of zebrafish sperm. *Methods Cell Biol* **60**: 365-372.

Ribes, V. and Briscoe, J. 2009. Establishing and interpreting graded Sonic Hedgehog signaling during vertebrate neural tube patterning: the role of negative feedback. *Cold Spring Harb Perspect Biol* **1**(2): a002014.

Riddle, R.D., Johnson, R.L., Laufer, E., and Tabin, C. 1993. Sonic hedgehog mediates the polarizing activity of the ZPA. *Cell* **75**(7): 1401-1416.

Rietveld, A., Neutz, S., Simons, K., and Eaton, S. 1999. Association of sterol- and glycosylphosphatidylinositol-linked proteins with Drosophila raft lipid microdomains. *J Biol Chem* **274**(17): 12049-12054.

Riobo, N.A., Saucy, B., Dilizio, C., and Manning, D.R. 2006. Activation of heterotrimeric G proteins by Smoothened. *Proc Natl Acad Sci U S A* **103**(33): 12607-12612.

Roelink, H., Augsburger, A., Heemskerk, J., Korzh, V., Norlin, S., Ruiz i Altaba, A., Tanabe, Y., Placzek, M., Edlund, T., Jessell, T.M., and et al. 1994. Floor plate and motor neuron induction by vhh-1, a vertebrate homolog of hedgehog expressed by the notochord. *Cell* **76**(4): 761-775.

Roelink, H., Porter, J.A., Chiang, C., Tanabe, Y., Chang, D.T., Beachy, P.A., and Jessell, T.M. 1995. Floor plate and motor neuron induction by different concentrations of the amino-terminal cleavage product of sonic hedgehog autoproteolysis. *Cell* **81**(3): 445-455.

Roessler, E., Belloni, E., Gaudenz, K., Jay, P., Berta, P., Scherer, S.W., Tsui, L.C., and Muenke, M. 1996. Mutations in the human Sonic Hedgehog gene cause holoprosencephaly. *Nat Genet* **14**(3): 357-360.

Rohatgi, R., Milenkovic, L., Corcoran, R.B., and Scott, M.P. 2009. Hedgehog signal transduction by Smoothened: pharmacologic evidence for a 2-step activation process. *Proc Natl Acad Sci U S A* **106**(9): 3196-3201.

Rohatgi, R., Milenkovic, L., and Scott, M.P. 2007. Patched1 regulates hedgehog signaling at the primary cilium. *Science* **317**(5836): 372-376.

Rohatgi, R. and Scott, M.P. 2008. Cell biology. Arrestin' movement in cilia. *Science* **320**(5884): 1726-1727.

Roy, S., Hsiung, F., and Kornberg, T.B. 2011. Specificity of Drosophila cytonemes for distinct signaling pathways. *Science* **332**(6027): 354-358.

Rubin, J.B., Choi, Y., and Segal, R.A. 2002. Cerebellar proteoglycans regulate sonic hedgehog responses during development. *Development* **129**(9): 2223-2232.

Sadowski, I., Ma, J., Triezenberg, S., and Ptashne, M. 1988. GAL4-VP16 is an unusually potent transcriptional activator. *Nature* **335**(6190): 563-564.

Sagai, T., Masuya, H., Tamura, M., Shimizu, K., Yada, Y., Wakana, S., Gondo, Y., Noda, T., and Shiroishi, T. 2004. Phylogenetic conservation of a limb-specific, cis-acting regulator of Sonic hedgehog (Shh). *Mamm Genome* **15**(1): 23-34.

Saha, K. and Schaffer, D.V. 2006. Signal dynamics in Sonic hedgehog tissue patterning. *Development* **133**(5): 889-900.

Sambrook, J. and Russell, D.W. 2001. *Molecular Cloning: A Laboratory Manual*. Cold Spring Harbor Laboratory Press.

Sasai, Y. and De Robertis, E.M. 1997. Ectodermal patterning in vertebrate embryos. *Dev Biol* **182**(1): 5-20.

Sasaki, H., Hui, C., Nakafuku, M., and Kondoh, H. 1997. A binding site for Gli proteins is essential for HNF-3beta floor plate enhancer activity in transgenics and can respond to Shh in vitro. *Development* **124**(7): 1313-1322.

Schafer, M., Kinzel, D., Neuner, C., Schartl, M., Volff, J.N., and Winkler, C. 2005. Hedgehog and retinoid signalling confines nkx2.2b expression to the lateral floor plate of the zebrafish trunk. *Mech Dev* **122**(1): 43-56.

Schauerte, H.E., van Eeden, F.J., Fricke, C., Odenthal, J., Strahle, U., and Haffter, P. 1998. Sonic hedgehog is not required for the induction of medial floor plate cells in the zebrafish. *Development* **125**(15): 2983-2993.

Scheer, N. and Campos-Ortega, J.A. 1999. Use of the Gal4-UAS technique for targeted gene expression in the zebrafish. *Mech Dev* **80**(2): 153-158.

Sharpe, J., Lettice, L., Hecksher-Sorensen, J., Fox, M., Hill, R., and Krumlauf, R. 1999. Identification of sonic hedgehog as a candidate gene responsible for the polydactylous mouse mutant Sasquatch. *Curr Biol* **9**(2): 97-100.

Sherer, N.M. and Mothes, W. 2008. Cytonemes and tunneling nanotubules in cell-cell communication and viral pathogenesis. *Trends Cell Biol* **18**(9): 414-420.

Shimeld, S.M. 1999. The evolution of the hedgehog gene family in chordates: insights from amphioxus hedgehog. *Dev Genes Evol* **209**(1): 40-47.

Shin, J., Park, H.C., Topczewska, J.M., Mawdsley, D.J., and Appel, B. 2003. Neural cell fate analysis in zebrafish using olig2 BAC transgenics. *Methods Cell Sci* **25**(1-2): 7-14.

Simons, K. and Vaz, W.L. 2004. Model systems, lipid rafts, and cell membranes. *Annu Rev Biophys Biomol Struct* **33**: 269-295.

Stamataki, D., Ulloa, F., Tsoni, S.V., Mynett, A., and Briscoe, J. 2005. A gradient of Gli activity mediates graded Sonic Hedgehog signaling in the neural tube. *Genes Dev* **19**(5): 626-641.

Steinhauer, J. and Treisman, J.E. 2009. Lipid-modified morphogens: functions of fats. *Curr Opin Genet Dev* **19**(4): 308-314.

Stone, D.M., Hynes, M., Armanini, M., Swanson, T.A., Gu, Q., Johnson, R.L., Scott, M.P., Pennica, D., Goddard, A., Phillips, H., Noll, M., Hooper, J.E., de Sauvage, F., and Rosenthal, A. 1996. The tumour-suppressor gene patched encodes a candidate receptor for Sonic hedgehog. *Nature* **384**(6605): 129-134.

Strahle, U. and Blader, P. 1994. Early neurogenesis in the zebrafish embryo. *FASEB J* **8**(10): 692-698.

Sugahara, F., Aota, S., Kuraku, S., Murakami, Y., Takio-Ogawa, Y., Hirano, S., and Kuratani, S. 2011. Involvement of Hedgehog and FGF signalling in the lamprey telencephalon: evolution of regionalization and dorsoventral patterning of the vertebrate forebrain. *Development* **138**(6): 1217-1226.

Tabata, T., Eaton, S., and Kornberg, T.B. 1992. The Drosophila hedgehog gene is expressed specifically in posterior compartment cells and is a target of engrailed regulation. *Genes Dev* **6**(12B): 2635-2645.

Taipale, J. and Beachy, P.A. 2001. The Hedgehog and Wnt signalling pathways in cancer. *Nature* **411**(6835): 349-354.

Taipale, J., Chen, J.K., Cooper, M.K., Wang, B., Mann, R.K., Milenkovic, L., Scott, M.P., and Beachy, P.A. 2000. Effects of oncogenic mutations in Smoothened and Patched can be reversed by cyclopamine. *Nature* **406**(6799): 1005-1009.

Taipale, J., Cooper, M.K., Maiti, T., and Beachy, P.A. 2002. Patched acts catalytically to suppress the activity of Smoothened. *Nature* **418**(6900): 892-897.

Tashiro, S., Michiue, T., Higashijima, S., Zenno, S., Ishimaru, S., Takahashi, F., Orihara, M., Kojima, T., and Saigo, K. 1993. Structure and expression of hedgehog, a Drosophila segment-polarity gene required for cell-cell communication. *Gene* **124**(2): 183-189.

Taylor, F.R., Wen, D., Garber, E.A., Carmillo, A.N., Baker, D.P., Arduini, R.M., Williams, K.P., Weinreb, P.H., Rayhorn, P., Hronowski, X., Whitty, A., Day, E.S., Boriack-Sjodin, A., Shapiro, R.I., Galdes, A., and Pepinsky, R.B. 2001. Enhanced potency of human Sonic hedgehog by hydrophobic modification. *Biochemistry* **40**(14): 4359-4371.

Teleman, A.A., Strigini, M., and Cohen, S.M. 2001. Shaping morphogen gradients. *Cell* **105**(5): 559-562.

Tenzen, T., Allen, B.L., Cole, F., Kang, J.S., Krauss, R.S., and McMahon, A.P. 2006. The cell surface membrane proteins Cdo and Boc are components and targets of the Hedgehog signaling pathway and feedback network in mice. *Dev Cell* **10**(5): 647-656.

The, I., Bellaiche, Y., and Perrimon, N. 1999. Hedgehog movement is regulated through tout velu-dependent synthesis of a heparan sulfate proteoglycan. *Mol Cell* **4**(4): 633-639.

Thisse, C., Thisse, B., Schilling, T.F., and Postlethwait, J.H. 1993. Structure of the zebrafish snail1 gene and its expression in wild-type, spadetail and no tail mutant embryos. *Development* **119**(4): 1203-1215.

Tokhunts, R., Singh, S., Chu, T., D'Angelo, G., Baubet, V., Goetz, J.A., Huang, Z., Yuan, Z., Ascano, M., Zavros, Y., Therond, P.P., Kunes, S., Dahmane, N., and Robbins, D.J. 2010. The full-length unprocessed hedgehog protein is an active signaling molecule. *J Biol Chem* **285**(4): 2562-2568.

Torroja, C., Gorfinkiel, N., and Guerrero, I. 2004. Patched controls the Hedgehog gradient by endocytosis in a dynamin-dependent manner, but this internalization does not play a major role in signal transduction. *Development* **131**(10): 2395-2408.

Udvadia, A.J. and Linney, E. 2003. Windows into development: historic, current, and future perspectives on transgenic zebrafish. *Dev Biol* **256**(1): 1-17.

van den Heuvel, M. and Ingham, P.W. 1996. smoothened encodes a receptor-like serpentine protein required for hedgehog signalling. *Nature* **382**(6591): 547-551.

Varjosalo, M. and Taipale, J. 2008. Hedgehog: functions and mechanisms. *Genes Dev* **22**(18): 2454-2472.

Vortkamp, A., Lee, K., Lanske, B., Segre, G.V., Kronenberg, H.M., and Tabin, C.J. 1996. Regulation of rate of cartilage differentiation by Indian hedgehog and PTH-related protein. *Science* **273**(5275): 613-622.

Vyas, N., Goswami, D., Manonmani, A., Sharma, P., Ranganath, H.A., VijayRaghavan, K., Shashidhara, L.S., Sowdhamini, R., and Mayor, S. 2008. Nanoscale organization of hedgehog is essential for long-range signaling. *Cell* **133**(7): 1214-1227.

Walton, K.D., Warner, J., Hertzler, P.H., and McClay, D.R. 2009. Hedgehog signaling patterns mesoderm in the sea urchin. *Dev Biol* **331**(1): 26-37.

Williams, E.H., Pappano, W.N., Saunders, A.M., Kim, M.S., Leahy, D.J., and Beachy, P.A. 2010. Dally-like core protein and its mammalian homologues mediate stimulatory and inhibitory effects on Hedgehog signal response. *Proc Natl Acad Sci U S A* **107**(13): 5869-5874.

Williams, K.P., Rayhorn, P., Chi-Rosso, G., Garber, E.A., Strauch, K.L., Horan, G.S., Reilly, J.O., Baker, D.P., Taylor, F.R., Koteliansky, V., and Pepinsky, R.B. 1999. Functional antagonists of sonic hedgehog reveal the importance of the N terminus for activity. *J Cell Sci* **112 (Pt 23)**: 4405-4414.

Yan, D. and Lin, X. 2009. Shaping morphogen gradients by proteoglycans. *Cold Spring Harb Perspect Biol* **1**(3): a002493.

Yao, S., Lum, L., and Beachy, P. 2006. The ihog cell-surface proteins bind Hedgehog and mediate pathway activation. *Cell* **125**(2): 343-357.

Yin, C. and Solnica-Krezel, L. 2007. Convergence and extension movements mediate the specification and fate maintenance of zebrafish slow muscle precursors. *Dev Biol* **304**(1): 141-155.

Zeng, X., Goetz, J.A., Suber, L.M., Scott, W.J., Jr., Schreiner, C.M., and Robbins, D.J. 2001. A freely diffusible form of Sonic hedgehog mediates long-range signalling. *Nature* **411**(6838): 716-720.

Zheng, X., Mann, R.K., Sever, N., and Beachy, P.A. 2010. Genetic and biochemical definition of the Hedgehog receptor. *Genes Dev* **24**(1): 57-71.